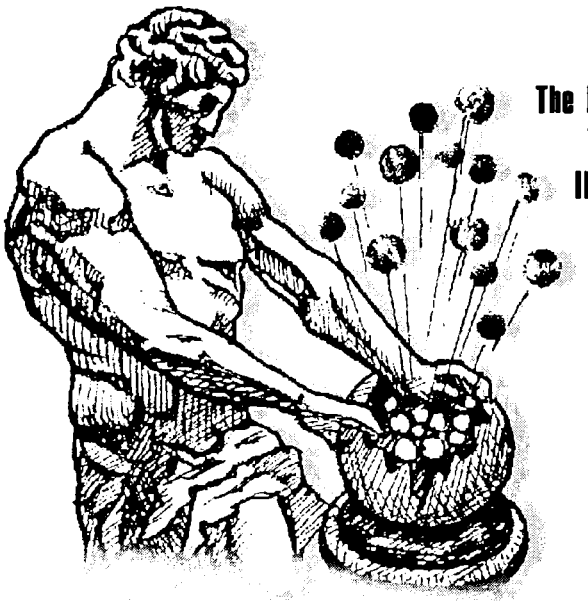

The Ministry of the Russian Federation for Atomic Energy
The State Scientific Center of Russian Federation
INSTITUTE FOR PHYSICS AND POWER ENGINEERING
named after Acad. A.I.Leipunskg

Nuclear Physics Department

ANNUAL REPORT
1998

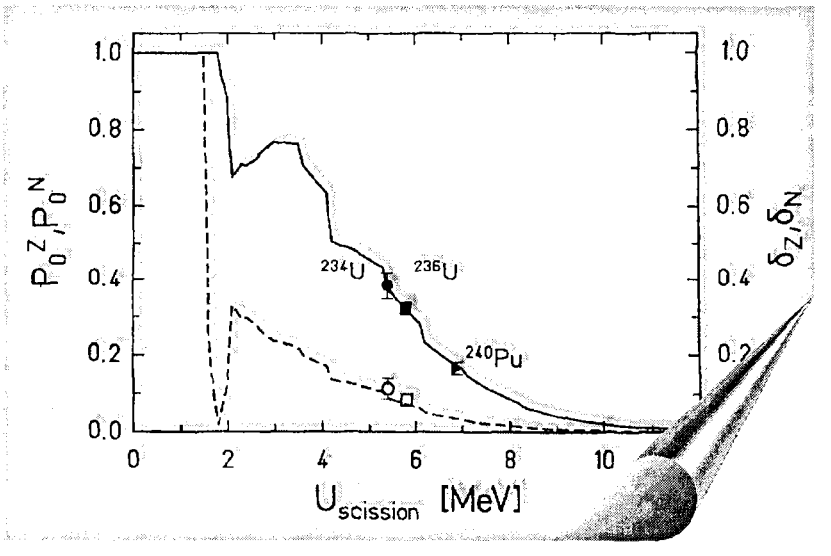

OBNINSK

Annual Report

Nuclear Physics Department

State Research Center of Russian Federation
A.I.Leypunsky Institute of Physics and Power Engineering.
Ministry for Atomic Energy of Russian Federation

For the year 1 January to 31 December 1998

Contacts: **Nuclear Physics Department**
State Research Center of Russian Federation
A.I.Leypunsky Institute of Physics and Power Engineering.
Ministry for Atomic Energy of Russian Federation.
249020, Obninsk, Kaluga Region, Russia
FAX: (095) 230 23 26, 8833112

Editor: **B.D.Kuzminov**

CONTENTS

PREFACE

This is the second issue of Annual Report, in which the achievements in scientific research for the last year in Nuclear Physics Department of IPPE are carried.

It includes measurement, compilation and evaluation of nuclear data for pure and applied science, the investigations in field of nuclear fission, nuclear structure and nuclear reactions, condensed matter physics, mathematical modeling, transmutation, high-voltage accelerators and applied research.

Main attention was concentrated to solve number of problems.

- The model has been formulated for interpretation of the even-odd structure in fission fragment yields.
- There was certain progress in formulating a microscopic theory of the cold and hot nuclei collective excitations.
- The new evaluations were made for the full files of americium isotope neutron cross sections.
- Calculations were made of isotope inventory, residual heat and helium content of AMOX fuel of BOR-60 reactor during the campaign and for cooling times up to 180 years.
- Some structural and dynamical properties of condensed matter were investigated in neutron scattering experiments.
- Mathematical modeling of some phenomena, connected with membrane apparatus, fast reactor transients, radioactive contamination migration in underground water, fluid mechanics, heat and mass transfer, crystal growth et cetera was realized.
- NPD continued efforts to investigate structural and selective properties of the nuclear track membranes, manufactured by fission fragments irradiation of polymeric film in nuclear reactor BR-10.
  The industrial production of polymer track membranes was created in IPPE.
- In 1998 NPD paid special attention to the experimental base advance, including accelerators EG-1, EGP-10 an EGP-15.
- The contribution of nonmonoenergetic neutrons from solid tritium-titanium - molybdenum target under the bombardment of proton beam was experimentally and theoretically investigated.

Department Director 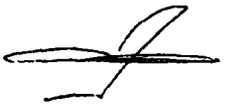 **B.Fursov**

1. DEPARTAMENT STRUCTURE

DIRECTORATE:

Director: B.I.FURSOV
Deputy Directors: B.D.KUZMINOV
V.E.RUDNIKOV

THEORETICAL NUCLEAR PHYSICS DIVISION
Head: A.V.IGNATYUK

THEORETICAL NUCLEAR PHYSICS LABORATORY
Head: Yu.N.SHUBIN
NUCLEAR DATA CENTER
Head: V.N.MANOKHIN

EXPERIMENTAL NUCLEAR PHYSICS DIVISION
Head: A.A.GOVERDOVSKI

NUCLEAR FISSION PHYSICS LABORATORY
Head: M.I.SVIRIN
NEUTRON SPECTROMETRY LABORATORY
Head: B.V.ZHURAVLEV
NUCLEAR REACTIONS LABORATORY
Head: V.M.PIKSAIKIN
NUCLEAR FISSION DYNAMICS LABORATORY
Head: Yu.B.OSTAPENKO
APPLIED NUCLEAR PHYSICS LABORATORY
Head: A.A.TUMANOV

HIGH-VOLTAGE ACCELERATORS DIVISION
Head: A.I.GLOTOV

CONDENCED MATTER PHYSICS LABORATORY
Head: A.V.PUCHKOV

MATHEMATICS AND SOFTWARE DIVISION
Head: V.P.GINKIN

NUMERICAL METHODS LABORATORY
Head: V.P.GINKIN
PRECISION METHODS LABORATORY
Head: V.K.ARTEMYEV
STATISTICAL METHODS LABORATORY
Head: S.V.PUPKO

2. SCIENTIFIC RESEARCH

2.1 NUCLEAR FISSION

Pair Breaking and Even-Odd Structure in Fission-Fragment Yields

F. Farget[*], *A.V. Ignatyuk, A.R. Junghans*[*], *K.-H. Schmidt*[*]

[*)]*Gesellschaft fuer Schwerionenforschung, Planckstraße 1, D-64291 Darmstadt, Germany*

The enhanced production of nuclei with even numbers of protons and neutrons is one of the prominent structural effects in nuclear fission from low excitation energies. The total even-odd effect in element yields, defined as the difference of even-Z and odd-Z yields divided by the total yield, has been found to vary strongly for different fissioning nuclei. Although the number of neutrons of the fission fragments produced at scission is difficult to measure, data from high kinetic energies where neutron evaporation is suppressed show that the even-odd effect in neutron number is considerably reduced as compared to the even-odd effect in proton number.

In an experiment recently performed at GSI Darmstadt with relativistic secondary heavy-ion beams, element yields have been determined for long isotopic series of neutron-deficient actinides and pre-actinides. For the first time, the systematic variation of the proton even-odd effect as a function of neutron and proton number of the fissioning system was measured over a large region of the chart of the nuclides. Due to the considerably increased data basis on even-odd effects in fission, the systematic appearance of an even-odd structure also in odd-Z fissioning nuclei has been revealed. In addition, the data show that an increased even-odd structure in extremely asymmetric charge splits is a general effect for even-Z fissioning nuclei. These new findings illustrate the prospects for a new insight into the mechanism of pair breaking in fission brought about by the progress in experimental technique.

In the present paper a model has been formulated for the interpretation of the even-odd structure in fission-fragment yields. The model is based on the number of available single-particle excitations of the nuclear system, calculated in the framework of the superfluid nuclear model. Assuming thermal equilibrium of quasiparticle excitations, the probability of pair breaking is given by the relative statistical weight of excitations which destroy the completely paired configuration of the proton, respectively neutron subsystem at the different stages of the fission process. The concept of the new model differs appreciably from that of previously proposed ones. Our approach seems to be more consistent with the basic principle of the statistical theory of nuclear reactions.

The model explains the experimental observation that neutron even-odd effects, even in cold fission, are considerably smaller than proton even-odd effects without invoking different influences of nuclear dynamics on the proton and neutron subsystems. The strongly different even-odd structures in proton and neutron number well comply with the assumption of thermal equilibrium in the effective scission configuration.

From the even-odd structure of measured fission-fragment element yields, the excitation energy acquired at scission was deduced. Contributions to the even-odd structure from the different phase spaces in the nascent fission fragments were considered. Indications have been found that the energy dissipation in fission scales with the Coulomb parameter $Z^2/A^{1/3}$ rather than with the fissility of the fissioning system. The deduced excitation energies at scission were found to increase less steeply with the Coulomb parameter of the fissioning nucleus than deduced previously.

Experimental Studies of the Absolute Delayed Neutron Yields from Neutron Induced Fission of ^{237}Np And ^{235}U in the Energy Range 0.340 - 5 Mev

V.M.Piksaikin, S.G.Isaev, L.E.Kazakov, B.D.Kuzminov, G.G.Korolev, V.G.Pronjaev

Experimental method and procedure of measurement

The measurements of the energy dependence of the total DN yields were carried out on the beams of protons and deuterons at the cascade generator KG - 2.5 of the IPPE. The monoenergetic neutrons were generated using reactions T(p,n)^{3}He and D(d,n)^{3}He in solid tritium and deuterium targets. The experimental method employed in measurements was based on a cyclic irradiation of fissionable samples by neutrons with the subsequent measurements of the time dependence of DN intensity.

Absolute measurements of the total delayed neutron yields from neutron induced fission reactions require the knowledge of the energy dependent absolute efficiency of the neutron detector used for delayed neutron registration. The absolute efficiency of the 4π neutron detector was determined by two different methods. The first one was the activation method based on the ^{51}V(p,n)^{51}Cr reaction. The second method was based on the measurements of the average number of prompt neutrons from spontaneous fission of ^{252}Cf source coupled with a surface barrier detector. The Monte Carlo calculations were used to determine the energy dependence of the relative efficiency of neutron detector.

The value of the fission rate in the fissionable samples was obtained on the basis of the pulse height distributions from two parallel-plate fission chambers positioned in the front of and behind the sample relative to ion beam.

Experimental results

The measurements of the absolute DN yields include two types of experiments. The first one consists of the measurements of the relative abundances and periods of separate DN groups. In this type of experiment the measurements with different irradiation and DN counting time intervals are foreseen to emphasize the certain DN groups. In the second type of experiment the measurements were performed using the irradiation time which is longer as compared to the longest DN period. DN counting time of 720 s was used that allows determining the neutron background value with high accuracy. The corrections for the neutron multiple scattering and neutron attenuation effects in the construction materials and samples as well as for the neutron self-multiplication effect in the samples were taken into account.

The experimental results of the present studies are shown in fig.1 where they are compared to the similar data of other authors. They represent the absolute DN yield from fission of ^{235}U by neutrons with energy E_n=1.165 MeV and the energy dependence of the relative total DN yields in the energy range E_n=0.77-5 MeV normalized to the value of the absolute DN yield at the neutron energy E_n=0.77 MeV obtained by the linear interpolation of the recommended values ν_d(En) for E_n=THRM (thermal neutrons) and E_n=FAST (fission spectrum neutrons) from the Tuttle's evaluation [2].

In the case of ^{237}Np the absolute DN yields were measured at neutron energies E_n=1.154 and 3.868 MeV and the energy dependence of relative total DN yield $\nu_d(E_n)$ in the energy range 1-5 MeV normalized at E_n=1 MeV on value $\nu_d(E_n)$ of the absolute total DN yield for E_n=1.154 MeV (obtained in the present work). The assumption was made

that the dependence $\nu_d(E_n)$ does not undergo considerable changes in the energy range E_n=1-1.154 MeV.

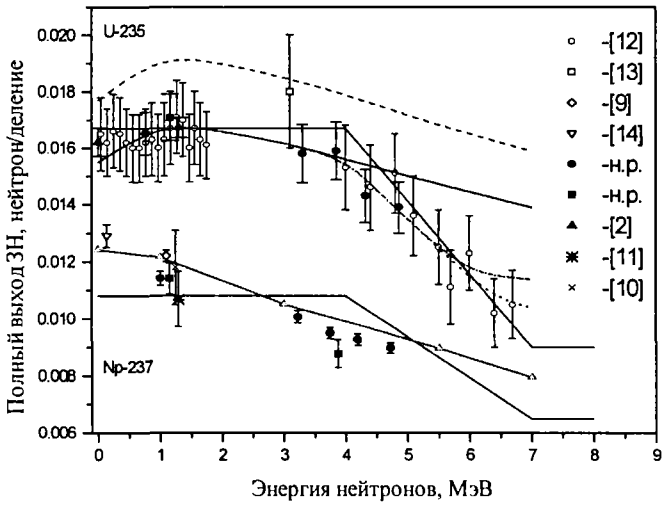

Fig. 1. Energy dependence of total DN yield $\nu_d(E_n)$ from fission of ^{235}U and ^{237}Np by neutrons. Experimental data of the present work: filled circles - relative data, filled squares - absolute data. Data obtained within the framework of parametrization [16]: dashed line (^{235}U) - calculation $\nu_d(E_n)$, based on independent fission yield IY (Z,A,E_n) from paper [3]; solid line (^{235}U) and triangle points, connected by a solid line (^{237}Np), - data $\nu_d(E_n)$, calculated in view of experimental data on independent fission yields IY (Z,A,E_n); a dash-dotted line (^{235}U) - data $\nu_d(E_n)$ taking into account a variation ν_p(En) with energy of neutrons En for a light fragment; dashed line (^{235}U) - the same as dash-dotted, but takes into account the contribution from the second chance fission.

References

2. Tuttle R.J.//Proc. of the consultants' meeting on delayed neutron properties, Vienna, 26-30 March 1979: IAEA, INDC(NDS)-107/G.Vienna, 1979. P. 29.
3. Report JAERI-M-89-204 / Ed. H. Ihara, 1989.
9. Benedetti G., Cesana A. et al. // Nucl. Sci. Eng. 1982. V. 80. P. 379.
10. Гудков А.Н., Живун В.М., Звонарев А.В. и др. // Атом.энергия. 1989. Т.66. С.100.
11. Waldo R.W., Karam R.A.// Trans. Am. Nucl. Soc. 1981. V. 39. P. 879.
12. Krick M.S., Evans A.E.// Nucl. Sci. Eng. 1972.V.47.P.311.
13. Masters C.F., Thorpe M.M., Smith D.B. // Nucl. Sci. Eng. 1969. V.36. P.202.
14. Saleh H.K., Parish T.H. et al. // Nucl. Sci. Eng. 1997. V.125. P.51.
16. Pronyaev V.G., Piksaikin V.M.// ВАНиТ. Сер.:Ядерные константы. М.: ЦНИИатоминформ, 1997. Вып.1-2. С.32.

Energy Dependence of Average Half-Life of Delayed Neutron Precursors in Fast Neutron Induced Fission of ^{235}U and ^{236}U

V.M. Piksaikin, S.G. Isaev, L.E. Kazakov, M.Z. Tarasko

The purpose of the present experimental study was to investigate the energy dependence of the average half-life of DN precursors in the fast neutron induced fission of ^{235}U and ^{236}U. So the group relative abundances a_i and half-lives T_i of delayed neutrons in the fast neutron induced fission of ^{235}U and ^{236}U were measured to obtain the average half-lives of DN precursors. On the basis of these data the energy dependencies of the average half-life of DN precursors in the fast neutron induced fission of ^{235}U and ^{236}U were obtained and the analysis of these dependencies was made.

Experimental method

The experimental method employed in the measurements is based on periodic irradiation of the fissionable samples by neutrons generated in a suitable nuclear reaction at the accelerator target and measurements of the decay of delayed neutron activity [2].

The $T(p,n)^3He$ and $D(d,n)^3He$ reactions were used in measurements as the neutron sources. Tritium and deuterium targets were irradiated by ion beam on the electrostatic accelerator KG-2.5 at the IPPE. The times of sample transportation from the irradiation position to the neutron detector were about 150 ms. The computer of the IBM type serves as a central processor controlling the irradiation time, the value of neutron flux at discrete time intervals, the number and width of the time channels for the delayed neutron counting. The computer controls also the operation of the pneumatic transport system and the accelerator mode switches. Time-channel widths of 0.01, 0.02, 0.1, 1.0, 10 s following in the automatic sequence were used in the present measurement. Two types of experimental data were used in the present experiment. The first type of data was obtained in the measurements with 15 s irradiation time and 424.5 s counting time. The second type of data was obtained in the measurements with 300 s irradiation time and 724.5 s counting time. Such procedure allowed to increase a relative contribution of delayed neutrons corresponding to definite groups of precursors in the integral decay curve.

Experimental results

The energy-dependencies of the average half-life of delayed neutrons precursors in the fast neutron induced fission of ^{235}U and ^{236}U are presented in Fig.1. Also in this figure the data obtained for fission neutrons spectra [3,4,6,8] are presented. The values of uncertainties for the average half-life were obtained without accounting of correlation between relative abundances and periods of delayed neutrons. The analysis of the correlation matrix of the relative abundances and periods shows that account of correlation between a_i and T_i reduce the uncertainty in the average half-life because the off diagonal elements are predominantly negative.

The analysis of the energy-dependence of the average half-life of delayed neutrons precursors for ^{235}U shows that in the incident neutron energy range 0.37 - 1.059 MeV the average half-life is constant. For ^{235}U and ^{236}U in the incident neutron energy range above 1 MeV the value of average half-life trends to reduce with increase of incident neutron energy. And in the case of ^{236}U this reduction is amounted to about 10 % in the considered energy range. This trend can be roughly explained by the increase of relative contribution

of the short half-life precursors in the fast neutron induced fission of ^{235}U and ^{236}U in the energy range above 1 MeV.

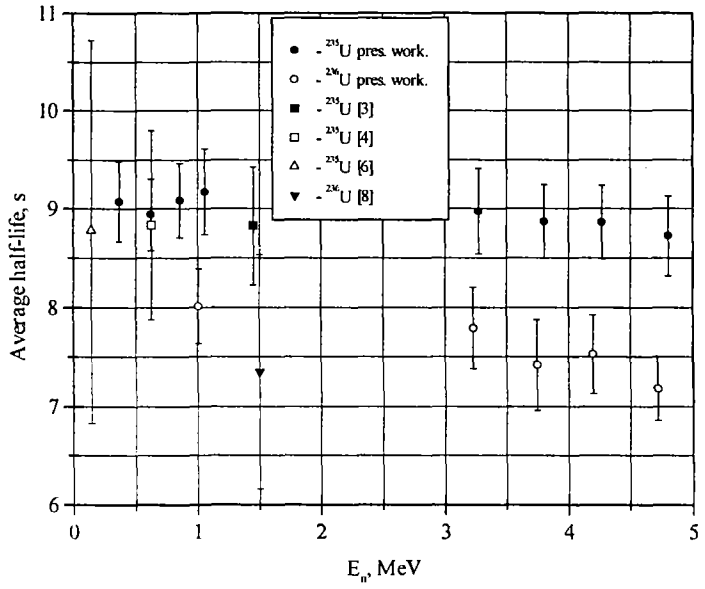

Fig.1. The energy-dependencies of average half-life of delayed neutrons precursors in fast neutron induced fission of ^{235}U and ^{236}U.

References

1. V.M. Piksaikin, S.G. Isaev. Correlation properties of delayed neutrons from fast neutron induced fission, Report-INDC(CCP)-415, IAEA, Vienna, 1998.
2. V.M. Piksaikin, Yu.F. Balakshev et. al.. Measurements of energy-dependence of delayed neutrons relative abundances and half-lives of delayed neutrons precursors in fast neutrons induced fission of ^{237}Np, Atomic Energy, Vol.85, No.1, 1998, P.51.
3. G.R. Keepin. Physics of Nuclear Kinetics, Addison Wesley Publishing Co., Reading, Massachusetts, 1965.
4. C.B. Besant, P.J. Challen, M.H. McTeggart, P. Tavoularidis, J.G. Williams. J.Br. Nucl.Energy Soc., Vol.16, 1977, P.161.
5. G. Benedetti, A. Cesana, V. Sangiust and M. Terrani. Delayed Neutron Yields from Fission of Uranium-233, Neptunium-237, Plutonium-238, -240, 241 and Americium-241, Nucl. Sci. Eng., Vol.80, 1982, P.379.
6. H.K. Saleh, T.A. Parish, S. Raman, N. Shinihara. Nucl. Sci. Eng., Vol.125, 1997, p.51.
7. R.W. Waldo, R.A. Karam, R.A. Meyer. Delayed Neutron Yields: Time Dependence Measurements and a Predictive Model, Physical Review C., Vol.23, No.3, 1981, P.1113.
8. A.N. Gudkov et al.. At. Energ., 1989, Vol.66, No.2, P.100,
   A.N. Gudkov et al.. At. Energ., 1989, Vol.67, No.3, P.702.
9. R.J. Tutle. Delayed-neutron yields in nuclear fission, Proc. of Consultants' Meeting on Delayed Neutron Properties, Vienna, 26-30 March, 1979, INDC(NDS)-107/G, P.29.

Correlation Properties of Delayed Neutrons from Fast Neutron Induced Fission

V.M. Piksaikin, S.G. Isaev

The experimental studies of the energy dependence of the delayed neutron parameters for various fissioning systems have shown that the behavior of a some combination of delayed neutron parameters (group relative abundances a_i and half lives T_i) has a similar features.

On the basis of the analysis of DN experimental data it was shown that the average half-life of DN precursors for Th, U, Pu, Am elements can be presented by the exponential dependence on the fissioning nucleus parameter $-(A_c-3Z)A_c/Z$ within experimental uncertainties (see Fig 1). It was shown that the total delayed neutron yield values for each considered elements correlate with the appropriate values of the average half life of DN precursors (see Figs. 2, 3). These properties of delayed neutrons allowed to obtain the independent systematics of the total DN yields for Th, U, Pu and Am elements. According to this systematics it was shown that the well known dependence of ν_d on $-(A_c-3Z)A_c/Z$ parameter has a more complex structure than it was assumed until now [1] - each of the considered element has its own ν_d dependence on this parameter (see Fig.4).

Preliminary analysis of ENDF/B-VI delayed neutron data on the basis of the present systematics showed that the DN parameters a_i and T_i obtained by the summation method must be carefully checked with the purpose to find the source of their disagreement with experimental data. As a result of the present findings some of the possible application of the reported results are the following. The obtained sistematics of DN parameters can be used

- for testing of DN measurement techniques and the LSF procedures;
- for testing the existing DN parameters data base;
- as a criteria for testing the summation calculation procedure and appropriate input data (P_n and fission yields as well as the distribution of precursors between the DN groups). Preliminary analysis of ENDF/B-VI data showed that the relative abundances and half lives data for the most studied in respect to fission yield data (fission yield is believed the main source of uncertainties in the summation method) ^{239}Pu and ^{235}U isotopes according to the present systematics are not correct;
- for the prediction of the DN parameters for elements for which there is no experimental data;
- for the evaluation of the DN parameters.

The present systematics gives the possibility to improve the total delayed neutron data ν_d through performing the measurements of the aggregate DN decay curves only.

It should be noted that in the present analysis only the restricted part of the available experimental information on the DN parameters were used. The uncertainties of the average half life values must be calculated using the information on the correlation between the DN group parameters [2]. Therefore the obtained results should be considered as preliminary data. The authors understand that the work must be continued with analysis of all available experimental information on the DN parameters.

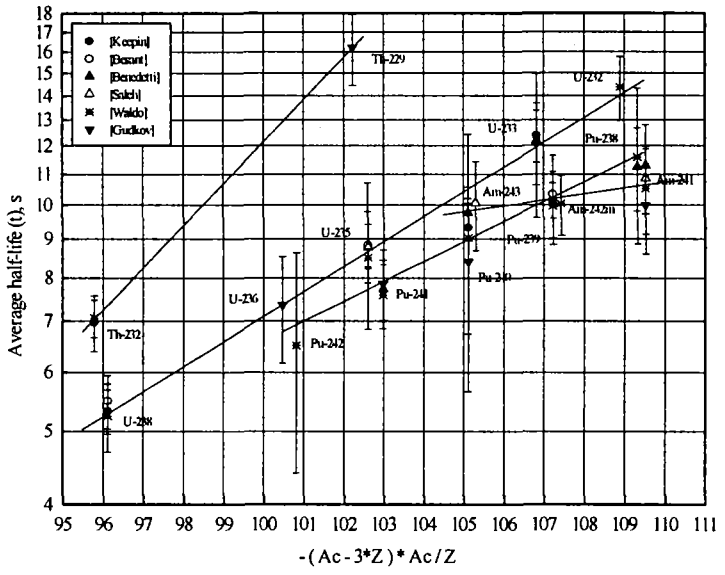

Fig.1. Systematics of the average half life of DN precursors for Th, U, Pu, Am elements.

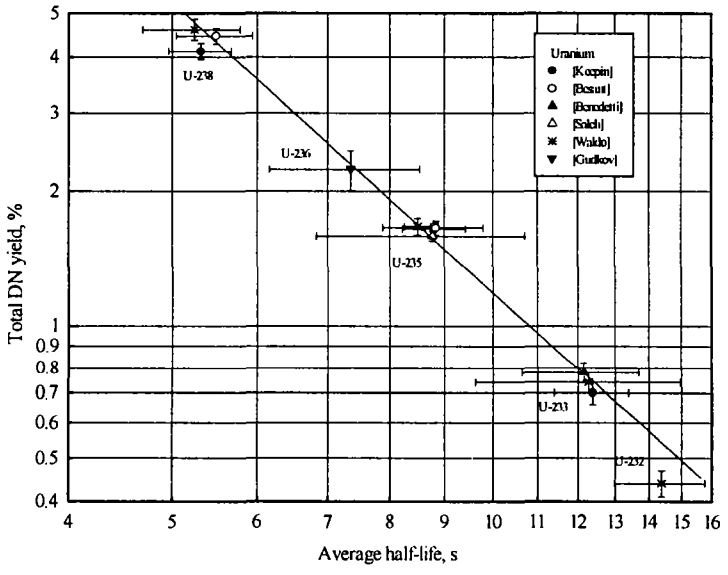

Fig.2. Total DN yield as a function of average half life of DN precursors for U.

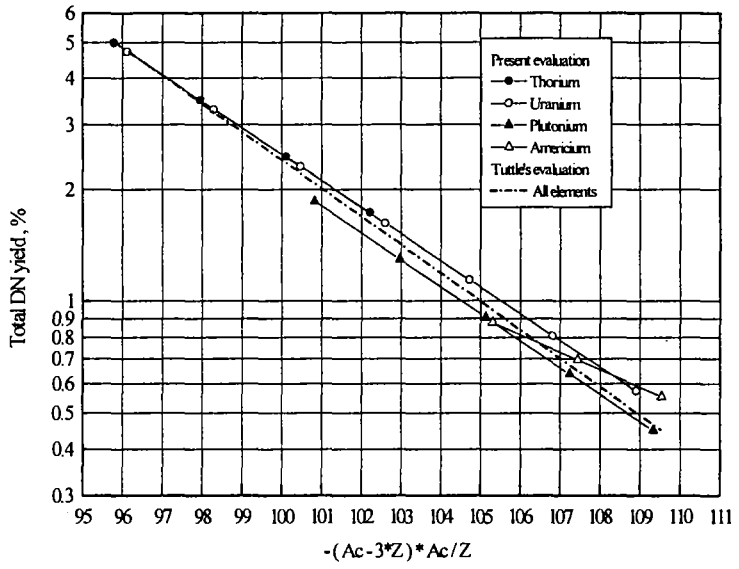

Fig.3. Dependence of the total DN yields on parameter $P = -(A_c - 3Z) \cdot A_c / Z$. Points connected by solid lines - present systematics, dach line - Tuttle's equation [1].

References

1. R.J. Tuttle, Delayed-Neutron Yields in Nuclear Fission, Proc. of consultants' meeting on delayed neutron properties, Vienna, 26-30 March, 1979, INDC(NDS)-107/G, P.29.
2. V.M. Piksaikin, Yu,F, Balakshev, S.G.Isaev, L.E.Kasakov, G.G.Korolev, V.I.Milshin, Measurements of Energy Dependence of Relative Abundances of Delayed Neutrons and Group Periods of their Precursors from Fast Neutron Induced Fission of ^{237}Np, Atomic energy (in Russian) to be published in 1998.

Features of the Neutron Spectra Accompanying the Fission of ^{238}U

G.N. Lovchikova, A.M. Trufanov, M.I. Svirin, A.V. Polyakov, V.A. Vinogradov

A scientific aspect of the investigated problems is connected with the appearance of unknown features (or maybe features that have not received sufficient attention) in the distributions of neutrons as the energy of the bombarding (primary) neutrons E_n is raising above the threshold of the reaction when nuclear fission becomes an emission process. As can see in fig these features are observed in comparing the measured spectra of neutrons at two groups of characteristic energies of E_n^I=2.9, 5 MeV and E_n^{II}=13.2, 14.7, 16.0, 17.7 MeV for the target nucleus ^{238}U [1-3]. In the first case, the excitation energies are below the energy threshold for (n,n'f) reaction, and secondary neutrons are emitted from exited fission fragments of compound nuclei A. In the second case the excitation energies lie much higher than the threshold for (n,n'f) reactions, and fission process has of an emission character- that is, the fission of the residual nuclei A-1 and A-2 formed after the emission of one or two neutrons is energetically possible. Under such conditions, not only fission fragments but also the fissile nuclei A and A-1 become sources of neutrons. At least in the measured energy range of secondary neutrons E=0.25-12 MeV for the reaction (n,f) induced by primary neutrons of energy E_n=2.9, 5.0 MeV the experimental distribution shape is close to Maxwell distribution $N_M(E,T)$ with an accuracy of the correction which takes into account some small deviations from $N_M(E,T)$. At E_n=13.2, 14.7, 16.0, and 17.7 MeV the distributions have a maximum at $E=E_n-B_f^{A-1}$ (B_f^{A-1} is the height of fission barrier) and rise with decreasing energy E in the region E<2 MeV. Under the assumption of two sources of neutrons (nuclei undergoing fission for prefission neutrons and fully accelerated fragments for postfission neutrons) the results of calculations can reproduce the shape of the observed distributions only in the region $E\geq$ 2 MeV. In the low-energy region (E<2 MeV) the experimental spectra display an anomalously large yield of soft neutrons in relation to the results of calculations. If the third source of neutron emission from nonaccelerated fragments is incorporated into the model calculations the results agree well with experimental data over entire range of measured secondary neutron energies, including the anomalous region E<2 MeV.

Further experiments to study this effect are necessary for obtaining deeper insight into the mechanism that is responsible for the emergence of soft neutrons. It should be noted that the additional experimental information about the neutron distributions especially in the low-energy region 10 keV-2 MeV would be useful.

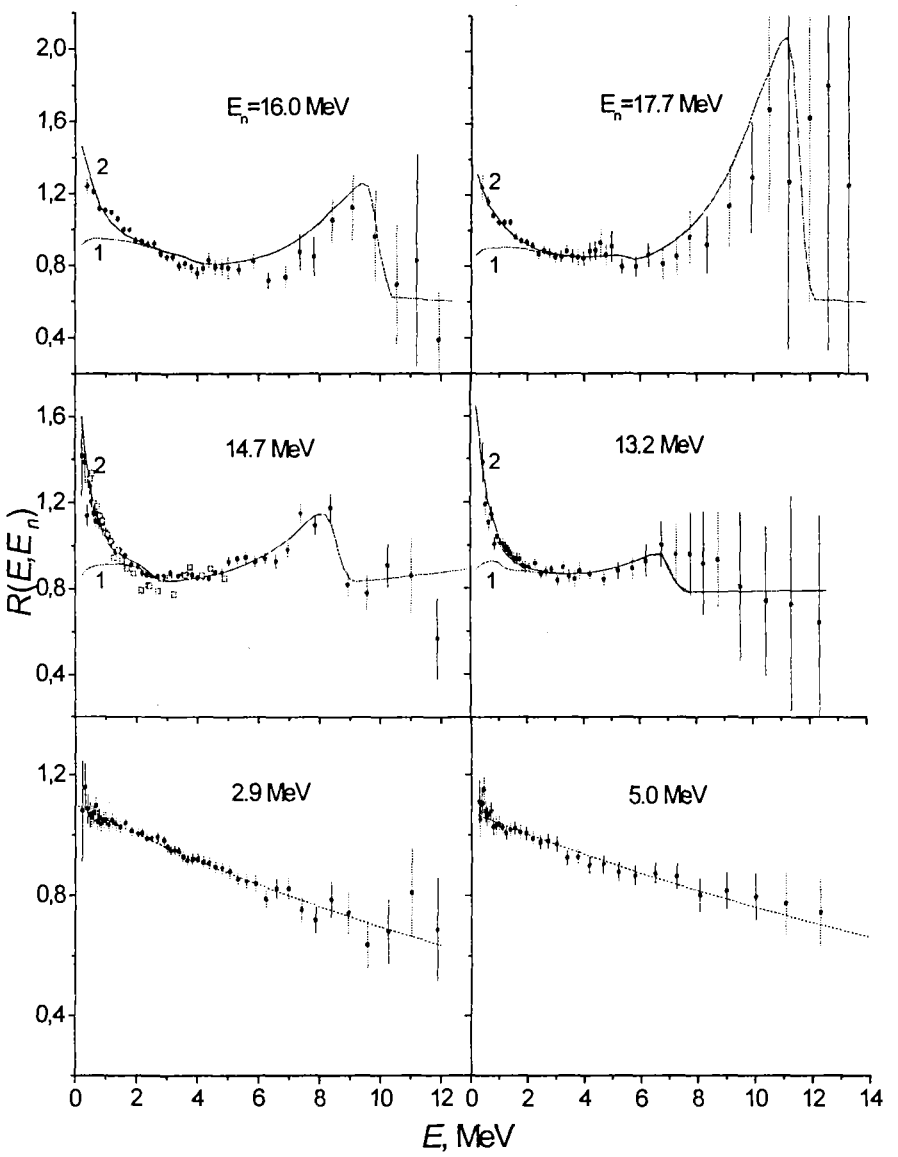

Fig. Ratios $R(E,E_n)$ of the spectra of fission neutrons from the reaction $^{238}U(n,xn'f)$ to the spectrum of neutrons from the spontaneous fission of ^{252}Cf: (points -solid circles [1-3], - open squares [4]) experimental values, (solid curves1) results of the calculation without allowance for the contribution of neutrons from nonaccelerated fragments, (solid curves 2) results of the calculation with allowance for the contribution of neutrons from nonaccelerated fragments, and (dashed lines) ratios of Maxwell distributions with temperatures T_U=1.332 MeV for E_n=2.9 MeV, T_U=1.353 MeV for E_n=5.0 MeV and T_{Cf}=1.42 MeV.

References

1. Svirin M.I., Lovchikova G.N., and Trufanov A.M., Yad. Fiz., 1997, vol.60, p.818.
2. Lovchikova G.N., Trufanov A.M., Svirin M.I. et al., Preprint of Inst. of Physics and Power Engineering, Obninsk, 1997, no. FEI-2648.
3. Lovchikova G.N., Trufanov A.M., Svirin M.I. et al., Preprint of Inst. of Physics and Power Engineering, Obninsk, 1998, no. FEI-2689.
4. Vasil'ev Yu.A., Zamyatnin Yu.S. et al., Zh.Eksp.Teor.Fis., 1960, vol.38, p.671.

2.2 NUCLEAR STRUCTURE AND NUCLEAR REACTIONS

Analysis of Cross-Sections and Mechanism of (n,xn) and (n,xγ) Reactions on Lead and Bismuth

V.P. Lunev, V.G. Pronyaev, S.P. Simakov, Yu.N. Shubin

Summary

Investigations of the interactions of fast neutrons with nuclei enable to study neutron reaction mechanism, the structure of discrete excited states and statistical properties unresolved levels of residual nuclei. In spite of comparatively long efforts in the development of fundamental approach to the description of nucleon-nucleus reactions in megaelectronvolt energy region the comprehensive understanding of the mechanisms of these reactions was not achieved yet. In our opinion, one of the main tasks in this region is the development of the approach, which combines, from one side, the fundamental grounds, and, from other side, is capable to predict qualitatively the reaction cross sections, in particular, the energy-angle distributions of secondary particles with experimental accuracy.

The present paper is the continuation of these investigations performed earlier for the other nuclei and reactions. The cross sections and energy distributions of neutrons and γ-rays from (n,xn) and (n,xγ) reactions on lead isotopes and bismuth have been analyzed up to incident neutron energies 26 MeV.

It is shown what degree of the accuracy can be achieved when up to date information on the optical potentials, the properties of low-lying discrete levels and the density of excited states is taken into account.

The reasonable agreement with experimental data was obtained when the compound, direct and precompound mechanisms and up-to date model parameters were used in the calculations.

On Two Mechanisms of Nuclear Superfluidity

A.V.Avdeenkov, S.P.Kamerdzhiev

It is well known that taking into account the quasiparticle- phonon interaction in the particle- particle channel is very important for quantitative and qualitative understanding of many phenomena both in odd and in even nuclei. However, the role of this interaction in the particle- particle channel is known to a considerably smaller extent. For the problem of nuclear superfluidity (pairing) this question was almost not studied on a microscopic level. First of all it is great interest to investigate this question in the g2 approximation (g- is the collective phonon creation amplitudes) which is suitable for semi-magic nuclei [1].

In the microscopic theory of nucleus only one mechanism of pairing is considered, as a rule. This is the known Bardeen-Cooper-Schrieffer (BCS) mechanism. It contains a particle- particle interaction, which is usually determined phenomenologically from comparison with experimental data. This means that the phenomenological pp- interaction contains the quasiparticle- phonon interaction in a non- explicit form, however in an explicit and quantitative form it was not yet taken consistently into account for nuclear pairing problem.

In Refs.[1], [2] main equations for the pairing gap have been formulated in the above- mentioned approximation. These non-linear equations take into account two mechanisms of nuclear pairing, namely one of the BCS type and the quasiparticle- phonon mechanism in an explicit form.

In this work we solved these equations for the first time. We obtained that for the semi-magic nucleus ^{120}Sn mean quantities of contributions of the first and second mechanisms are equal to 74% and 26% of observed pairing gap, respectively. Thus, pairing, at least in semi- magic nuclei, has a mixed nature in the sense that it is caused by both of these two mechanisms. The first one has volume origin while the quasiparticle-phonon mechanism has mainly a surface origin.

References

1. A.V.Avdeenkov, S.P.Kamerdzhiev, Yad.Fiz. 62(1999)No.4
2. S.Kamerdzhiev, J.Speth, G.Tertychny, Acta Phys.Pol. 29B(1998)2231

Temperature Generalization of the Continuum Quasiparticle Random-Phase Approximation

S.P.Kamerdzhiev,E.V.Litvinova, V.I.Tselayev***

**Institute of Nuclear Power Engineering,Obninsk, Russia,*
***Institute of Physics, St.Petersburg State University, St. Petersburg, Russia.*

In Ref.[1] we have generalized the well-known quasiparticle random- phase approximation (QRPA) to include the single-particle continuum (CQRPA) and describe properties of giant resonances and some gamma- ray reactions. That was necessary because the inclusion of the continuum allows to obtain a real physical envelope of a multipale giant resonance (GR). The continuum is important for the description of some unstable nuclei, partial reactions, GRs of large multipolarity etc.

The main direction of modern GR physics is the investigation of GR in hot nuclei. But hot (temperature) nuclei are very interesting by themselves, of course. Therefore, it is necessary to add to our CQRPA a taking into account of temperature to obtain the TCQRPA approach.

In this work we generalized the CQRPA [1] to include temperature and realized our TCQRPA approach numerically for some stable and unstable Sn isotopes.

Our calculations for 120Sn have shown, in particular, that inclusion of the continuum increases the energy weighted sum rule (EWSR) by about 6% for T<Tc and only by 2-3% for T>Tc where Tc is critical temperature at which pairing is absent. The results are similar to those [2] obtained within the standard theory of finite Fermi systems (without taking the continuum into account) for deformed nuclei. However, they differ noticeably from the result [3] for spherical nuclei obtained within a simple version of the QRPA.

In order to obtain a better description of hot nuclei it is necessary to include more complex configurations than those accounting for in the TCQRPA. But this problem is very cumbersome for non- magic nuclei, it has been not yet realized within a reasonable approach (which would include, for example, the single- particle continuum and ground state correlations).

References

1. S.Kamerdzhiev, R.J. Liotta, E.Litvinova, V.Tselyaev, Phys.Rev. C58 (1998)172.
2. S.Kamerdzhiev, D.Zawischa Phys.Lett. B275(1992)1.
3. G.G. Dussel, H.Fortunato, H.M. Sofia, Phys.Rev. C42(1990)2093.

The Role of Ground State Correlation in the Single-Particle Strength of Odd Non-Magic Nuclei

A.V.Avdeenkov, S.P.Kamerdzhiev

A method based on the consistent use of the Green function formalisms has been developed to calculate the distribution of single- particle strength in odd nuclei with pairing [1]. The method takes into account the quasiparticle- phonon interaction, ground state correlation and a "refinement" of phenomenological single- particle energies and pairing gap values from the quasiparticle- phonon interaction under considaration. The calculations for

^{121}Sn and ^{119}Sn, which were performed in the quasiparticle+phonon approximation, have shown a reasonable agreement with experiment.

In this work we have investigated the role of ground state correlations (GSC) in the single-particle strength of the odd nuclei under consideration. In general, the GSC caused by taking into account complex configurations (this is our case) are more physically interesting and important than the well-known RPA GSC.

We obtained that the GSC plays a noticeable role and mostly improve the agreement with experiment or shift the results to the right direction. In the Fig.1 we show their noticeable role of our GSC for 1g9/2 states in 119Sn.

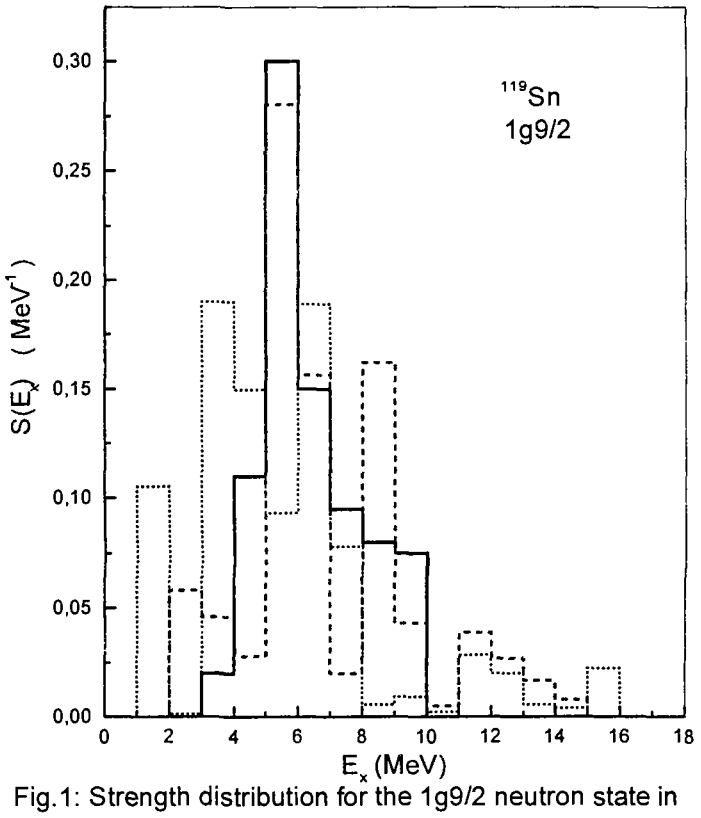

Fig.1: Strength distribution for the 1g9/2 neutron state in ^{119}Sn.The solid line gives the experimental data. The dashed line gives the results with taking into account GSC, the dotted line gives the results without them.

References

1. A.V. Avdeenkov, S.P. Kamerdzhiev, Yad.Fiz. 62 (1999) No.4

There is no Missing Isoscalar Monopole Strength in ^{58}Ni

*S.Kamerdzhiev, J.Speth *, G.Tertychny, and F.Osterfeld **

* *Instiut fuer Kernphysik, Forschungszentrum Juelich, D-52425, Germany*

Till very recently there were still many questions connected with the IS E0 giant resonance in nuclei with A<90. An important one being the problem of distribution of E0 strength and small amount of it observed in several nuclei. In Ref. [1] only 32% (at best <50%) of the IS E0 EWSR was observed in the (12 - 25) MeV region. In fact, these ^{58}Ni results increased uncertainties for the A<90 nuclei.

In our preliminary calculations [2] we compared with the theory *only the form of the experimental spectra* for ^{58}Ni(α,α') reaction in the observed (12-25) MeV interval because there were no data about the corresponding absolute values in Ref. [1]. A good agreement with this experiment was obtained but our value of the IS E0 EWSR was equal to 71.4%. We concluded that a considerable part of the strength might be hidden in the experimental background [1].

Recently it was reported by the authors of Ref. [1] that they have extended the observed energy interval up to 35 MeV in several of the A<90 nuclei including ^{58}Ni and found some additional IS E0 strength at higher excitation energies [3]. Thus, due to this fact and also with taking into account a continuum under the monopole peak 75-100% f the EWSR might be present below 35 MeV excitation energy [4]. In addition, absolute values of experimental cross sections are known at present [3]. It was necessary in Refs. [3,4] to substract another background and therefore another additional strengts should appeare under the previous (12-25) MeV interval. This can be clearly seen from Fig.1.

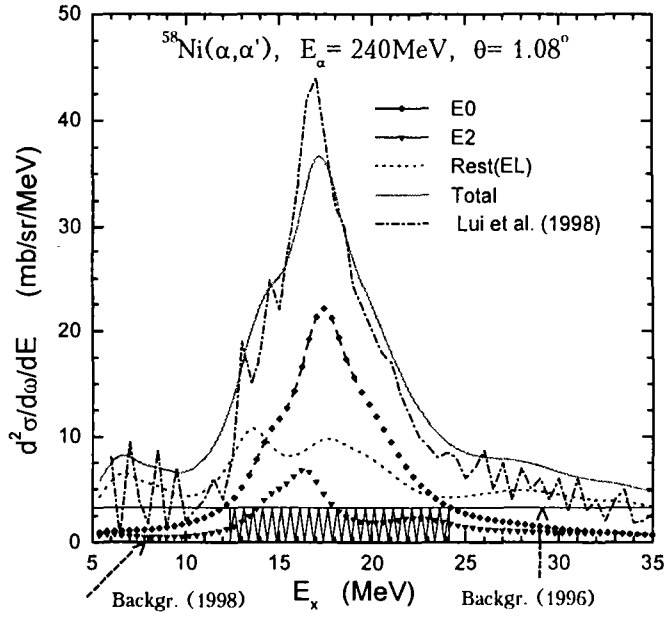

Fig. 1. The cross section of ^{58}Ni(α,α') reaction at $E_α$=240MeV and θ=1.08°. The experimental data (dash-dotted curve) were taken from Ref. [3]. The solid curve gives the total (summed) theoretical cross section, the dotted line ("Rest(EL)") corresponds to sum of the IS and IV E1, and IS E3 and E4 multipoles. The dashed area shows an additional IS E0 strength which could not be observed in the experiment of Ref. [1], see text. This area corresponds to 22% of the IS E0 EWSR.

In Ref.[1] the background was substracted beginning from 25 MeV as it is shown by the upper border of the shaded area in Fig.1. In other words, only the part of the E0 resonance which is higher than this upper border could be observed in Ref.[1]. In recent exeperiment [3,4] the background was substracted beginning from about 35 MeV, to be exact, the experimental data given in Fig.1 were counted from the new background which corresponds to zero on the vertical axis. So the shaded area in Fig.1 corresponds to the IS E0 strength which could not be observed in Ref. [1] and was observed in the newest experiment in addition to the old result in Ref. [1]. It is possible to estimate approximately the part of the IS E0 EWSR corresponding to this shaded area. The square of the area which is the sum of the shaded one and that of the E0 resonance upper than the shaded area is about 138.3 mb/sr/MeV. This figure corresponds to our 71.4% of the EWSR. The shaded area gives 42.6 mb/sr/MeV which corresponds to 22% of the IS E0 EWSR and was missed in the Ref. [1] experiment.

References

1. Youngblood, H.L. Clark, and Y.-W. Lui, Phys. Rev. Lett. 76, 1426 (1996).
2. Kamerdzhiev, J. Speth, and G. Tertychny, in Proceeding of the Intern. Conference on Nuclear Structure and Related Topics (Dubna, Sept. 1997), p.347; in Proceeding of the Workshop on the Structure of Mesons, Barions and Nuclei (Cracov, May 1998), Acta Phys. Pol. 28,2231 (1998)
3. W. Lui, D.H. Youngblood, and H.L. Clark, Contribution to the Topical Conference on Giant Resonances (Varenna, May 1998).
4. A. van der Woude, Summary talk at the Topical Conference on Giant Resonances (Varenna, May 1998), to be published in the Proceedings of the Conf. in Nucl. Phys. A.

Comparison of Threshold Reaction Cross Sections for the Ti, V, Cr, Fe, Ni, Cu and Zn Isotopes from Evaluated Data Libraries

A.I.Blokhin, V.N.Manokhin, S.M.Nasyrova

The most of excitation functions in evaluated data libraries are calculated on the basis of theoretical models with the parameters adjusted to the experimental data available. However, because of the differencies in models and codes, input parameters and experimental data used for the adjustment there are large discrepancies in evaluated data, presented in different evaluated data libraries even for the isotopes and reactions of great importance for technological applications. We compared some evaluated threshold reaction excitation functions from the libraries BROND-2, ENDF/B-VI, JEF-2, JENDL-3, ADL-3, EAF-97.

To solve the problem of selection of more reliable excitation functions from these libraries we propose our recommended curves which are evaluated on the basis of empirical systematics without using any theoretical model calculations. These systematics are obtained from an analysis of experimental data. Because our evaluation method is independent from model calculations we consider more reliable those theoretical excitation functions, which are in more close agreement with our recommended excitation functions.

The recommended excitation functions were evaluated on the basis of the systematics developed in the works /1-3 /. Below the essential items of the systematics and procedure of evaluation of our recommended curves are given only for (n,p) and (n,,α) reactions.

- The shapes of (n,p) reaction excitation functions are similar for the isotopes with the same (N-Z). The maximum (n,p) reaction cross sections decrease linearly as a function of A for the isotopes of a given element and increase linearly as a function of Z for the isotopes with the same (N-Z).
- The shapes of (n,α) reaction excitation functions are similar for the isotopes with the same (N-Z). The maximum (n,α) reaction cross sections decrease linearly as a function of A for the isotopes of a given element and increase linearly as a function of Z for the isotopes with the same (N-Z).
- The position of the maximum of (n,p) excitation function relative to the threshold is proportional to the difference (Q_{nnp} -Q_{np}).
- The position of the maximum of (n, α) reaction excitation function relative to the threshold is proportional to the difference ($Q_{nn\alpha}$ -$Q_{n\alpha}$).

The results of comparison and evaluation of 70 excitation functions are presented in the work /4/. As example two Figures are given below.

In conclusion we should like to note that we are far from idea to consider our recommended curves as the most accurate. However, our recommendations are based on the systematical trends, which were extracted from analysis of available experimental data and from our point of view in better agreement with physics of processes. We propose that the curves with considerable deviation from our recommendations should be checked. There is great chance that some of such curves may be wrong.

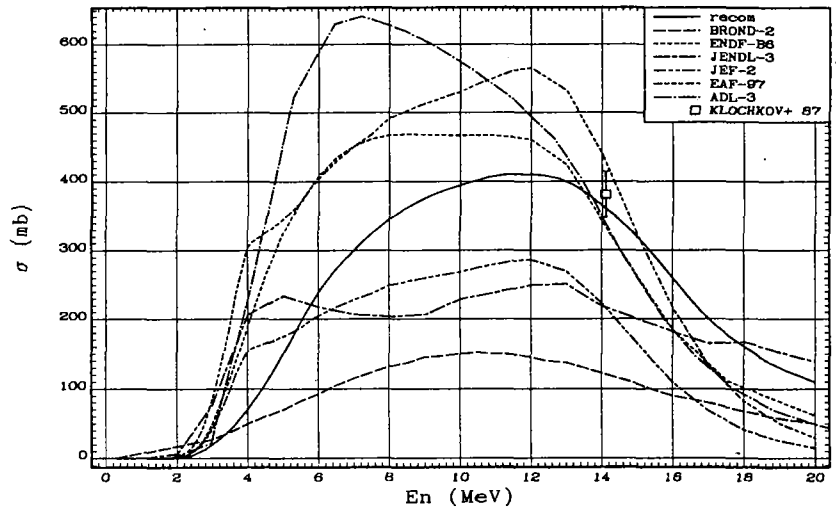

Fig.1. Cross section of $^{50}Cr(n,p)^{50}V$ reaction.

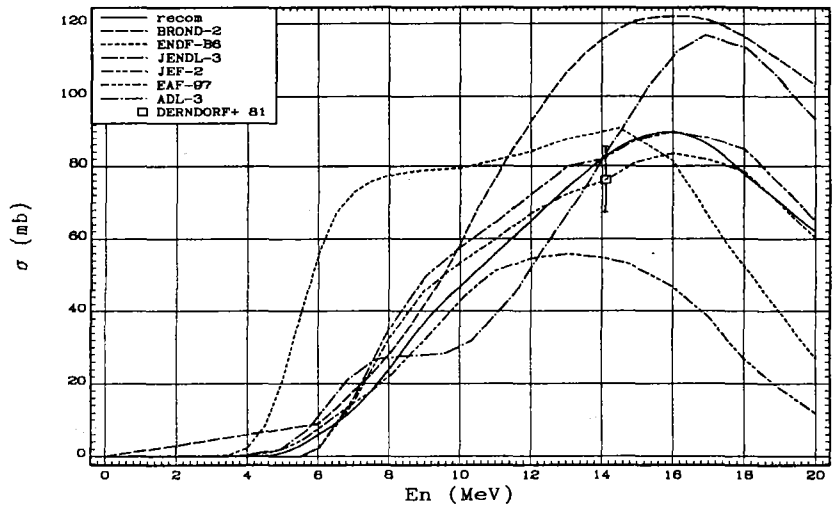

Fig.2. Cross section of $^{50}Cr(n,\alpha)^{47}Ti$ reaction.

References

1. V.N.Manokhin. VANT, Yadernye Konstanty, 1996, N2, p.73. Report INDC(CCP)-387, 1997, Vienna. Yadernye Konstanty, 1994, N1, p.18. Report INDC(CCP)-398,Vienna, 1996.
2. A.I.Blokhin, V.N.Manokhin. In: Conference Proceedings, Vol.59. "Nuclear Data for Science and Technology", Bologna, Italy, 1997, 1,p.871.
3. A.I.Blokhin, V.N.Manokhin, S.M.Nasyrova. Preprint FEI - 2620, 1997 (in Russian).
4. A.I.Blokhin, V.N.Manokhin, S.M.Nasyrova. VANT, Yadernye Konstanty, N 1-2, 1997, p.50. Report INDC(CCP)-411, 1998, Vienna.

Evaluations of Neutron Cross Sections for ^{241}Am and ^{243}Am

A.V. Ignatyuk, A.I. Blokhin, V.P. Lunev, V.N. Manokhin,
G.Ya. Tertychny, V.A. Tolstikov, K.I.Zolotarev

In recent years the new evaluations were made for the full files of americium isotope neutron cross sections: ENDF/B-VI /1/ for Am-241 and Minsk's group for Am-241, -242m and -243 /2-3/. These evaluations are based on all available experimental data and the cross sections of many reactions in these files are improved essentially in comparison with previous evaluations. However in our opinion the recommended data in the new evaluations of fission cross sections do not describe optimally the available experimental data. For Am-241 and Am-243 we analyzed independently the experimental data of fission, (n,xn) and radiative capture cross sections and prepared the modified files of the evaluated neutron cross sections for BROND-3 library.

For the evaluation of ^{241}Am and ^{243}Am fission cross sections all experimental information available in the neutron energy region from 2 keV to 20 MeV was analyzed. The data were corrected with the new recommended monitor reaction cross sections. The most ^{241}Am(n,f) and ^{243}Am(n,f) reaction cross sections were measured relative to the ^{235}U fission cross section. For the normalization of such data the fission cross section of ^{235}U from ENDF/B-VI library was used.

In some works the ^{241}Am(n,f) and ^{243}Am(n,f) cross sections were measured relative to ^{239}Pu fission cross section. The ^{239}Pu(n,f) reaction cross sections from JENDL-3.2 were used to obtain absolute values of ^{241}Am(n,f) reaction cross sections. The cross sections of the monitor ^{238}U(n,f) and ^{237}Np(n,f) reactions were taken from ENDF/B-VI and from new evaluation made in IPPE.

To fit the recommended curve of the fission cross section the method of the statistical analysis of correlated data was used. The evaluated fission cross sections for Am-241 are given in Fig.1 together with the renormalized experimental data and other evaluations.

The experimental information for the Am-243 fission cross section in the energy region of 1 keV - 20 MeV are poorer than for Am-241. There are only seven experimental works in which ^{243}Am(n,f) excitation function was studied in relatively wide intervals of neutron energy. The analysis of experimental data after their renormalization to the new standards shows that there are noticeable systematic discrepancies between the data of different authors. For selection of more reliable data the microscopic experimental data were averaged on the spectra of Cf-252 spontaneous fission neutron source and Zebra-reactor and compared with the results of integral measurements in those spectra.

The analysis and correction of the experimental data permitted to remove considerably the contradictions in the Am-243 fission cross section measurements. The data for the Am-243 fission cross section are very scarce in the energy region above 10.5 MeV and measured with large uncertainties. That is why the neutron energy dependence of fission cross section in the region above 10 MeV, calculated in the frame of the optical-statistical model was used in the procedure of statistical evaluation of the cross sections in addition to the experimental data.

The Am-243 fission cross section evaluation obtained by statistical analysis of the correlated data is shown in Figs.2 together with renormalized experimental data and evaluations of other laboratories. For both americium isotopes the correlation matrices of uncertainties were also prepared and included into the section MT=33 of the full files of the evaluated cross sections.

The experimental data for the neutron radiative capture cross sections exist only in the energy region 1-400 keV for Am-241 and only in the neutron energy region up to 250 keV for Am-243. These data were renormalized to the present day standards, the systematic and statistical uncertainties were taken into account and the correlation coefficients for each data set were evaluated as well

For the neutron energy above upper experimental points the energy dependence of the radiative capture cross sections obtained from optical-statistical calculations and empirical systematics of capture cross sections for the neutron energy above 14 MeV were used.

The approximating curve for the capture cross section was obtained by the same method as for the fission cross sections. The correlation matrices of the uncertainties were included into the section MT=33 of the full files of the evaluated cross sections. More detailed description of the radiative capture cross section evaluation for the ^{241}Am and ^{243}Am was given in the work /4/.

The recent evaluations of the actinide total cross sections are in good agreement, however there are some discrepancies in the fast neutron absorption cross sections. From consideration of all the data we came to the conclusion that for Am-241 the scheme of 5 coupled levels with the following optical potential parameters is optimal:

The depth of real part of the potential V_r was adjusted to the neutron strength function value, determined from the resolved resonance region, and the depth of imaginary part of the potential in the energy region above 8 MeV was determined on the basis of optimal description of the fission and (n,xn) reaction cross sections. For Am-243 the same energy dependence parameters of the optical potential were used with slightly different values. As far as the neutron elastic and inelastic scattering cross sections, obtained in our calculations, are close to the ENDF/B-VI evaluations, the relevant sections of the integral and differential cross sections of neutron elastic and inelastic scattering from the ENDF/B-VI were included without changes to the new data file for BROND-3.

The discrepancies in the evaluations of absorption and fission cross sections effect the (n,2n) and (n,3n) reaction cross section evaluations. Because we evaluated also the (n,2n) and (n,3n) reaction cross sections consistently with the absorbtion and fission cross sections.

The neutron energy spectra were taken from ENDF/B-VI evaluations.

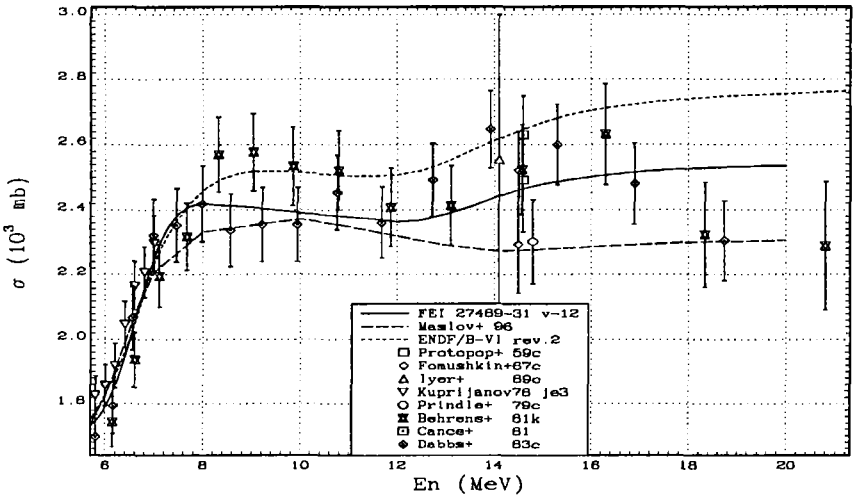

Fig. 1. Recommended fission cross section for ^{241}Am in comparison with evaluated and experimental data.

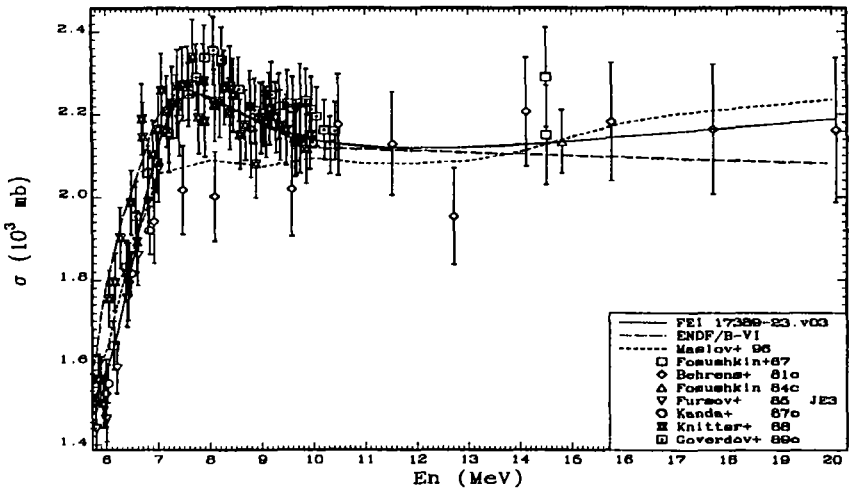

Fig. 2. Recommended fission cross section for ^{243}Am in comparison with evaluated and experimental data.

References

1. P.Young, D.Madland. ENDF/B-VI, MAT 9543, 1994.
2. V.M.Maslov et al. Report INDC(BLR)-005, IAEA, Vienna, 1996.
3. V.M.Maslov et al. Report INDC(BLR)-006, IAEA, Vienna, 1996
4. Zolotarev et al. VANT, Yadernye Konstanty, 3-4, 1997, c.79. Report INDC(CCP)-416, 1998, Vienna, p. 25.

Systematical Trends in the Behaviour of Fission and (n,2n) Reaction Cross Sections of Fissile Isotopes

V.N.Manokhin, A.I.Blokhin

In this paper the consistent analysis and comparison are made of the fission and (n,2n) cross sections in fast neutron energy range.

An analysis of available experimental data on fission cross sections for the isotopes from thorium up to curium shows that all energy dependences of fission cross sections in the neutron energy region of 1-20 MeV have similar structural features: maxima in the energy intervals of 1-3 MeV and 8-9 MeV and minima in the energy intervals of 5-6 MeV and 11-13 MeV.

Because these maxima and minima are situated practically in the same neutron energy intervals for all isotopes it is possible to compare fission cross sections in these intervals in dependence on A and Z. It should be noted that in the 5-6 MeV interval there is (n,nf) reaction threshold, in the 11-13 MeV there is (n,2nf) reaction threshold. In the energy interval of 11-13 MeV the maximum of (n,2n) reaction of excitation function and (n,3n) reaction threshold are located.

Theoretical model calculations show that at 11-13 MeV the inelastic scattering cross section is small (50-100 mb) and the main contribution to nonelastic interaction in this energy range gives the fission and (n,2n) reactions.

In Fig. 1 the available experimental and calculated data for the fission cross section are given. The fission cross sections of a given element may be approximated by straight lines.

In Fig.2 the calculated and experimental (n,2n) reaction cross section in the maximum of excitation function are presented. There is practically linear dependence of these cross sections as a function of atomic mass number A.

The sum of the fission and (n,2n) reaction cross sections in the incident neutron energy interval of 11-13 MeV changes weakly against atomic mass number of isotopes and in the first approximation can be considered as constant in all range of isotopes from Th up to Am and equal to 2580±50 mb.

In the work /1/ the universal normalized function for (n,2n) reaction was given that describes quite well the shape of the (n,2n) reaction excitation functions from the threshold up to the maximum of the cross section for a wide region of atomic mass number A = 10-200. The use of this normalized function for description of the (n,2n) reaction cross section shape gives good results for ^{232}Th, ^{238}U and ^{237}Np and there are some grounds to believe that this normalized function will be universal as well for the description of (n,2n) cross sections of other fissile isotopes.

Comparison of (n,3n) reaction cross section for ^{235}U and ^{238}U shows linear increase of maximum cross section with increase of atomic mass number. In /2/ the more detailed description of the systematical trends for fissile isotopes is given.

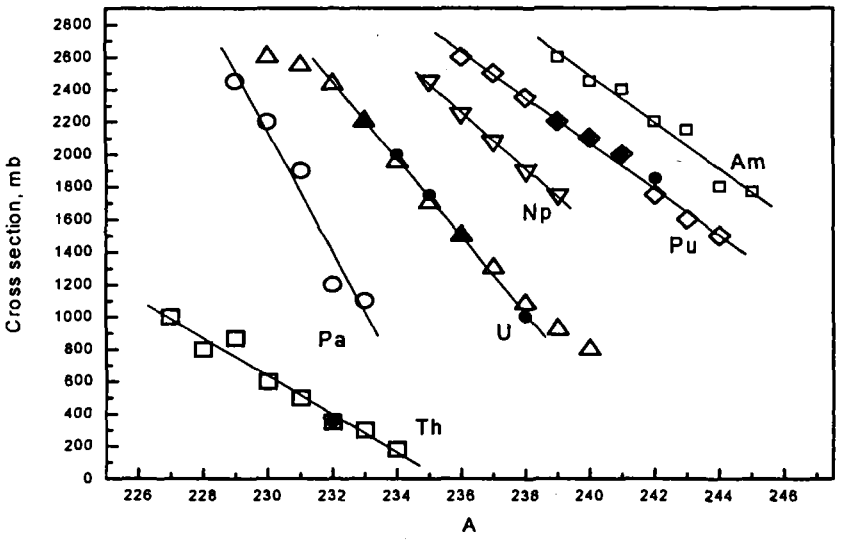

Fig.1. Fission cross section as a function of À. Dark symbols - experiment, light - calculation /7/.

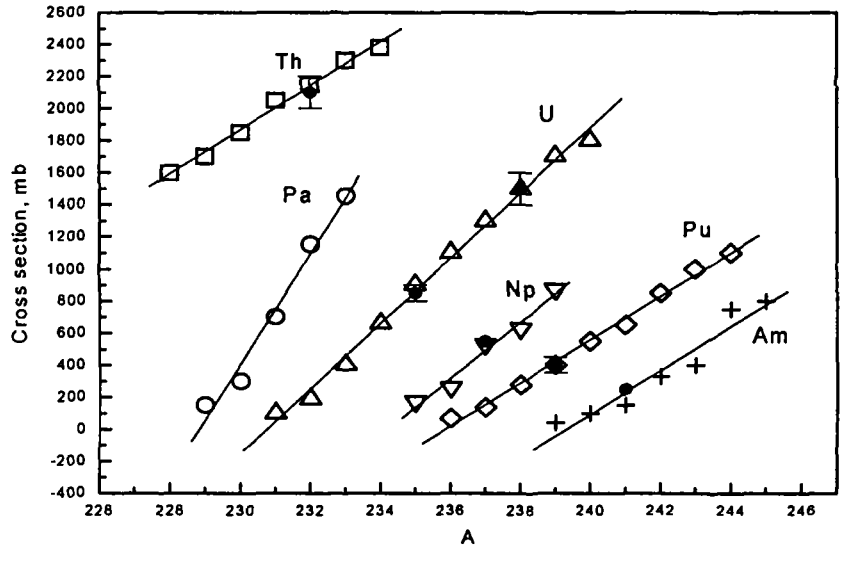

Fig.2. The (n,2n) reaction cross section at 12-13 MeV (in the maximum of excitation function).

References

1. V.N.Manokhin. Voprosy Atomnoi Nauki i Techniki, Ser. Yadernye Konstanty, v.2, 1997, p.73.Report INDC(CCP)-397, Vienna, 1997.
2. V.N.Manokhin, A.I.Blokhin. Voprosy Atomnoi Nauki I Techniki, Ser. Yadernye Konstanty, v.2, 1998, p.30. See also Preprint IPPE-2715, 1998, Obninsk.

Discrepancies in (n,2n) Reaction Excitation Functions of Rare Earth Isotopes. Recommendations for Selection of the Reliable Data

A.I.Blokhin, V.N.Manokhin, S.M.Nasyrova

An activity in creation of international data libraries (for example, FENDL library) leads to the problem of selection of more reliable data from different national or regional libraries. Because of large discrepancies in many cases it is not easy to decide which data are reliable. As a rule, there are no serious arguments to reject the data even if they differ essentially from the others. To solve the problem we proposed the systematics that permits to select reliable excitation functions.

An analysis of threshold reaction cross sections from different data libraries shows considerable discrepancies in the excitation functions. These discrepancies are particularly large, when there are no or too little experimental data. As a rule the evaluated data are calculated on the basis of theoretical models taking into account the 14-15 MeV systematics and discrepancies among these calculated data exist for most reactions and isotopes. We think that it is useful to publish the results of this comparison. We understand that it is very difficult to correct the existing libraries but hope that our recommendations will be taken into account.

In this paper the (n,2n) reaction excitation functions for rare earth isotopes from the libraries BROND-2, ENDF/B-VI, JENDL-3, ADL-3 and EAF-3 were compared.

As a criteria for determination which evaluated data from the libraries mentioned above seem to be more reliable, the (n,2n) reaction excitation functions, calculated on the basis of the excitation function systematics, are given together with those from the data libraries. As the systematics' excitation functions are obtained independently from the experimental data and model calculations it seems to us reasonable to consider the systematics curves or those excitation functions which are close to the systematics as more reliable.

A description of the systematics used in this work for calculation of the (n,2n) reaction excitation functions in the energy region up to 20 MeV is given in the works /1-3/.

The recommended data obtained on the basis of our method are presented in 50 Figures in the work /4/.

Now we would like to make some general remarks. The comparison of evaluated curves show, that in most cases the (n,2n) cross section values at the maximum of excitation functions are rather close. However, there are great discrepancies in shapes of the excitation functions. Many curves have very steep slope above the threshold that contradicts new experimental data. One can see a fast decrease of the (n,2n) cross sections in the energy region above the energy value at which the cross section maximum is observed. It was proved, on the basis of the experimental data, that the maxima of (n,3n) reaction cross sections are lower than those of (n,2n) reactions. Also the cross section increase above the threshold is weaker for (n,3n) reactions than for (n,2n) ones. The fast drop in cross sections after the maximum seems to be unreasonable. It contradicts also available experimental data.

It should be mentioned that similar discrepancies for the (n,2n) reactions are also observed for many other elements. Preliminary analysis indicates the same problems also for the (n,p) and (n,α) reactions.

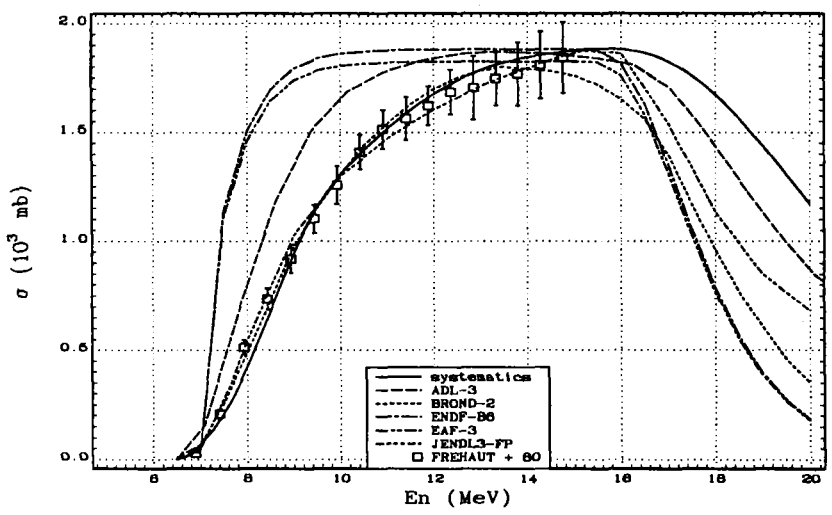

Fig 1. Cross section of ^{155}Gd(n,2n)^{154}Gd reaction.

References

1. V.N.Manokhin, "Systematics of the (n, 2n) and (n, 3n) reaction excitation functions", Jadernye Konstanty, (1994), v.1. See also: Report INDC(CCP)-398,Vienna, 1996.
2. V.N.Manokhin, Some criteria for selection of evaluated threshold reaction excitation functions. Report INDC(CCP)-397/G, Vienna, 1997.
3. A.I.Blokhin, V.N.Manokhin, "Empirical dependence of parameters of neutron threshold reaction excitation functions on A, Z, (N-Z)", in: Proc. Int. Conf. on Nuclear Data for Science and Technology, Trieste, Italy, 1997, p.871.
4. A.I.Blokhin, V.N.Manokhin, S.M.Nasyrova, Discrepanñies in (n,2n) reaction excitation functions of rare earth isotopes. Recomendations for selection of more reliable curves. Report INDC(CCP)-411, 1998, Vienna.

Formation of Activation Products in Interactions of Medium Energy Protons with Na, Si, P, Cl, Ca and Fe

M. Fassbender, Yu.N. Shubin and S.M. Qaim**

* *Institut fur Nuklearchemie, Forschungszentrum Juelich GMBH, D-52425 Juelich, Germany*

Summary

Excitation functions of (p,x) - processes on the elements , leading to the formation Na, Si, P, Cl, Ca and Fe, leading to the formation of 22,24Na and the medium mass activation products ^{42,43}K, ^{47}Ca, ^{44m,47}Sc, ^{48,51}Cr, ^{52,54}Mn, ^{52}Fe and ^{55}Co, were measured over the proton energy range of 70 to 355 MeV sing the stacked-foil technique. The product activity could be measured non-destructively via γ-ray spectrometry.Experimental results were compared with theoretical data obtained using modified hybrid nuclear model code ALICE-IPPE (1998) for intermediate energies. The agreement was found to be generally satisfactory below 70 MeV. The processes ^{nat}Cl(p,x)^{22}Na, ^{nat}Si(p,x)^{22,24}Na, ^{31}P(p,x)^{22}Na and ^{nat}Fe(p,x)^{48}V, ^{55}Co, ^{54}Mn, ^{51}Cr are described reasonably well by theory even at high energies. An activity estimate showed that the contribution of medium mass activation products to the total tissue and bone activation during proton therapy is negligible.

Semi-Empirical Systematics for *(N,T)* Reaction Cross Sections at the Energy of 14.6 MeV

*A.Yu. Konobeyev**, *V.P. Lunev*, *Yu.N. Shubin*

* *Institute of Nuclear Power Engineering, 249020 Obninsk,*

Summary

A new semi-empirical systematics for the *(n,t)* reaction cross section at the energy of 14.6 MeV is presented. The systematics is based on the account for nonequilibrium reaction mechanism and the corresponding analytical formulas of the preequilibrium exciton model. It is shown that the new semiempirical systematics not only ensures better description of the available experimental data as compared with the systematics suggested earlier, but enables to obtain the more realistic cross section values for the nuclei remote from the stability valley than those predicted by the empirical systematics.

Reference

1. Konobeyev[a]A.Yu., Lunev[b,1]V.P., Shubin[b,1]*Yu.N. Semi-Empirical Systematics for *(N,T)* Reaction Cross Sections at the Energy of 14.6 MeV. ***Il Nuovo Cimento***, **Vol.** 11A, **No.** 5, pp. 445-456, 1998.

Nuclear Data Needs for Accelerator Driven Subcritical Systems with Heavy Metal Coolant

A.V. Ignatyuk, Yu.N. Shubin

Abstract

The nuclear data needed for the calculations and analysis of the properties of accelerator driven subcritical systems and heavy liquid metal fast reactors (LMFR) for the transmutation problem are discussed on the example of investigation of the nuclei concentrations and long-lived residual radioactivity accumulated in Pb and Pb-Bi targets irradiated by high energy proton beam. Status of nuclear data in various energy regions is outlined The dominating components to the total radioactivity of radionuclides resulting from fission, spallation reactions and radiative capture by target nuclei for various irradiation and cooling times were analyzed. The volatile nuclide concentrations were determined also. The estimations of spectral component contributions of neutron and proton fluxes to the accumulated activity were carried out. It was shown that main contribution to the long-lived radioactivity give a high energy (> 20 MeV) part of the neutron and proton spectra. The contributions of fission products to the target activity and partial activities of main long-lived fission products were evaluated. The accumulation of Po isotopes due to the reactions of radiative capture were determined together with spallation reaction products giving the main contribution to the long-lived radioactivity. The production of tritium in the targets and its contribution to the total target activity was considered and the status of data needed for this task is discussed. The nuclear data connected with beam attenuation, gas production and radiation damage in the accelerator-target window was considered also.

For the liquid metal fast blankets conceived for the transmutation of actinides the traditional energy region is important. The attention is drawn to the large discrepancies in reaction cross sections for the both fission and multiple neutron emission. Recent evaluations for minor actinides are presented and nuclear data for thorium cycle are discussed. The necessity of the consisted evaluated cross section data base development at intermediate energies is stressed.

New Version of the Advanced Computer Code ALICE - IPPE

A.I. Dityuk, A.Yu. Konobeyev[*], *V.P. Lunev, Yu.N. Shubin,*

[*] *Institute of Nuclear Power Engineering, 249020 Obninsk*

Abstract

A new version of the ALICE code - ALICE-IPPE - is described. The main changes are briefly outlined. The new version of ALICE-IPPE differs from the ALICE-92 in a following aspects. Algorithm for the level density calculation according to the generalized superfluid model was tested, corrected and improved. Preequilibrium cluster emission calculation was included in the code. Calculation of the alpha-particle spectra is performed taking into account both the pick-up and knock-out processes. The phenomenological approach is used to describe direct channel for the deuteron emission. The triton and He-3 spectra are calculated according to the coalescence pick-up model of Sato, Iwamoto, Harada. Double precision calculations is used in all code. The correction taking into account gamma-ray emission was made for cross-section calculations. The contribution for residual (Z,A) nucleus production due to photon emission and following particle emission from residual (Z,A-1) or (Z-1,A-1) is considered directly. The corrections were made for the algorithm of multiple precompound proton emission spectra calculation near threshold and Kalbach systematic treatment.

Reference

1. A. I. Dityuk, A.Yu. Konobeyev[1], V.P. Lunev, Yu. N. Shubin, IAEA INDC(CCP)-410, Vienna, 1998.

Inelastic Neutron Scattering and Prompt Fission Neutron Spectra for ^{237}Np

N.V. Kornilov, A.B. Kagalenko, V.Ya. Baryba, V.G. Demenkov, S.V. Pupko, P.A. Androsenko

The ^{237}Np is a dominant nucleus among the nuclei from atomic power waste and the knowledge of the neutron data for this nucleus is of paramount importance for transmutation problem. Till now there are no any experimental data for inelastic cross section and scattering neutron spectra that complicates the data evaluation. The first experimental results are presented in this paper.

The measurement of the inelastic neutron spectra and cross section for ^{237}Np is complicated by the following factors:

1. A rather massive sample is required for a such measurement, that is, the measurement may be carried out if hundred grams sample of Np is available;
2. The neptunium oxide powder is the only material available for sample preparation. Hence, the detail simulation of the experiment and careful investigation of the neutron source spectra are required for correct estimation of the inelastic neutron spectra and cross sections;
3. Np sample produces very intensive γ-rays background, that should be proper reduced for successful measurements;
4. The total secondary neutron spectra (inelastic, elastic and fission) may be measured for Np. Hence, one should know the spectrum of prompt fission neutrons (PFNS) to estimate the inelastic neutron spectrum. This is a typical problem for fissile nuclei, however, due to lack of experimental data for Np, an additional measurements are required to made correct subtraction of the PFNS contribution.

In this paper we describe how the mentioned above problems have been overcome. The secondary neutron spectra (inelastic, elastic, fission) for ^{237}Np were measured by the neutron time of flight spectrometer of the IPPE at the incident energy range 1-2.5 MeV. The solid tritium target was used as a neutron source. The neptunium oxide (189 g) packed in the low mass stainless steel container was used as a scattering sample. The neutron background due to scattering on the target environment and tritium into the target backing was measured and was calculated with the appropriate model of the neutron source. The data were corrected for neutron background, the scattering on the oxygen and iron nuclei, and the effect of the finite sample size. The fission neutron spectra were measured, evaluated and subtracted from the emission neutron spectra to estimate inelastic neutron spectra and cross sections. The experimental results were compared with ENDF/B-VI, BROND-2, JENDL-3 neutron data libraries.

On the Contradiction Between Microscopic and Macroscopic Data for ^{235}U Fission Neutron Spectrum at Thermal Energy

N.V. Kornilov, A.B. Kagalenko, K.I.Zolotarev

The ^{235}U is a most important nucleus for practical applications. So this explain a particular interest to measurement and evaluation of the ^{235}U neutron data. The prompt fission neutron spectrum (PFNS) for ^{235}U at thermal point have been investigated in many works, but some problems still exist. The PFNS may be investigated in a several kind of the experiments. The direct information is extracted from microscopic experiment in which the spectrum shape is measured at fixed neutron incident energy. The detector efficiency is the only function which required for spectrum shape estimation from these experiments. The average cross section measured in integral experiment also may be used for PFNS evaluation. However, in this case one should know not only the reaction cross section but the real shape of the spectrum exposed the investigated sample. In benchmark experiments the reaction rates are measuring in various type of the reactors and critical assemblies. The difference between experimental and calculated results (if it exists) may be applied for PFNS correction. However, the final result will depend very much on the neutron data accuracy and the accuracy of the codes and model that were used for these calculations.

All recent ^{235}U PFNS evaluations ([1-3]) were based on the experimental data however, they give very different spectrum shape (>15%) and different average energy of the fission neutrons 1.964±0.019MeV [1], 2.027MeV [2], 2.033MeV[3], In paper [1], we used only microscopic data for PFNS evaluation. The authors of [2] took into account all set of data: microscopic, integral and benchmark data to find the parameters of the Watt distribution. As a result, the low energy part of the spectrum was mainly based on the microscopic data but the PFNS shape in the high energy region was constructed to describe the average cross sections and benchmark experiments [4]. It seems that the parameters of the Madland-Nix model [3] were also adjusted to compromise the microscopic and integral data.

The low average energy 1.97±0.02MeV was reported in many experimental works. The authors [2] pointed out this value however, they were obliged to increase to ~3% the average energy to describe the results of integral experiments and benchmark data. They concluded that may exist another sources of the discrepancy, however the large uncertainties for the microscopic PFNS at high energy allowed them to correct neutron spectrum and include such data in ABBN-93 [5].

In this report it was shown that already existing microscopic experimental data for spectrum of the ^{235}U prompt fission neutron at thermal point allow us to estimate the spectrum shape with high accuracy. The average neutron energy calculated on the basis of experimental data 1.977±0.008MeV contradicts to values from ENDF/B-VI and ABBN-93 libraries. It was emphasized that the "old" contradiction between microscopic and macroscopic experimental data is not solved till now.

References

1. Kornilov N.V., Kagalenko A.B., Hamsch F.-J., J. Nucl. Phys. in press.
2. Khomjakov Yu. S., et al VANT(Nuclear data), 1992,1,70.
3. Madland D.G, Nix J.R., Nucl. Sci. Eng. 1982. V.81. P.213.
4. Zvonarev A.V., et al. VANT(Nuclear Data), 1990,3,67.
5. Manturov L.N., Nikolaev M.N., Tzibula A.M., VANT(Nuclear data), 1996, 1.

Evaluation of Non-Rutherford Proton Elastic Scattering Cross Section for Silicon

A.F.Gurbich

The Ion Beam Analysis techniques that deduce the information about the composition and the structure of the sample by comparing a simulated spectrum of detected ions to the measured spectrum become more and more widespread. In distinct of relative measurements using standard reference samples the methods, which are based on the computer simulation, strongly rely on the available absolute cross section data.

The evaluation of the proton elastic scattering cross sections for silicon was made in the framework of the approach previously described [1,2]. Briefly it consists in parameterisation of the available experimental data using the theoretical model which involves relevant physics. The interaction between the proton and the target nucleus is represented, in the center of mass of the equivalent single particle problem, by an optical model potential. The compound nucleus levels contribution is taken into account by addition of Breit-Wigner resonances to the optical amplitude. The model parameters are adjusted using the experimental information taken from different sources. Once the optimal in a statistical sense set of model parameters is obtained, the required excitation functions for analytical purposes may be calculated for any scattering angle.

The cross section for natural silicon was calculated as a sum of the cross sections for its three stable isotopes weighted by the relative abundance. The resonance parameters for compound ^{29}P nucleus were fixed at the values taken from [12]. Three strong resonances mainly influence the cross section in the energy range under consideration. Resonances at proton energies of E_p=1.66 MeV ($1/2^-$) and E_p=2.88 MeV ($3/2^-$) in the p+^{28}Si system are known [3,5] to have a single particle configuration. Therefore these resonances were not explicitly included in the calculations being reproduced by potential scattering. In addition to the strong resonance at E_p=2.085 MeV the width of which is Γ=15.6 keV [12] the resonances located up to 4 MeV were included in order to take account of the influence of their tails. The optimization procedure was the same as specified in [1]. Relatively narrow resonances are only observed for proton scattering from ^{29}Si and ^{30}Si in the energy range under investigation. These resonances are too weak to remarkably affect the cross section for natural silicon. So resonance scattering was neglected for the minor isotopes of silicon. The contribution of these isotopes was taken into account using a standard optical model with global parameters [13]. The following changes were only made. The imaginary potential was discarded and the real well depth of the central potential was adjusted by fitting to the experimental data taken from Refs. [14,15] and [16] for ^{29}Si (V_R=65.3 MeV) and ^{30}Si (V_R=65.7 MeV) respectively.

The evaluated theoretical curves $d\sigma(E)/d\Omega$ for the elastic proton scattering from natural silicon along with available experimental data are shown in Fig.1 for three scattering angles. As is seen from the figures the theoretical curves are in a fair agreement with the experimental data in the energy region greater than approximately 1.5 MeV. It is worth noting that the contribution of the minor silicon isotopes to the total cross section is significant when ^{28}Si cross section is far from the Rutherford value. For instance, the ^{29}Si and ^{30}Si isotopes give in sum about a half of the observed cross section for 170° excitation function at the center of the broad dip near 2.8 MeV.

At energy lower than ~1.5 MeV the theory predicts higher cross sections for the 150° and 170° scattering angles as compared with the data from Ref.[10]. The most prominent

discrepancy (up to factor 1.5) is observed for 110° scattering angle at energies lower than ~1.2 MeV. Unfortunately the only experimental data set [10] is available in this case. The discrepancy has been thoroughly studied but no reasons for such a deviation of the cross section from Rutherford one was found in the present analysis. It is up to a potential user to decide whether to rely upon the measured or on the evaluated data.

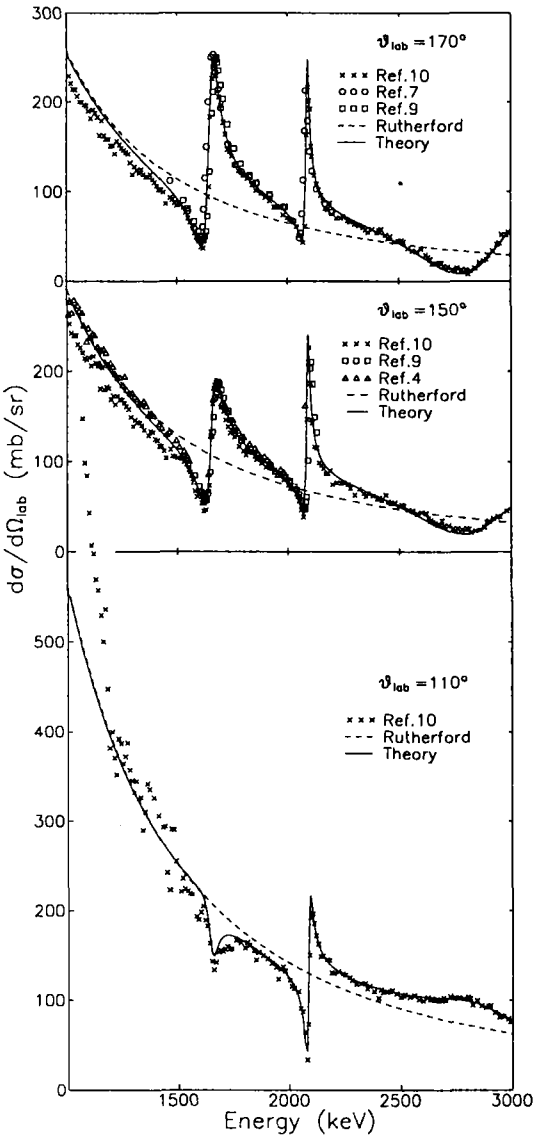

Fig.1. The evaluated differential cross sections and the available experimental data for proton elastic scattering from silicon.

References

1. A.F. Gurbich, Nucl. Instr. and Meth. B 129 (1997) 311.
2. A.F. Gurbich, Nucl. Instr. and Meth. B136-138 (1998) 60.
3. A.K. Valter, I.I. Malakhov, P.V. Sorokin, A.I. Taranov, Izvest. Akad. Nauk S.S.S.R. Ser. Fiz. 22 (1958) 871.
4. S. Rubin, L.E. Bailey, T.O.Passel, Phys. Rev. 114 (1959) 1110.
5. J. Vorona, J.W. Olness, W. Haeberli, H.W. Lewis, Phys. Rev. 116 (1959) 1563.
6. T.A. Belote, E. Kashy, J.R. Risser, Phys. Rev. 122 (1961) 920.
7. E.Rauhala, Nucl. Instr. and Meth. B 12 (1985) 447.
8. J. Liu, T. Xie, H.J.Fischbeck, Nucl. Instr. and Meth. B 79 (1993) 468.
9. R.Salomonovič, Nucl. Instr. and Meth. B 82 (1993) 1.
10. R.Amirikas, D.N.Jamieson, S.P.Dooley, Nucl. Instr. and Meth. B 77 (1993) 110.
11. P.M. Endt, Nucl. Phys. A 521 (1990) 294.
12. F.G. Perey, Phys. Rev. 131 (1963) 745.
13. A.N. Lvov, A.I. Popov, P.V. Sorokin, V.E. Storizhko, Izvest. Akad. Nauk S.S.S.R. Ser. Fiz. 30 (1966) 439.
14. R.O. Nelson, E.G. Bilpuch, C.R. Westerfeldt, Phys. Rev. C 27 (1983) 930.
15. A.K. Valter, A.I. Popov, V.E. Storizhko, J. Exp. Theor. Phys. 43 (1962) 2038.

Benchmarking of Evaluated Neutron Data for Vanadium by a 14 Mev Spherical Shell Transmission Experiment

S.P. Simakov, B.V. Devkin, B.I. Fursov, M.G. Kobozev, V.A.Talalaev, U. von Möllendorff[1], M.M. Potapenko[2]

[1]*Forschungszentrum Karlsruhe, Institut für Neutronenphysik und Reaktortechnik, Karlsruhe, Germany*
[2]*Institute of Inorganic Materials, Moscow, Russia*

Vanadium-based alloys are interesting, in several respects, as potential structural materials for fusion reactors. From the point of view of neutronics, one of the interesting features is a possible superior neutron economy, i.e., a favourable balance between absorption by (n,x) reactions and multiplication by (n,2n) reactions. According to calculations using evaluated nuclear data for vanadium from the EFF-1 file, vanadium as structural material instead of steel may open the possibility of attaining a sufficient tritium breeding ratio in the blanket of a DEMO-like reactor without requiring a specific neutron multiplier such as beryllium or lead, resulting in considerable engineering and economic advantages. This is not possible in a blanket having steel structures. For a reliable assessment of vanadium in this respect, its evaluated nuclear data should be verified, 'benchmarked', by integral experiments, i.e., experiments on thick samples. A very suitable type of experiment consists in measuring the spectral leakage flux from spherical shells with a central neutron source.

In the experiment reported here, two spherical shells having wall thickness of 3.5 cm (0.6 λ) and 10.5 cm (1.8 λ) were used. The present experiment was performed in collaboration between IPPE Obninsk and Forschungszentrum Karlsruhe. It appears to be the first integral fast-neutron experiment ever performed on vanadium. Similar experiments on vanadium are being performed at Japan Atomic Energy Research Institute, and at the Technical University of Dresden.

Measurements of neutron leakage spectra from two shells of pure with a 14 MeV neutron source at the center have been performed at 14 MeV pulsed neutron generator of IPPE. The neutron leakage spectra were measured by the time-of-flight method from 15 MeV down to 50 keV. Descriptions of the experimental arrangement, the time-of-flight spectrometer, the measurements and data reduction procedures are given. Corrections connected with neutron multiple scattering in the neutron source, deviations from spherical symmetry and others were estimated by the Monte-Carlo technique. Also, the response function of the spectrometer was determined and folded with the calculated spectra to allow meaningful calculation-experiment comparisons even near the 14 MeV peak. As an example the experimental data are shown in Fig. 1 for the case of vanadium shell #2.

Three-dimensional Monte-Carlo calculations were made with the MCNP code, using the EFF-3, FENDL-1 and JENDL-FF nuclear data libraries. The total leakage fluence is correctly predicted or slightly overestimated by all these evaluated data. However, its breakdown into energy bins (Fig. 1) shows considerable overestimation near 0.1 MeV for FENDL-1 and JENDL-FF and near 10 MeV for JENDL-FF, while EFF-3 on the whole reproduces the leakage spectra best. An analysis of existing differential experimental V(n,xn) data at 14 MeV incident energy agrees with these findings.

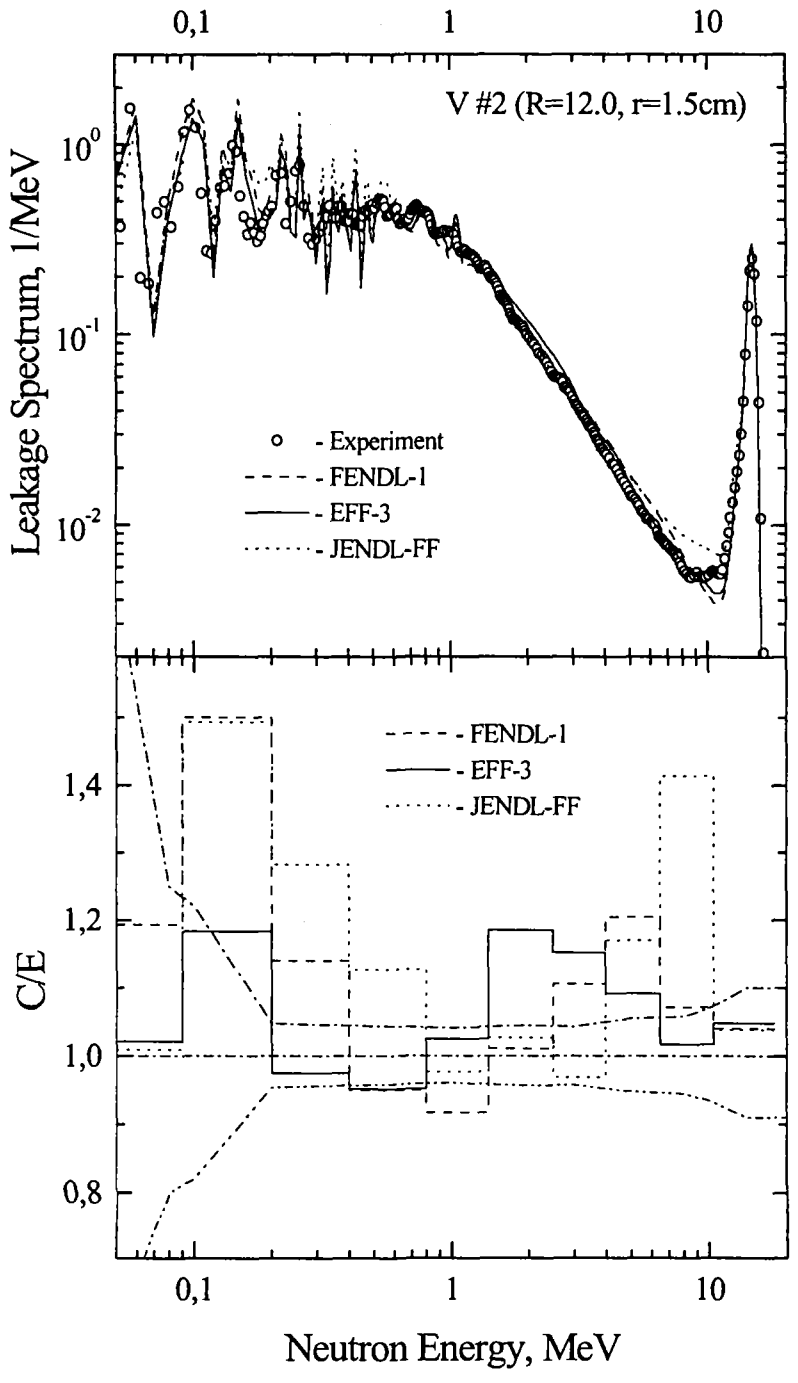

Fig. 1. Comparison of experimental and calculated neutron leakage spectra (top) and ratio C/E (bottom) for vanadium sphere #2. Dash-dotted curve denotes the experimental uncertainty corridor.

Benchmarking of Evaluated Neutron Data for Nickel By 14-MeV Spherical Shell Transmission Experiments

S.P. Simakov, B.V. Devkin, M.G. Kobozev, U. von Möllendorff[1], D.Yu. Chuvilin[2]

[1]Forschungszentrum Karlsruhe, Institut für Neutronenphysik und Reaktortechnik, Karlsruhe, Germany;
[2]Kurchatov Institute of Atomic Energy, Moscow, Russia

Nickel is an important constituent of stainless steels and other alloys used, e.g., as structural and shielding materials in fusion technology. While the low-activation materials being presently developed for fusion power reactors will be free of nickel, the validation of evaluated nuclear data for nickel is still important in view of near-term applications. Such validation or benchmarking should be done by integral experiments, i.e., involving thick layers of the material, in order to be close to the application case.

Several laboratories have measured the spectral neutron leakage fluence from nickel spheres by different techniques. In 1992, our group at Obninsk measured the neutron leakage spectrum from a metallic nickel shell with 7.5 cm wall thickness [1] by the time-of-flight (TOF) technique. Using the same shell, measurements of the neutron leakage spectrum have been made also at Kiev University [2] by the same technique and at the Institute of Dosimetry, Prague [3], by the scintillator pulse height unfolding technique. For a larger sphere having 14.5 cm wall thickness, the leakage spectrum has been measured by the TOF method at the OKTAVIAN facility of Osaka University [4].

The results of our transmission experiment on a spherical nickel shell of 7.5 cm wall thickness with a 14 MeV neutron point source at the center are shown in Fig.1 in comparison with three-dimensional Monte Carlo calculations using data from the libraries FENDL-1, EFF-2.4 and JENDL-FF. It is seen that the FENDL-1 library predicts the neutron leakage from nickel with better accuracy than the others, but some improvements are still needed.

The comparisons with the data of the other groups have shown that there is discrepancies which sometimes exceed the experimental uncertainties ascribed. This make it difficult to derive conclusions on the reliability of the nickel evaluated if we taking into account all available experimental data sets.

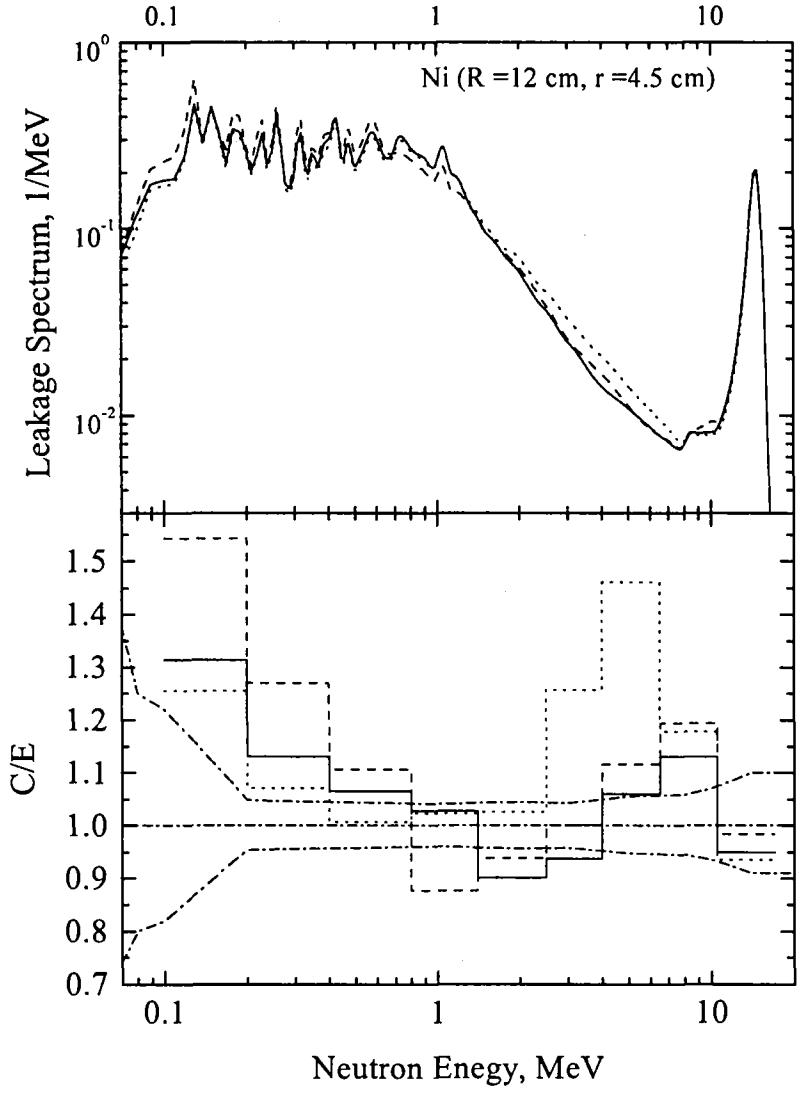

Fig. 1. Comparison of experimental and calculated neutron leakage spectra (top) and ratio C/E (bottom) for nickel sphere. Points – experiment. Solid curve - Monte Carlo calculation with FENDL-1, dashed - JENDL-FF, dotted - EFF-2.4. The dashed-dotted curve shows the corridor of estimated experimental uncertainties.

Reference

1. S.P. Simakov, A.A. Androsenko et al., in: *Fusion Technology 1992,* C. Ferro et al. (eds.), Elsevier (1995) p. 1489; B.V. Devkin, V.G. Demenkov et al., report INDC(CCP)-378, International Atomic Energy Agency, Vienna (1994)
2. Yu. N. Onishchuk, B. E. Leshchenko et al., *Conference Proceedings* **59** (1997), p. 1212, G. Reffo et al. (eds.), Editrice Compositori, Bologna
3. D. Yu. Chuvilin, Doctor Thesis, Kurchatov Institute, Moscow (1992)
4. T. Kasahara, H. Hashikura et al., report OKTAVIAN A-84-04, Osaka University (1984)

Neutron Leakage Spectra from Iron Spheres with ^{252}Cf Neutron Source

B.V. Devkin, M.G. Kobozev, S.P. Simakov, V.V. Sinitsa, V.A. Talalaev, U. Fischer[1], U. von Möllendorff[1]

[1]*Forschungszentrum Karlsruhe, Institut für Neutronenphysik und Reaktortechnik, Karlsruhe, Germany*

Testing of neutron data in spherical benchmarks is considered as important step on the way of validation of evaluate data libraries. Traditionally scintillation detectors and pulse height technique was used for neutron spectroscopy in the benchmarks with ^{252}Cf source [1]. In 1988 we have proposed and tested the time of flight method for the spectroscopy of the neutrons leaking from the spheres with ^{252}Cf source in the center [2]. The source was a fast ionzation fission chamber. The advantage of this technique is that neutron leakage spectra and efficiency are measured simultaneously in the one experiment (Cf in the sphere and bare source, respectively). In the present work we report the results of the measurements and comparison with transport calculations for five iron spheres, the parameters of which are listed in the Table 1.

Table 1. Parameters of iron spheres.

Sphere No.	Sphere Radius, cm		Wall thickness		Hole diameter, cm	Weight kg
	outer	inner	cm	λ		
1	4.5	2.0	2.5	0.6	2.0	2.4
2	12.0	4.5	7.5	1.7	3.0-3.2	50.9
3	12.0	2.0	10.0	2.3	2.0-3.2	53.3
4	20.0	1.9	18.1	4.2	1.9-2.5	258.0
5	30.0	2.0	28.0	6.4	2.0-4.0	874.0

Transport calculations have been made with one-dimensional code ANISN and three-dimensional - MCNP 4.a, data files being taken from the BROND-2, FENDL-1, ENDF-B6, JENDL-3. The MCNP code was used as well for estimation of the specific corrections. For example, the effect connected with the employing of the time of flight method in the experiment. These results to the shifting of the resonance like structure in the experimental spectrum to the lower energy, because of the time delay of the scattered neutrons in the shell. Fig. 1 demonstrates this effect for the case of thickest sphere #5, where time independent and time-dependent (neutron time of arrival spectrum was converted to energy one) Monte Carlo calculations are shown.

The comparison of transport calculation with experimental data did not indicate any significant discrepancies except for the case of the shell #5.

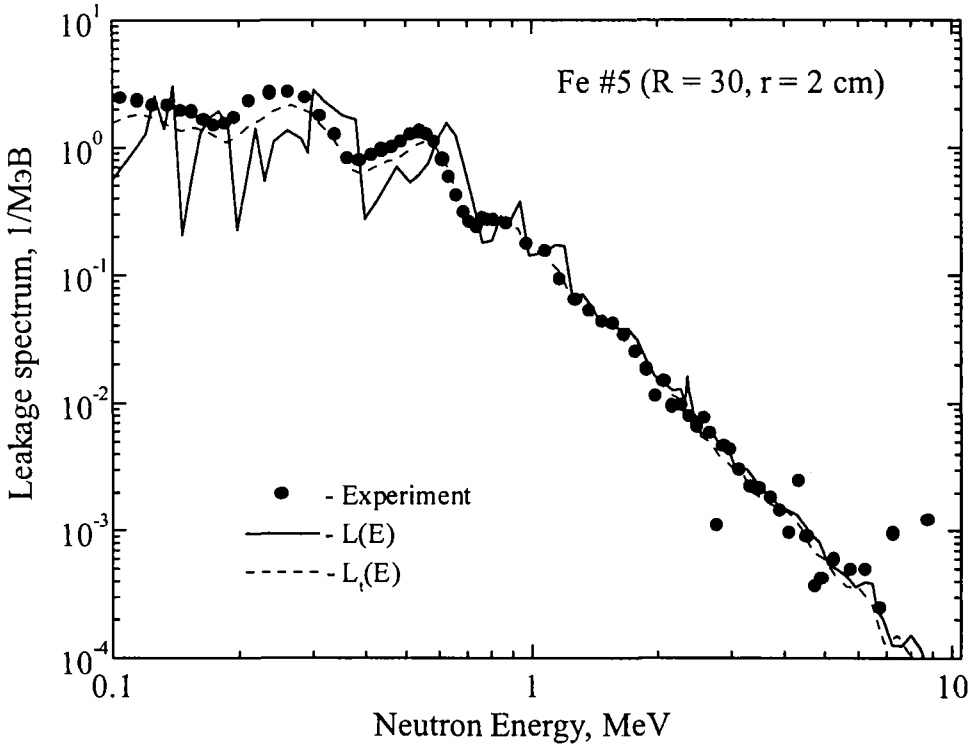

Fig. 1. Neutron leakage spectrum for Fe shell #5. Points – experiment, solid curve –time-independent calculation MCNP4.a/FENDL-1, dashed – the same, but time-dependent.

References

1. В.И. Горячев, Ю.И. Колеватов и др. Интегральные эксперименты в в проблеме переноса ионизирующих излучений. М.: Энергоатомиздат, 1985
2. S.P. Simakov et al. Report ZFK-646, Dresden, 1988, p. 111

2.4 TRANSMUTATION

Calculations of Isotopic Composition, Residual Heat and Helium Content of Spent Amox Fuel (Americium Containing Fuel) of BOR-60 Reactor

E.V.Gai, A.E.Ivanov, A.L.Kochetkov, N.S.Rabotnov

Summary

As a stage in preparations for "RECYCLE" experiment on BOR-60 fast reactor calculations were made of isotope inventory, residual heat and helium content of AMOX fuel during the campaign and for cooling times up to 180 years (ten periods of Cm-244).

Following assumptions were made on the fuel composition:

1. Basic fuel element is 75% enriched uranium.

2. 20 or 50 per cent mass are added of Am-Cm fraction extracted from reprocessed SNF of VVER-1000 reactor with initial enrichment of 4.4% and burnup of 40 GW days/t cooled for ten years. Basic components of the fraction are (per cent): Am-241 - 83.746; Am-242m - 0.101; Am-243 -13.163; Cm-242 - 2.46E-04; Cm-243 - 0.029; Cm-244 - 2.731; Cm-245 - 0.227; Cm-246 - 3.59E-03; Cm247 - 6.31E-05; Cm248 - 6.25E-06.

3. This fraction contains the admixture of 10 per cent mass of lantanides unseparated from americium and curium.

4. Following chemical forms were assumed for the actinides: UO_2, Am_2O_3 and Cm_2O_3.

Similar calculations were also made for standard MOX fuel of BOR-60 with Am-Cm added in the same proportions. The results may be outlined as follows.

If Am is added to standard fuel, 21% of Am-241 and 13% of Am-243 are transmuted during the campaign. As compared to the case of pure standard MOX-SNF piling up of Cm isotopes increases thousands of times, Pu-238 and Pu-242 dozens and hundreds of times, helium production hundreds of times.

There is no Pu in AMOX fuel based on 75% U, so there are considerable quantitative differences: Am transmutation rate is about 16.5% per campaign, the mass of accumulated Cm is about 13% of the mass of transmuted Am, the mass of accumulated Pu - 45% for initial Am-Cm concentration of 20% and 35% for initial Am-Cm concentration of 50%. Accumulated Pu consists almost entirely of non-fissioning isotopes. Total accumulation of helium may be as high as 1 kg/thm and helium pressure in fuel pin plenum may reach dozens of MPa.

The residual heat (RH) was at first calculated only for long cooling times in 3-180 years interval for both actinides and fission products as components of SNF. But the fact that actinides contribution in all this interval was much higher than that of the FPs indicated the necessity to extend the calculations into shorter cooling times, from one hour to one year. According to the results, RH of the actinides makes even with RH of FPs in three days after shutdown for 20% of Am-Cm and in three hours for 50% of Am-Cm (or uranium fuel it happens in dozens of years). And absolute value of the total RH stays above 1 MW/t for about a month with important consequences for both planned and emergency cooling after shutdown.

No single satisfactory numerical criterion of the efficiency of MA transmutation was proposed up to now, so various parameters influencing the efficiency are discussed for the case analyzed: M - total transmuted mass; m- total burned mass (turned into FPs); c_i - isotopic concentrations of the actinides, including heavier MA produced by neutron absorption both on transmuted isotopes and on fuel matrix fissionable and fertile components; n - total number of neutrons absorbed by the actinides; E - total energy release; in-core life-time and cooling time before reprocessing. If the mass of re-accumulated MA and even isotopes of U and Pu is subtracted from the transmuted mass, the balance is negative for 20% of Am-Cm case and positive for 50% of Cm-Am case.

Potentials of Molten Tin as a Coolant for Electronuclear Systems

G.L. Khorasanov, A.P. Ivanov, and A.L. Shimkevich

One of the first proposals to use liquid tin for nuclear power facility was done by J.R.Weeks in 1971 /1/. He considered melts of natural tin and its eutectic alloys, Bi-Sn, Pb-Sn, and Bi-Pb-Sn as potential coolants for fast reactors. The attractive features of tin such as high boiling point ($T_{boil.}$ = 2270 °C), low vapor pressure (~ 100 Pa for 800 °C), and low melting point ($T_{melt.}$ = 231.9 °C), were mentioned. Meanwhile it was noted that molten tin is one of the agressive liquid metals. It interacts with steel to form $FeSn_2$. So Cr, Mo, W or Ti as potentially satisfactory structural materials appear to be used for high temperatures. Later Zr alloys were also considered to be a compatible material with liquid tin.

The next proposal to use molten tin in fast reactors was done by L.Qian in 1992 /2/. He analyzed the possibility for changing sodium by tin coolant to increase the safety of minor actinides burner. The share of delayed neutrons in a core with liquid tin can be increased in doping a small amount of Pu and diluted U. This is impossible in the core with liquid sodium due to the void effect of reactivity. In general, it was shown that tin is a promising alternative for sodium, and its using essentially improves fast reactor safety properties.

The first proposal to use liquid tin in electronuclear systems was done by G.L.Khorasanov et al in 1996 /3-5/. It is known that the neutron yield from a tin target-converter irradiated with 100–400 MeV protons is slightly less than the one of the lead target. This fact requires an increase of accelerator power to provide the necessary intensity of neutrons, 10^{18}–10^{19} neutron/s, for full-scale electronuclear systems. Meanwhile, the use of Sn instead of Pb or Bi-Pb can sufficiently improve thermal and physical and ecological characteristics of target assembly.

In comparing liquid tin and liquid lead characteristics, one can conclude the following.

- The low melting point of tin in comparison with lead allows the inlet temperature of a coolant to decrease.
- Due to the higher boiling point of tin, the operation range of temperatures for tin coolant, $\Delta T = T_{boil} - T_{melt}$, is wider than the one for lead coolant.
- Requirements to liquid tin circulation are easier than that to liquid lead in systems with positive motion.
- Consideration of thermal and physical properties (such as heat conductivity, heat capacity, dynamic viscosity, and etc.) gives also some advantage for tin over lead.
- Due to the mentioned thermal and physical properties of tin, it is possible very effective heat removal up to 1 GW/m^3. In this case, the required coolant temperature is of order 400–600 °C and coolant flow velocity is about 2 – 4 m/s.
- The estimated radioactivity of tin as well as bismuth-lead is high enough after irradiation with 400 MeV proton flux of $5 \cdot 10^{13}$ proton/cm^2·s during 1 year. It requires a cooling time of several thousand years to decrease target activities to the acceptable hands-on level, which is about 10^8 Bq/kg for beta-active nuclides /6/.
- A completed absence of alpha-active nuclides (Po-210, Pb-202) in the radioactive wastes of tin makes it less radiotoxic material than lead or bismuth-lead.

- Tin target may also compete with lead target as an effective proton-to-neutron converter; to enhance the neutron yield heavy tin isotope, Sn-124 (6 percent in the natural mixture), must be used. It was calculated that neutron yields Pb-208, Hg-204, and Sn-124 differ less than 15 percent.
- As concerned the compatibility of liquid tin with steels it must be noted that an increased oxygen content in a heat transfer system with liquid metal coolant causes the intensive corrosion of structural materials. The scale of oxygen effect on steel corrosion is defined not by oxygen mass concentration in liquid metal but a level of its oxidation potential in saturation on oxygen. For example, the corrosion in sodium is less than the one in lead at equal oxygen mass content in them and all other things as temperature, hydrodynamics, surface state of structural materials. One can assume that liquid tin intervening sodium and lead on the oxidation potential in saturation state is to be characterized by temperate oxygen-dependent corrosion activity in comparison with lead and eutectic alloy of bismuth-lead. In this case, one can do away with classic technology for oxygen passivation of structural materials and recommend a development of oxygen-less coolant technology as for sodium /7/.

Thus, the cited arguments and estimation permit tin to be considered as a target-converter material in beam-reactor systems. The use of molten tin can improve thermal and physics, safety, and ecology of an electronuclear system at increasing a price of 15–30 percent beam power.

Outstanding calculations of Dr. A.Yu.Konobeyev are gratefully acknowledged. Research performed in part is supported by the Russian Foundation for Basic Research, grant # 98-02017398.

References

1. J.R.Weeks. Lead, Bismuth, Tin and Their Alloys as Nuclear Coolants. / Nuclear Engineering and Design, v. 15, p. 363-372 (1971).
2. L. Qian et al. / In: Proc. of Int. Conf. on Advanced Nuclear Power Plants, Oct. 25-27, 1992, Tokyo, Japan, v. I, p. P3.2-1 – P3.2-7 (1992).
3. G.L.Khorasanov et al. Melted Tin Target-Converter for a Proton Accelerator-Based Neutron Generator. / In: Proc. of the 8th Int. Conf. on Emerging Nuclear Energy Systems, ICENES'96, June 24-28, 1996, Obninsk, Russia, v. II, p. 603-610 (1996).
4. A.N.Didenko et al. External Neutron Generator for Safe Nuclear Power Plant and Nuclear Wastes Transmutation Facilities. / In: Proc. of Int. Conf. on Future Nuclear Systems, GLOBAL'97, Oct. 5-10, 1997, Yokohama, Japan, v. II, p. 1355-1359 (1997).
5. G.L.Khorasanov et al. Accelerator-Driven Subcritical Fast Reactors for Closing the Nuclear Fuel Cycle. / In: Proc. of the 9th Int. Conf. on Emerging Nuclear Energy Systems, ICENES'98, June 28 – Iuly 2, 1998, Tel-Aviv, Israel, v. 1, p. 227 – 234 (1998).
6. IAEA–TECDOC-885. Clearence Levels for Radionuclides in Solid Materials, Vienna (1996).
7. A.L. Shimkevich. Author's Summary of D.Sc. Thesis «Principles for Fluctuation Theory of Inhomogeneous Melts», Moscow: RAS' Institute of High Temperatures (1997).

Lead Coolant for Fast Reactor-Burner with Hard Neutron Spectrum

G.L.Khorasanov, A.P.Ivanov, V.V.Korobeinikov, A.I.Blokhin, and A.L.Shimkevich

The incineration of long-lived radiotoxic minor actinides (MA) is one of the important problems in the development of the future nuclear power engineering. Potentials of fast reactor for burning Np-237, Pu-240, Pu-242, and Am-243 fissile preferentially under hard neutron spectrum are well known. Our main concern is with ways for further hardening of conventional fast reactor neutron spectra.

The use of coolants with low moderating properties is one of the ways to get the hard neutron spectrum in the fast reactor. In this paper, the stable lead isotope, Pb-208, which 52.3 percent are contained in natural lead of, is proposed as the one of such coolants. The neutron inelastic scattering cross-section of Pb-208 is 3-3.5 times less than the one for other lead isotopes. These data are taken from JENDL-3.2 library /1/ and given in Table 1.

Table 1. Neutron inelastic scattering cross-sections of natural lead and his stable isotopes, averaged up on fission neutron spectrum, barns.

Nuclide	Pb-204	Pb-206	Pb-207	Pb-208	Pb-nat
Cross-section, σ_{in}	1.325	1.316	1.265	0.361	0.804

Calculation of the MA transmutation rates in the fast reactor with different coolants is performed with Monte Carlo code MMKFK /2/. The analysis of obtained results for the blanket containing neptunium and americium and having thickness of 50 cm was carried out. The composition of this blanket is listed in Table 2.

Table 2. The composition of the blanket including (MA + coolant), nuclides·10^{-24}/cm^3.

Nuclide	Model 1 (Np+Na)	Model 2 (Np+Pb-nat)	Model 3 (Np+Pb-208)	Model 4 (Am+Na)	Model 5 (Am+Pb-nat)	Model 6 Am+Pb-208)
Np-237	0.00126	0.00126	0.00126	0.0	0.0	0.0
Am-241	0.0	0.0	0.0	0.00114	0.00114	0.00114
Am-243	0.0	0.0	0.0	0.00040	0.00040	0.00040
O	0.00252	0.00252	0.00252	0.00236	0.00236	0.00236
Na	0.01030	0.0	0.0	0.01030	0.0	0.0
Pb-nat	0.0	0.01430	0.0	0.0	0.01430	0.0
Pb-208	0.0	0.0	0.01430	0.0	0.0	0.01430

For all the models, the composition of structural materials is the same. Nuclear concentration values for structural materials used in homogeneous blanket are listed in Table 3.

Table 3. The nuclear concentration of structural materials in homogeneous blanket model, nuclides·10^{-24}/cm^3.

Nuclide	Model 1-6
Fe	0.014
Cr	0.00308
Ni	0.00168
Mo	0.000242
Mn	0.000164
Zr	0.00216
C	0.00216

The obtained results are given in Table 4.

Table 4. The portion of fission in cross-section of neutron capture and fission for neptunium and americium in the fast reactor blanket with different coolants, $\sigma_{fis}/(\sigma_{fis}+\sigma_{cap})$.

MA	Na coolant	Pb-nat coolant	Pb-208 coolant
Np-237	0.2000	0.2100	0.2650
Am-241	0.1770	0.1750	0.2150
Am-243	0.2170	0.2260	0.2800

As follows from Table 4, the fast reactor with natural lead coolant practically does not differ of the reactor with sodium coolant in terms of their ability to MA incineration. The use of Pb-208 in the fast reactor results in increasing that to incinerate MA of 20–30 percent in comparison with a conventional fast reactor. This fact has to be taken into account for using the lead coolant.

References

1. JEF Report 14.Table of Simple Integral Cross Section Data from JEF -2.2, ENDF/B-VI, JENDL-3.2, BROND-2 and CENDL-2, Paris, NEA (1994).
2. L.B. Kazakova et al. In Proceedings of the 7th Topical Meeting on Monte Carlo Methods, Novosibirsk, Russia (1985).

Lead and Tin Targets for Reducing Polonium Waste

G.L.Khorasanov, A.P.Ivanov, A.I.Blokhin, and A.L.Shimkevich

Polonium isotope, Po-210, and lead isotope, Pb-210, are the most toxic alpha-active nuclides resulted of nuclear reactions for natural lead and bismuth as target materials in ADTT. A calculation shows that activity of Po-210 produced in lead reaches the value of 10^{11} Bq/kg after the irradiation during 30 years, and it decays to the clearance level of 10^{4} Bq/kg by cooling time of 100 years. In order to reduce accumulation of Po-210, and Pb-210, a new forthcoming technique of isotopic tailoring is proposed to use. It is calculated that the activity of Po-210 arising from stable lead isotope, Pb-207, decreases to the value of 10^{9} Bq/kg under the same irradiation conditions as from Pb-natural. In the case of Pb-207, the irradiation cooling time of 7 to 8 years only is required to reach the clearance level. These calculations were carried out in using FISPACT-3 code and FENDL-2 library for typical fast reactor neutron spectrum and neutron flux of $5 \cdot 10^{15}$ n/cm^2/s.

As opposed to projects providing for target of heavy metals, we also consider liquid tin target that is lighter and has better thermal, physical, and ecological properties than lead or bismuth. A complete absence of alpha-active nuclides, high boiling point, wide operation temperature range gives some advantages for tin over lead. Tin target can compete with lead target as an effective proton-to-neutron converter. In order to enhance the neutron yield, heavy tin isotope of Sn-124 is to be used. The calculation performed with DISCA code shows that the neutron yield of Sn-124 is 15 % less than the one of Pb-natural for protons with the energy of 400 to 800 MeV.

From this data lead enriched by isotope, Pb-207, and tin enriched by isotope, Sn-124, can be considered as an effective target-converter materials for reducing toxic alpha-active wastes such Po-210, Pb-210.

Comparative Analysis of Ionic and Hydrophobic Hydration Effects

A.G.Novikov, M.N.Rodnikova and O.V.Sobolev*

* *Kurnakov Institute of General and Inorganic Chemistry, Russian Academy of Sciences, 117907, Moscow, Russia*

Neutron scattering experiments on LiCl, CsCl, $[CH_3]_4NCl$ (2M) and $[C_4H_9]_4NCl$ (1M) aqueous solutions curried out by our group in last years and the analysis of these experiments allow us to perform the comparison of the effects of ionic and hydrophobic hydration on the molecular level. Experiments and data handling methods were described in our previous papers [1-4].

The GFD of pure water molecules and GFDs of water molecules comprising the hydration shells of Cs^+, Li^+ and Bu_4N^+ ions are shown in Fig.1. Although Li^+ and Cs^+ ions belong to different types of ionic hydration (positive and negative), as it follows from presented data, both of these ions lead to H-B network disruption in the hydration shell. That is evidenced by decreasing of the weight of the fist translation mode (the most low-frequency one) corresponding to deformation of tetrahedral angle O-O-O, which is usually regarded as the evidence of the H-B network existence [5]. The primary water structure distortion in the vicinity of the dissolved ion is also witnessed by libration bands shift to the low frequency, which is more obvious in the case of Cs^+ ion and weaker in the case of Li^+.

The Bu_4N^+ ion affects molecules GFD of their hydration shell differently from ions mentioned above. It follows from Fig.1c there is no any significant changes in the low-frequency part of spectra. This fact is indicative of persistence of H-B network existing in pure water in the vicinity of large hydrophobic particle. In our opinion, this result directly correlates with the results of neutron diffraction investigations on water structure in hydration spheres of thetraalkilammonium ions [6-9]. There was shown clearly the absence of significant influence of these ions (at least, up to and including Bu_4N^+) on hydration water molecular structure, which appears as practically indistinguishable from pure water. As it was pronounced repeatedly earlier, the reason of such result is the structural features of these ions, which allow them to enter into inherent tetrahedral water structure without its distortion. The geometrical model of such structural organization for Me_4N^+ was formulated [8].

It should be noted that the study of hydrophobic effects by Raman scattering and infrared adsorption also did not show the remarkable growth of intermolecular interactions and space coordination of H-B network in hydration water surrounding the hydrophobic particles [10].

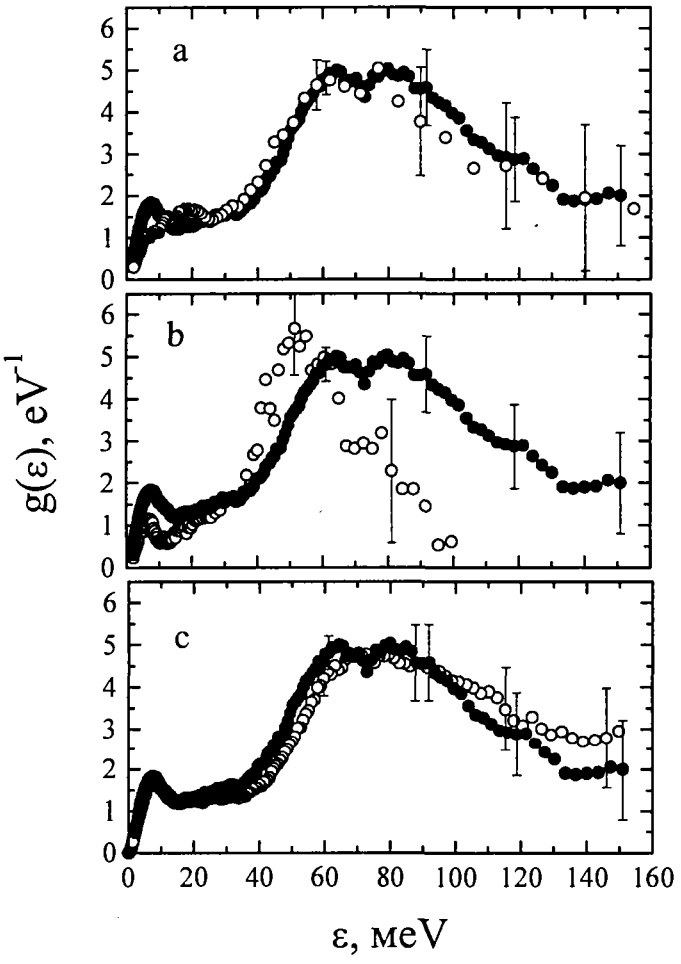

Fig.1 Generalized frequency distributions of water molecules. Solid circles – pure water, open circles – hydration water: (a) - Li^+ ion; (b) - Cs^+ ion; (c) – TBA^+ ion.

References

1. A.G.Novikov, M.N.Rodnikova, V.V.Savostin, O.V.Sobolev. Rus. J. Phys. Chem. 70, 1011, (1996).
2. A.G.Novikov, M.N.Rodnikova, V.V.Savostin, O.V.Sobolev. Chem. Phys. Letters. 259, 391, (1996)
3. A.G.Novikov, M.N.Rodnikova, V.V.Savostin, O.V.Sobolev. Physica B. 234-236, 340, (1997).
4. A.G.Novikov, M.N.Rodnikova, V.V.Savostin, O.V.Sobolev. Rus. J. Inorg. Chem. 42, 1428, (1997).
5. M.Seats, S.Rice. J. Chem. Phys. 72, 3236, (1980).
6. J.Turner, A.Soper, J.Finney. Mol. Phys. 70, 679, (1990).
7. J.Turner, A.Soper, J.Finney. Mol. Phys. 77, 411, (1992).
8. J.Turner, A.Soper. J.Chem. Phys. 101, 6116, (1994).
9. J.Turner, A.Soper, J.Finney. J. Chem. Phys. 102, 5438, (1995).
10. Z.Kecki, P.Dryjnski. J. Mol.Structure. 275, 135, (1992)

Some Structural and Dynamical Properties of Liquid $POCl_3$

A.G. Novikov, D.I. Seliverstov, O.V. Sobolev.

The liquid $POCl_3$ (chlorine oxide of phosphor) is known as a main component of a mixture, constituting the liquid based laser system (typical composition: $POCl_3$ + $SnCl_4$, activated by Nd^{3+} ions) [1]. If the chemical properties and electron excitation spectrum of this liquid are widely studied, the information, concerning with its molecular structure and microdynamics is very scarce. At the same time it is well established, the elementary excitation spectrum of phonon subsystem and its correlation with electronic excitations are directly related to the nature of electron excitation transfer, its relaxation and quenching [2]. This is why we have undertaken a set of neutron scattering experiments on liquid $POCl_3$ with the spectrometer DIN-2PI, using it in diffraction as well as in inelastic scattering modes. The present report contains the short information about our first results.

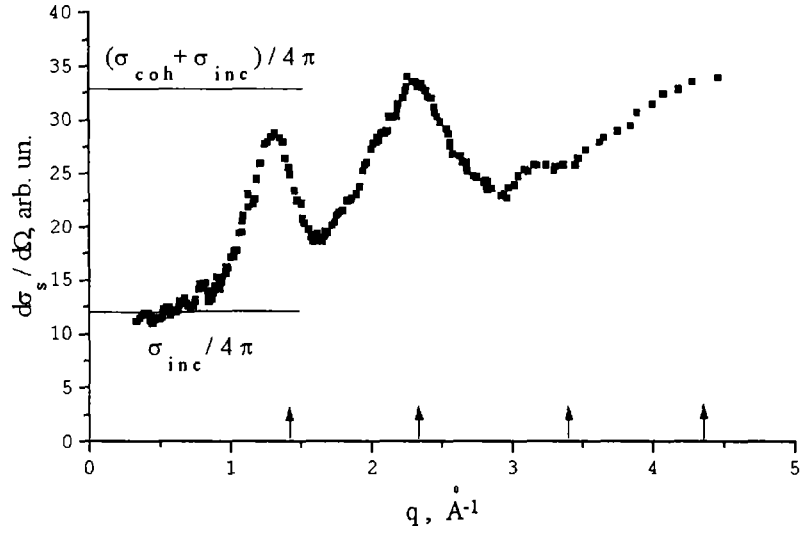

Fig. 1. Angular differential scattering cross section for liquid $POCL_3$

Fig. 1 shows the angular differential scattering cross section. The arrows point to the positions of the coherent peaks, found by X-ray diffraction [3]. The double differential scattering cross sections, measured at small scattering angles, where coherent effects can be neglected (see initial part of $d\sigma/d\Omega$ on fig.1), were used to extract the generalized frequency distribution (GFD) of chlorine atoms (87% of scattering events on $POCl_3$ molecule are connec-ted with chlorine) by application of the method, elaborated for incoherent scatterers [4] (fig. 2). The arrows show the location of the intramolecular modes, discovered in optical experiments by IR- absorption and Raman scattering of light [5]. It can be concluded from fig. 2, the region of intramolecular modes to be restricted by the energy transfers $\varepsilon \geq 20$meV. Thus, the part of GFD to the left from these energies can be related to the intermolecular modes. It should be supposed, that the wide peculiarity with the maximum about ε~(4-5) meV contains effects of molecular vibration motions (hindered translations) as well as effects of molecular librations in the force field of neighbours. There is no information about the intermolecular interactions in the liquid under study, but in [6] the method is suggested to estimate the frequency of intermolecular vibrations for liquids on the basis of their evaporation heats. Taking for $POCl_3$ $H_{ev} \cong 8$ kCal/mole, we get $\varepsilon_{tr} \sim$ (7-8) meV. If we suppose the intermolecular part of GFD

can be described by superposition of two Gaussians, we get one centered near ε~(7-8) meV (supposed, translational), and the second (librational) near ε~(4-5) meV (see inset of fig. 2). The wide overlap of these curves can be explained by the proximity of effective masses, which molecule participates in these two kinds of motions with.

The analysis of the quisielastic component of scattering in the region of small q has allowed to estimate the selfdiffusion coefficient for $POCl_3$ liquid as D ~(1.6±0.2) cm^2/c.

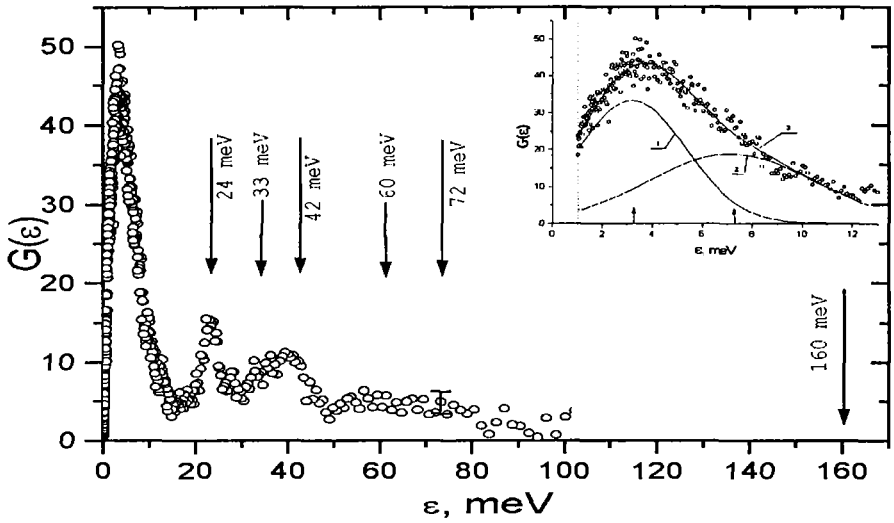

Fig. 2. Generalized frequency distribution G(ε) for chlorine atom in $POCL_3$ molecule. Inset: intermolecular part of G(ε). 1 -libration mode; 2 -translation mode; 3 - common approximating curve.

References

1. Yu.G. Anikeev, M.E. Zhabotinski, V.B. Kravchenko. Lasers on Inorganic Liquids. M., ''Nauka'', 1986, 248 p.
2. V.L. Ermolaev, E.N. Bodunov, E.B. Sveshnikova, T.A. Shahverdov. Emissiveless Transfer of Electron Energy Excitation. L., ''Nauka'', 1977, 311p.
3. A.K. Dorosh. Structure of Condensed Substances. Lviv, ''Vissha Shkola'', 1981, 176p.
4. A.G. Novikov, Yu.V. Lisichkin, N.K. Fomichev. Russ. J. Phys. Chem. 1986, v.60, p.1337.
5. K. Nakamoto. Infrared Spectra of Inorganic and Coordination Compounds. J. Wiley & Sons Inc., New York, London, 1984.
6. N.G. Bahshiev, V.S. Libov. Dokladi RAN, Phys.Chem., 1990, v.312, p. 1384.

Isochoric Specific Heat and Anharmonicity for Liquid Potassium

M.V. Zaezjev, A.G. Novikov, V.V. Savostin

1. Introduction

Liquid alkali metals are assumed to be nearly 'harmonic liquids' with small anharmonicity. The Grüneisen constant, which is of order 1.5, and $1 \leq C_P/C_V \leq 1.5$ are the features of these liquids. An inelastic neutron scattering experiment for liquid potassium at temperatures of 340, 440 and 550 K was performed and frequency spectrum (FS) of oscillations of potassium's atoms was obtained [1]. Neutrons with initial energy of 4 meV were used and the average energy of potassium atoms' oscillations was about 7 meV [1]. The temperature dependence of the spectrum is small compared to the energies of the spectral components in the temperature range studied, the Grüneisen constant has been found to be 1.3. This temperature dependence indicates an anharmonicity in oscillations of potassium atoms and makes possible the evaluation of the isochoric specific heat, C_V, at the same time.

2. Theoretical background

The internal energy of a system per one mole can be represented via a system's FS as following:

$$U(T) = E_0 + 3N_A \int_0^\infty \varepsilon\, g(\varepsilon) f(\varepsilon,T)\, d\varepsilon\,, \tag{1}$$

$g(\varepsilon)$ is the frequency spectrum, N_A is the Avogadro number, ε is excitation energy, i.e. change of neutron energy in the scattering process, and the function $f(\varepsilon,T)$ is:

$$f(\varepsilon,T) = \left[\exp\left(\varepsilon/k_BT\right) - 1\right]^{-1} + 1/2\,, \tag{2}$$

k_B is the Boltzmann constant. Taking into account the revealed deformation of $g(\varepsilon)$ with temperature the specific heat per one mole is:

$$C_V(T) = \frac{\partial U(T)}{\partial T} = 3N_A \int_0^\infty \left[\frac{\partial g(\varepsilon)}{\partial T} f(\varepsilon,T) + g(\varepsilon)\frac{\partial f(\varepsilon,T)}{\partial T}\right] \varepsilon\, d\varepsilon\,. \tag{3}$$

The first term in square brackets represents the anharmonic contribution to the specific heat.

3. Results

At three temperatures of our experiment $g(\varepsilon)$ has been represented by the following [1]:

$$g(\varepsilon) = g_L(\varepsilon) + g_T(\varepsilon) = \frac{4\varepsilon^2}{\sqrt{\pi}}\left[\frac{A_L}{\varepsilon_L^3}\exp(-\varepsilon^2/\varepsilon_L^2) + \frac{A_T}{\varepsilon_T^3}\exp(-\varepsilon^2/\varepsilon_T^2)\right]. \tag{4}$$

A_L and A_T are weight coefficients independent of temperature, ε_L and ε_T are excitation energies corresponding to the peaks of components, $g_L(\varepsilon)$ and $g_T(\varepsilon)$, respectively. The dependence of $g_i(\varepsilon)$ $(i = L,T)$ and ε_i on temperature is an evidence of anharmonicity. The function $\partial g(\varepsilon,T)/\partial T$ and the anharmonic contribution in Eq. (3) can be defined now (Fig.1).

The second term in Eq. (3) represents harmonic component and if $\varepsilon \ll k_BT$ (that is really the case) it is approximately that of the Dulong-Petit law: $C_V^{har} \approx 3N_Ak_B$.

Before comparing the result with known data [2] it should be remembered that the FS, $g(\varepsilon,T)$, does not contain a diffusion component of the total mobility of atoms. Only

inelastic contribution to neutron scattering pattern was considered to obtain FS [1]. So now the diffusion contribution is to be considered, and C_V takes the form:

$$C_V(T) \cong (1 - S_d)\left(C_V' - \frac{3}{2} N_A k_B T \frac{\partial S_d}{\partial T} \right) + \frac{3}{2} N_A k_B S_d . \qquad (5)$$

Here C_V' is the specific heat of Eq. (3), and S_d is relative part of diffusive modes in the FS.

For solid potassium near the melting point the anharmonic contribution has been found [3]:

$$C_V^{an}(T) = 3 N_A k_B T A , \qquad (6)$$

where $A = 1.7 \cdot 10^{-4}$ K^{-1}. Being extrapolated to temperatures from 340 to 550 K this contribution is shown on Fig.1. More appropriate comparison comes with the result [4] where the anharmonicity has been considered as a small correction to harmonic law connected with the structure of liquid that finally yields the upper limit of the anharmonic contribution:

$$C_V^{an} \leq 1.5 N_A k_B S_m(T) . \qquad (7)$$

$S_m(T)$ is the structure factor, $S(q)$, at $q = (18\pi^2 n)^{1/3}$ [2], n is particle density. It is seen on Fig.1 that our result as regards to the anharmonic contribution, C_V^{an}, is consistent with both [3] and [4]. Total specific heat, C_V, calculated with Eq. (5) matches in general the reference data [2] but are 1 to 1,5 J/mole K smaller. Configurational contribution caused by thermal expansion of metal and restructuring corresponding to the expansion could be taken into account. It does not exceed 1.5 J/mole K in the considered temperature range.

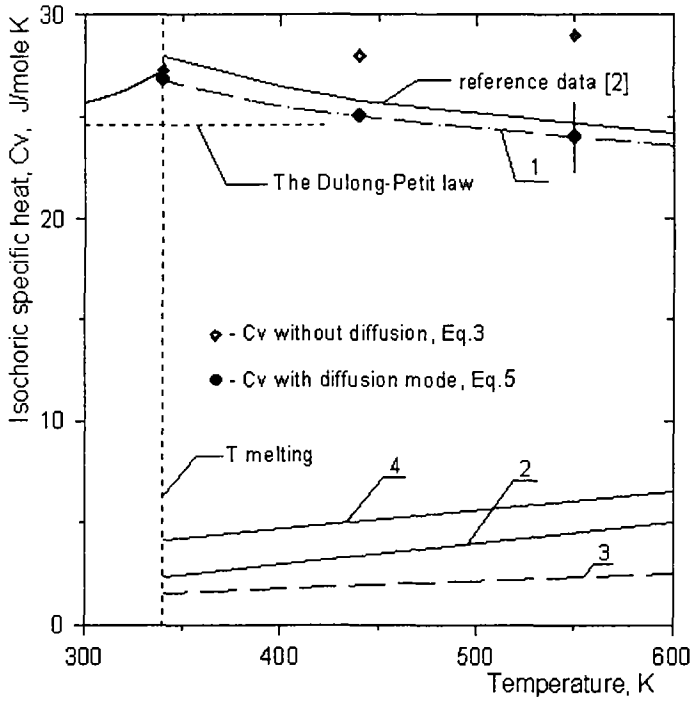

Fig.1. Isochoric specific heat for liquid potassium.
1 – approximation curve;
2 – anharmonic contribution, C_V^{an}, of Eq. (3);
3 – extrapolation of data [3], Eq. (6);
4 – upper limit of the anharmonic contribution, Eq. (7).

References

1. M.V.Zaezjev, M.N.Ivanovsky, A.G. Novikov, V.V.Savostin and A.L.Shimkevich, Russian J. Phys. Chem. (New York, Plenum) 68 (1994) 240.
2. Handbook of Thermodynamic and Transport Properties of Alkali Metals, ed. R.W. Ohse (Blackwell, Oxford, 1985) p. 753.
3. D.L. Martin, Phys. Rev. 139 (1965) A150.
4. P. Bratby, T. Gaskell, N.H. March, Phys. Chem. Liq. 2 (1970) 53.

Oxygen Microscopic Dynamics in Liquid Potassium Studied by Inelastic Neutron Scattering

A.G. Novikov, V.V. Savostin, A.L. Shimkevich, M.V. Zaezjev

1. Introduction

The investigation of liquid alkali metals (LAM) represents an especial interest over a period of years because of their wide using as coolants for nuclear power systems and high-temperature heat pipes. As a result, there is an ample experimental and theoretical information on thermodynamic, thermal and physical properties, structure, and atomic dynamics of LAM.

Meanwhile LAM form multicomponent impurity solutions in technological practice. Oxygen is the one of most important impurities. The raise of oxygen solubility in any coolant dramatically activates the steel corrosion. However the current knowledge of structural and dynamic properties of oxygen state in LAM is extremely insufficient.

In the present work we set a task to obtain microscopic dynamics characteristics of oxygen impurity in liquid potassium from data on inelastic neutron scattering.

The conditions of our experiment were chosen in such a way as to avoid an existence of K_2O oxide in the system. On account of low oxygen concentration in the melt, an assumption has been used that dynamic influence of oxygen on potassium atoms is absent [1].

2. Experimental

The inelastic-neutron-scattering experiment on liquid potassium-oxygen (K-O) system was performed at 550 K. Oxygen dissolved in the melt was investigated at concentration of 1.8, 5.1, and 8.5 at.%. The DIN-2PI time-of-flight spectrometer was used. It is located at one of the neutron beams of the IBR-2 pulsed reactor (Frank Laboratory of Neutron Physics, JINR, Dubna). The energy of incident neutrons was of 7.5 meV with resolution of 0.37 meV.

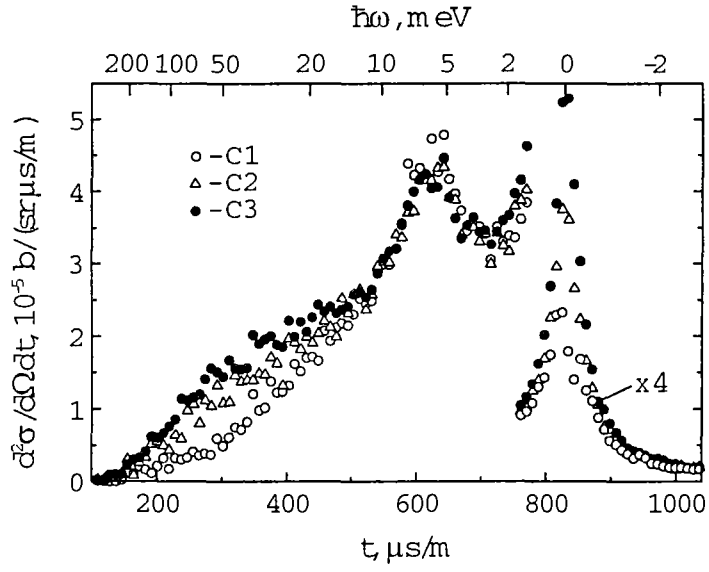

Fig. 1. DDSCS of slow-neutrons by K-O melt for the scattering angle of 28° at three oxygen concentrations: C_1 = 1.8 at.%, C_2 = 5.1 at.%, C_3 = 8.5 at.%. t and $\hbar\omega$ is neutron time-of-flight and energy transfer under scattering respectively.

A sample placed directly in the neutron beam was a thin-wall (0.15 mm) cylindrical container of stainless steel of 10 cm in diameter and 16 cm in height. It was filled with pure (99.9%) potassium. The cylinder was rigidly held into aluminum jacket of 12 cm in diameter and 1 mm in thickness. The jacket performed a strength function. The sample was a part of potassium loop with a cold trap controlling the concentration of dissolved oxygen impurity.

3. Results

From the experimental double-differential scattering cross-sections DDSCS (Fig.1), the liquid potassium DDSCS has been subtracted. The residual is considered as oxygen contribution which is converted to partial frequency spectrum (FS) of oxygen atomic vibrations (Fig. 2) using incoherent approximation.

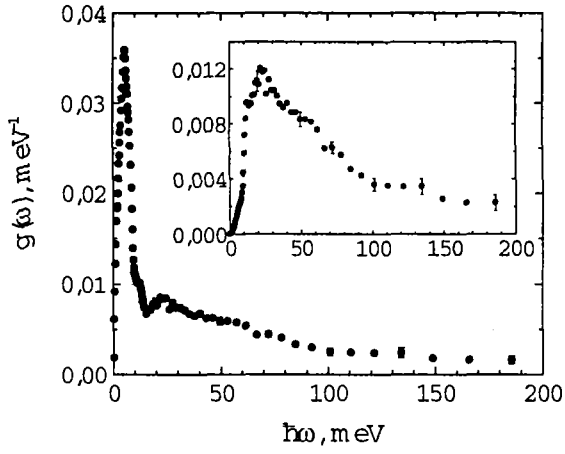

Fig. 2. The frequency spectrum of the liquid K-O system. The partial oxygen FS is shown in inset, being averaged over all three oxygen concentrations.

The partial oxygen FS has a value of average energy and extends to energies higher than those for potassium. This fact indicates that the oxygen-oxygen interaction is more strong than the metal-metal one. Such the observation is consistent with known information on oxygen atomic dynamics in cesium and rubidium [2]. It was shown that oxygen structure in them is of a cluster character (e.g., $Cs_{11}O_3$, Rb_9O_2). As obtained Raman spectra [2], there is also specific distinction of low energy metal modes and high energy oxygen vibrations in K-O system. From the Raman scattering [2], it has been revealed that vibrational modes of oxygen in Cs_7O clusters give a wide band in the region of 20–35 meV. In the case of the K-O system, the partial oxygen FS is like a single but rather wide peculiarity with maximum of $\hbar\omega \approx 20 - 25$ meV. Based on such the comparison, one can assume a cluster type formation in the K-O melt that is in accordance with the assumption [1].

In estimating the decay time of the velocity autocorrelation function obtained from the partial FS, we get the value of about 0,2 ps for the life time of oxygen atomic vibrations, which we prescribe to the oxygen-oxygen interaction by means of metal atoms. This life time is an order of magnitude less than that for potassium vibrations. It proves the statement that oxygen clusters exchange quickly metal atoms with the melt.

References

1. M.N. Ivanovsky, V.A. Morozov, A.L. Shimkevich and B.A. Shmatko, Liquid Metal Engineering and Thechnology, Vol. 3 (BNES, London, 1984) p. 15.
2. T.P. Martin, H.-J. Stolz, G. Ebbinghaus and A. Simon, J. Chem. Phys. 70 (1979) 1096.

Neutron Scattering Study of the Liquid Helium Excitation Spectrum

I.V.Bogoyavlenskii[1], A.V.Puchkov, A.N.Skomorokhov[2]

[1]Kharkov Institute of Physics and Technology, Kharkov, Ukraine;
[2]Joint Institute for Nuclear Research, Dubna, Moscow Region, Russia.

A neutron scattering experiment on the spectrometer DIN-2PI was oriented towards the study of a phonon-maxon region of the liquid helium excitation spectrum. One of the aims of the experiment was to verify the existence of a zero-sound mode in the maxon region. To solve this problem, the measurement was focused on temperatures quite close to the superfluid transition temperature, as expected by Glyde and Griffin [1,2] and from experimental results [3,4].

$S(Q,\omega)$ of liquid ^{4}He was measured at T=1.53; 1.81; 1.96; 2.1; 2.22K covering the wavevector range from 0.2 to 1.2Å^{-1}. To obtain the resolution function, measurements at a low temperature were also carried out. A low initial neutron energy (2.37meV) and reduced angular uncertainties provide an instrumental resolution between 0.105 and 0.07meV (FWHM) as a function of the scattering angle.

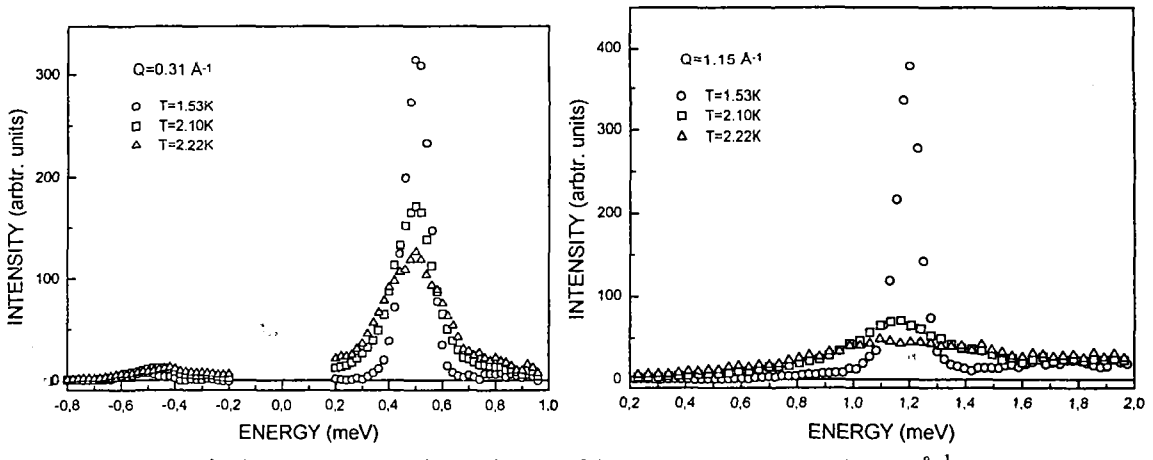

Fig.1 Temperature dependence of S(Q,ω) at Q=0.31 and 1.15 Å^{-1}.

It is found that the temperature dependence of $S(Q,\omega)$ depends notably on Q. At Q<0.5Å^{-1}, the phonon broadens as the temperature increases though retains a well-defined excitation above T_λ. The peak position varies slightly with temperature. In the maxon region (Q about 1.0Å^{-1}) the temperature dependence is quite different. Maxon change abruptly at T_λ, leaving no sharp peak at temperature above. In the Q region from 0.5 to 0.8Å^{-1}, $S(Q,\omega)$ exhibits additional intensities at $\omega>\omega_0$, that increase with temperature. This peculiarity can be explained as the temperature dependence of the interference terms of $S(Q,\omega)$ or the remnant zero sound mode.

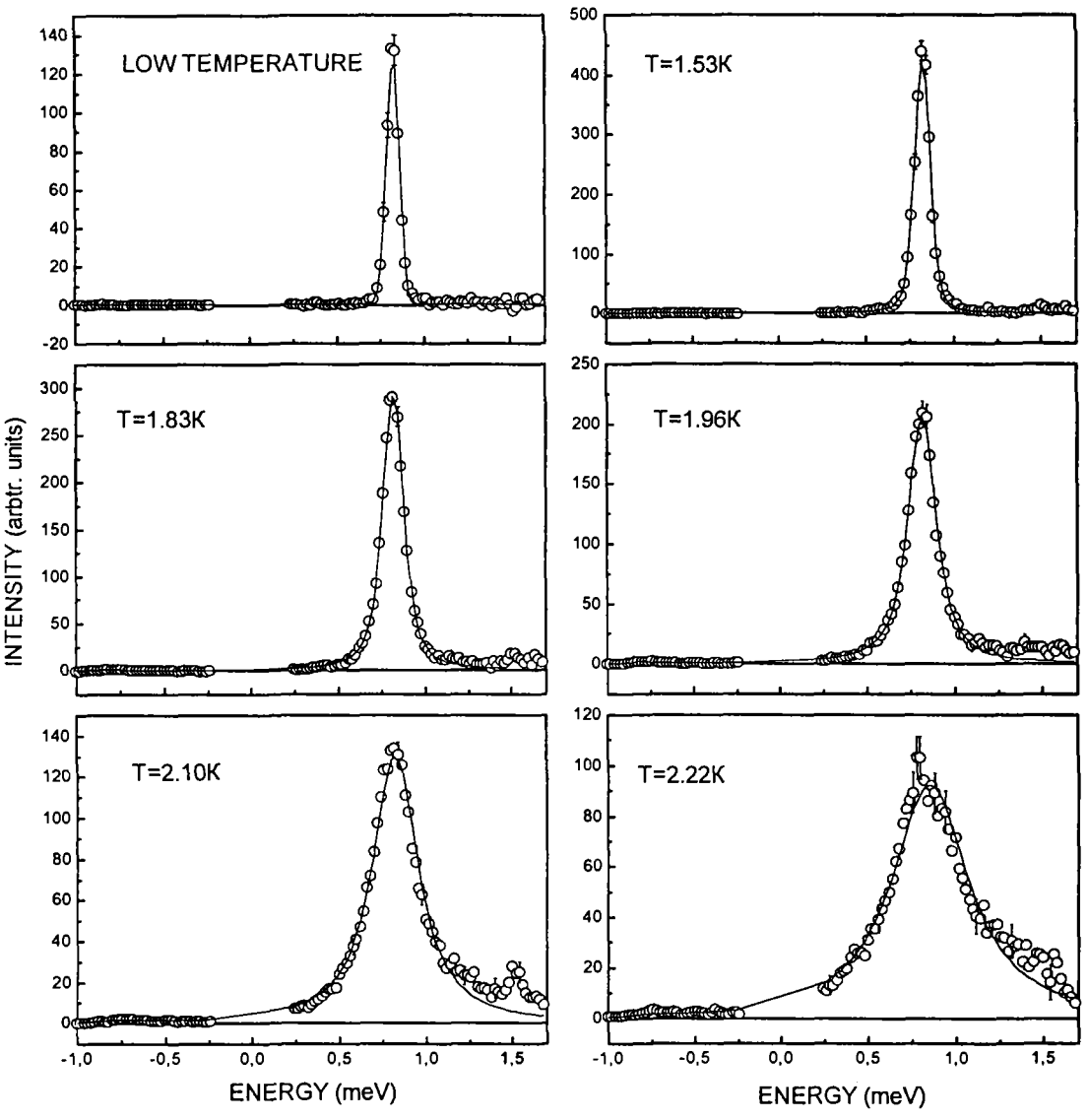

Fig.2. Temperaure dependence of S(Q,ω) at Q=0.51 $Å^{-1}$. Solid lines represent best fits to the data obtained by convolution of the resolution function and the function a damped harmonic-oscillator.

References

1. H.Glyde, Exitations in liquid and solid helium, Clarendon Press.,Oxford,(1994)
2. H.R.Glyde and A.Griffin, Phys.Rev.Lett.65(1990),1454
3. R.M.Crevcoeur, H.M.Smorenburg, I.M. de Schepper, W.Montfrooij and E.C.Svensson, Czech. J. of Phys.46(1996)257
4. I.V.Bogoyavlenskii, A.V.Puchkov, A.N.Skomorokhov and S.V.Poupko, Physica B 234-236(1997)324.

Hydrogen Vibrations in Austenitic Stainless Steels

S.Danilkin, D.Delafosse[1], H.Fuess[2], V.Gavriljuk[3], A.Ivanov[4], T.Magnin[3], H.Wipf[4]

[1] *Ecole Nationale Superieure des Mines de Saint-Etienne, Saint-Etienne, France*
[2] *Darmstadt University of Technology, Darmstadt, Germany*
[3] *Institute for Metal Physics, Kiev, Ukraine*
[4] *Institut Max von Laue - Paul Langevin, Grenoble France*

The aim of this INS experiment is in clarification of the hydrogen state and hydrogen effect on the interatomic bonding in FCC iron-based disordered solid solutions with and without H. The chosen alloys - Fe18Cr16Ni10Mn and Fe25Cr20Ni belong to the corrosion resistant engineering materials (stainless steel) which have to be resistant under hydrogen attack. The Fe18Cr16Ni10Mn steel does not transforms into ε-phase at any cold work and cooling down to 4K, and only H load induces the ε-phase. The Fe25Cr20Ni steel is less stable. The studied steels were melted in the induction furnace under argon atmosphere. After annealing in vacuum, samples were doped with hydrogen in the furnace with H pressure p=170÷190 bar at temperature of t=500°C. Thereupon for a time 20÷30 minutes the samples were cooled down to the room temperature in furnace and placed in liquid nitrogen where they were stored up to the neutron scattering experiment. Hydrogen content in steels was equal to 0.373 at. % in Fe18Cr16Ni10Mn and 0.326 at. % in Fe25Cr20Ni alloy. During the measurements the sample was mounted in an aluminium frame in an ILL cryofour. Vibrational spectra were measured in energy range from 15 to 380 meV at 77K (2K) at a constant scattering angle of 90° and reflection scattering geometry from the flat sample. The measured spectra were corrected for a background and normalised by the incoming neutron flux. The generalised vibrational density of states (GVDS) θ(ε) was obtained from the measured spectra in frames of one-phonon incoherent scattering approximation.

Fig. 1 shows the low-frequency part of GVDS in Fe18Cr16Ni10Mn, which corresponds to the metal atom vibrations. Hydrogen modifies GVDS only slightly, changing the form of the transversal band in GVDS. However the second moment of GVDS, which is proportional to the mean interatomic force in crystal, increases in the both steels.

Fig. 2 shows hydrogen vibrations in Fe25Cr20Ni alloy with H at 77K and 2K. The spectrum of the H-free alloy was used as background. In Fig. 2 we observe peaks at ε≈130 meV and ≈260 meV. High frequency peak is the second harmonics. Despite of cubic symmetry of the octahedral position in the FCC structure both peaks have shoulders at the side of the higher energies. The least-square analysis shows that each peak may consist of two with the energies: $\varepsilon^{(1)}_1$=128 meV ,$\varepsilon^{(2)}_1$=147 meV and $\varepsilon^{(1)}_2$=256 meV, $\varepsilon^{(2)}_2$=285 meV at 77K. Ratio $\varepsilon^{(1)}_2/\varepsilon^{(1)}_1$ equals 2 with an accuracy of 1% in all measured spectra. For second peak, the ratio $\varepsilon^{(2)}_2/\varepsilon^{(2)}_1$ equals 2 within experimental error. At 2K two-peak structure became more pronounced (Fig. 2), however room temperature data, obtained for Fe18Cr16Ni10Mn show only two broad peaks. The similar shoulders observed in FeH, $MnH_{0.86}$ and NiH hydrides were connected with dispersion of the optical modes. However, in studied solid solutions with low H content the observed peaks should correspond to the dispersionless localised vibrations. According to the X-ray data precipitation of hydrides and formation of γ*-phase is not observed in these steels. [1]. The possible reason for the two-component structure of the H peaks could be short

ordering of the metal atoms, taking into account that H vibrational frequency in CrH (ε=121 meV) is rather close to $\varepsilon^{(1)}_{I}$ in studied steels.

The performed measurements provide information about hydrogen effect on the interatomic bonding and hydrogen vibrational bands at very low H contents when diffraction study fails to observe structure changes. This shows that inelastic neutron scattering data on hydrogen state in steels are quite important for the understanding of first stages of the embrittlement process – short ordering and decomposition of the solid solution.

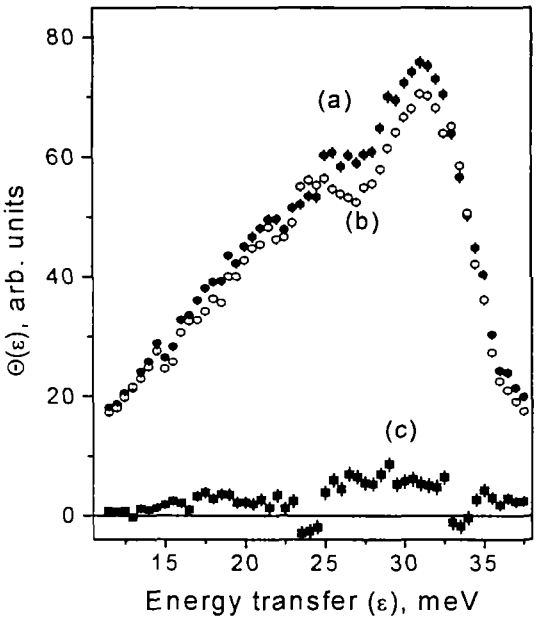

Fig.1. Metal atom vibrations in Fe18Cr16Ni10Mn alloy.
(a) hydrogen content 0.326 at.%
(b) after hydrogen removal at 900°C
(c) difference

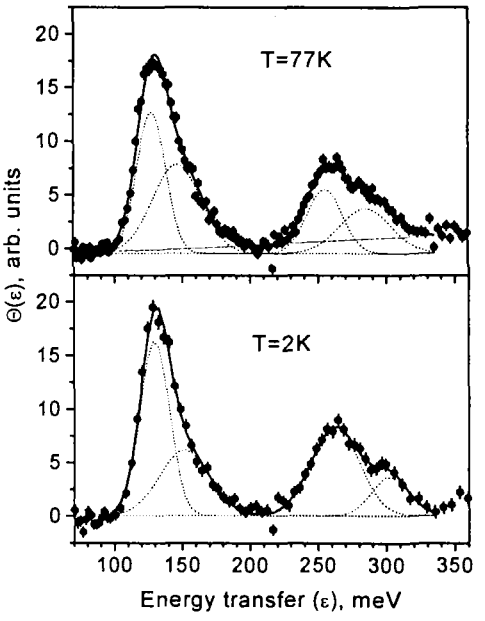

Fig.2. Hydrogen vibrations in Fe25Cr20Ni alloy.

References

1. V.G.Gavriljuk, H.Hanninen et al. Acta metall. Mater. 43 (1995) 559.

Mn Effect on the Crystal Structure and Lattice Dynamics of Fe-Cr-Mn-N Austenitic Alloys

A.Beskrovni[1], S.Danilkin, E.Jadrowski[1], M.Neova-Baeva[2]

[1] *Joint Institute for Nuclear Research, Dubna, Russia*
[2] *Institute of Solid State Physics, Sofia, Bulgaria*

High nitrogen austenitic steels are of high strength and corrosion resistance and offer the structure stability at low temperature and during cold working. The steel properties depend on the interstitial (N) and metal (Cr, Ni, Mn) atom content.

Present report concerns to the effect of Mn on the crystal structure and lattice dynamics of nitrogen austenitic alloys. Alloys with compositions Fe-19Cr-xMn-0.5N (x=9÷23 wt.%) were studied. To our knowledge the dependence of the lattice parameter on Mn content in these alloys are not studied yet. As for Mn effect on the interatomic interactions in steel, elastic constants have been studied by ultrasonic method [1].

The diffraction measurements were carry out with Philips-Micro III X-ray diffractometer with Fe K_α radiation and Mn filter. Inelastic neutron scattering spectra were measured with DIN-2PI spectrometer [2] at initial neutron energy E_0 = 18.4 meV. Spectra of scattered neutrons were measured at 10 fixed detectors in the scattering angle range 2ϑ = 71÷134°. The vibration density of states $G(\varepsilon)$ was calculated from the experimental data in frame of one-phonon approximation for incoherent scattering.

The measured diffraction patterns of studied alloys correspond to FCC structure. The linear increase of the lattice parameter with an increase of the Mn content was observed: a(Å) = 3.603 + 0.0013 x_{Mn} (wt.%). Vegard's low predicts a value of $100 \cdot k_a/a_0$ = 0.032 in comparison with 0.036 calculated from experimental data. The atomic radii used in these estimations for Mn and Fe are 1.3 Å and 1.26 Å. This shows that the lattice expansion produced by Mn atoms could be explained by simple atomic model.

INS measurements show modification of the metal frequency spectrum with increasing Mn content. The differences of the frequency distributions $G(\varepsilon)$(Mn=9%) and $G(\varepsilon)$(Mn=14, 19 and 23% Mn were calculated (Fig.1). There are no changes between frequency distributions in alloys with 9 and 14% of Mn. The effect of Mn is seen in difference [$G(\varepsilon)$(Mn=9%) - $G(\varepsilon)$(Mn=19%)] and in [$G(\varepsilon)$(Mn=9%) - $G(\varepsilon)$(Mn=23%)]. The positive difference in the energy region between ε_l and ε_m reflects the shift of the frequency spectrum boundary in the low-energy direction with increasing Mn content. Mainly this effect cause the decrease of the second moment of frequency distribution $<\varepsilon^2_{Me}>$ from 705 meV^2 at Mn=9% to 660 meV^2 at Mn=23%. The negative difference for the same alloys at energies less then 20 ÷ 25 meV reflects the increase of the density of states with increasing Mn content. This corresponds to decrease of the sound velocities and should cause the decrease of Debye temperature. Indeed, Debye temperature Θ_D calculated from the low - energy part of the experimental frequency distributions is decreased with increasing Mn content from 413K at Mn=9% to 401K at Mn=23%.

The softening of the metal atom frequency distribution agrees with data on elastic constants [1] and with a decrease of the shear and bulk moduli caused by Mn. The softening of interatomic bonding is in agreement with predictions of a theoretical model based on volume changes. These results disclose that Mn produces no significant change in the character of chemical bonding.

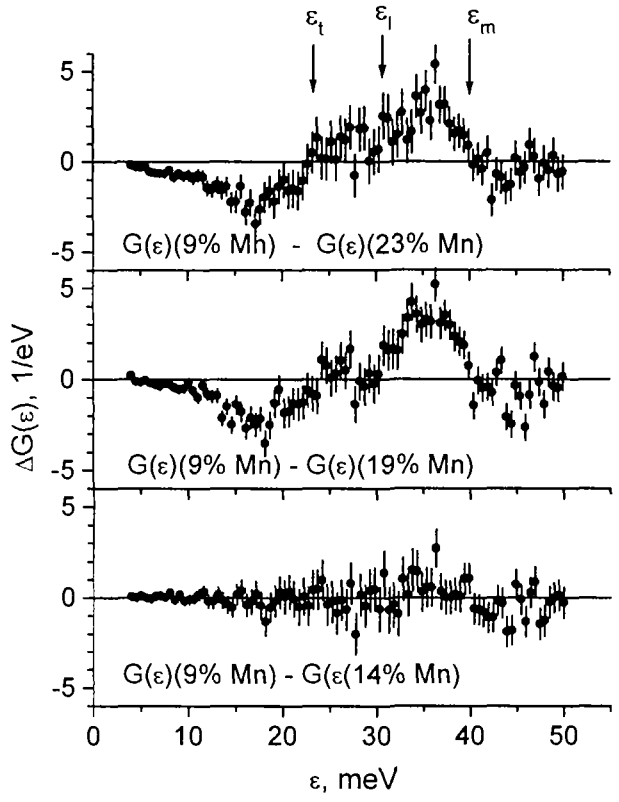

Fig. 1 Difference of the frequency distributions of Fe-19Cr-xMn-0.5N alloys with different Mn contents. ε_m – metal spectrum boundary, ε_l and ε_t - positions of longitudinal and transversal vibration bands.

References

1. S. Kim, H. Ledbetter Journal of Materials Science 29 (1994) 5462.
2. Neutron Experimental Facilities at JINR, User Guide, Frank laboratory of Neutron Physics, Joint Institute for Nuclear Research, Dubna, 1992.

Neutron Study of Dynamic Atomic Correlations in Amorphous Isotopic Ni-B Alloys

S.N.Ishmaev, Y.V.Lisichkin, A.V.Puchkov, V.A.Semenov, E.Svab**, G.F.Syrykh**

* *RRC Kurchatov Institute, 123182 Moscow, Russia*
** *Research Institute for Solid State Physics, Budapest, Hungary*

The dynamics of metallic glasses $^{i}Ni_{65}{}^{11}B_{35}$ is investigated by the inelastic slow neutron scattering method on isotopic substituted (i= natural, 60 and <b>=0) samples using the time-of-flight spectrometer DIN-2PI at the pulsed reactor IBR-2 in Dubna, and earlier at reactor IR-8 in Moscow [1]. The density of vibration states splits into two distinct regions: 0-40 and 40-90 meV, corresponding to predominant vibrations of heavy (Ni) and light (B) atoms (Fig.1). The first results obtained on the spectrometer DIN-2PI on the Q-dependence of the dynamic structure factor $S(Q,\varepsilon)$ at fixed energies (Fig.2) show small deviations from the Q^2 behaviour possibly due to short range structure and dynamic atomic correlations.

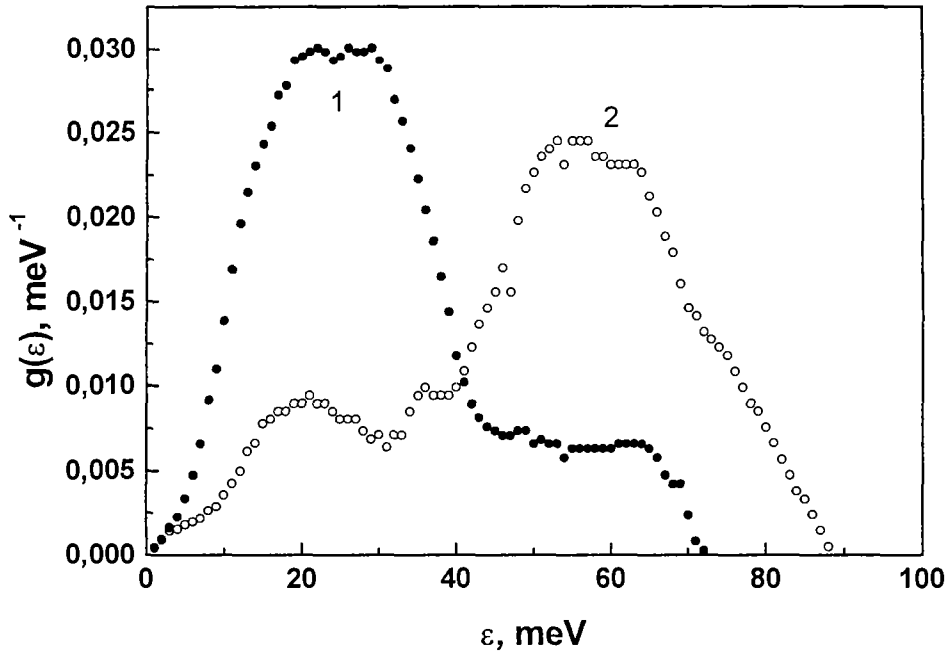

Fig.1 Partial densities of vibration states of Ni (curve 1) and B (curve 2) atoms in the amorphous alloy $Ni_{65}B_{35}$.

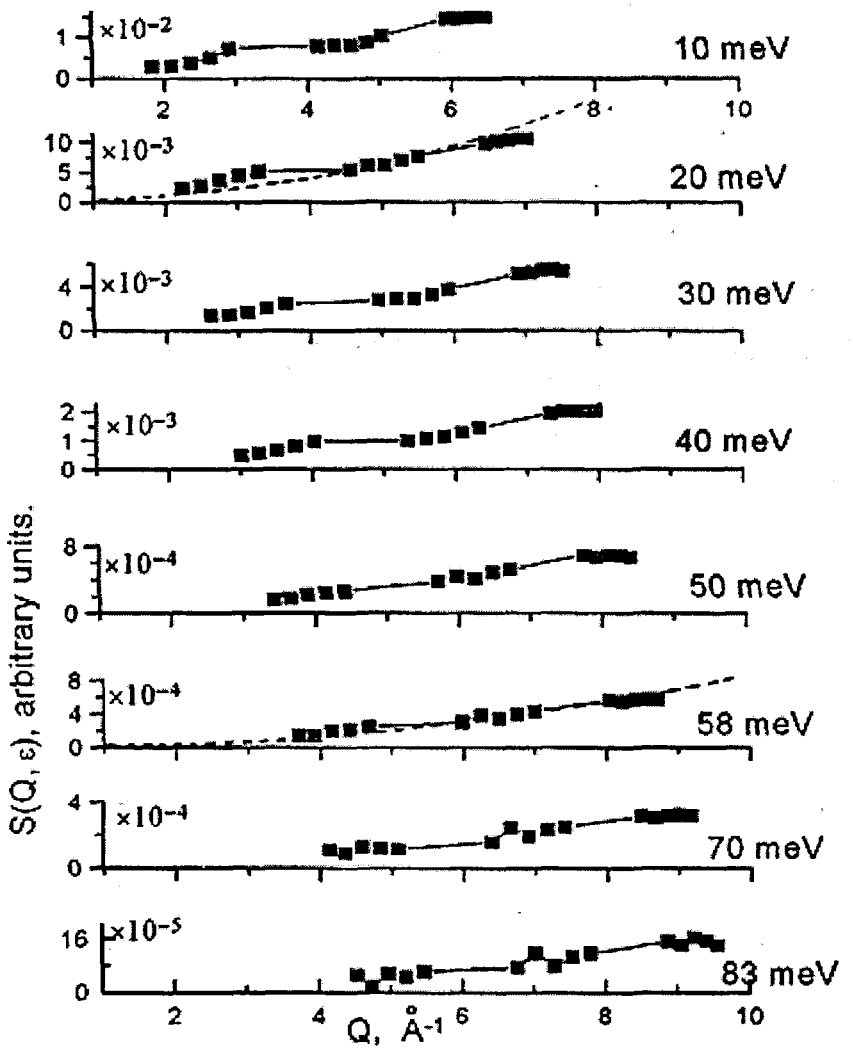

Fig.2 Q variations, $S(Q)$, for the amorphous alloy $Ni_{65}B_{35}$ at different energy transfers ε [2].

References

1. M.G.Zemlyanov, G.F.Syrykh, N.A.Chernoplekov and E.Svab, ZhETP, 94(1998)365 (in Russian).
2. S.N.Ishmaev, Yu.V.Lisichkin, A.V.Puchkov, V.A.Semenov, E.Svab and G.F.Syrykh, Proc.of 6-th European Powder Diffraction Conference EPDIC-6, Aug.22-25, Budapest, Hungry,1998.

Identification of Biphonons by Peculiarities of Angular and Energetic Dependences of Inelastic Crossection of Neutrons, Fissioning Biphonons

O.A. Dubovsky, A.V.Orlov

The spectra of multiphonon vibrations in solid state materials of different type - hydrieds of transient metals, ionic crystals, semiconductors -are investigated in recent years by methods of inelastic scattering of neutrons, photons and electrons. New narrow resonance lines, seen recently in spectra are interpreted as bound (due to anharmonicity of vibrations) multiphonon vibrations - biphonons and triphonons [1] and was investigated previously by other authors theoretically [2]. This interpretation is based now only on energetic balance in series of spectral one-phonon and multiphonon resonances, and this sircumstances gives foundation for alternate explanation of additional resonances as connected with possibility of defects, peculiarites of one-phonon density of states, ets.

It was proposed in [3] to use analysis of angular and energetic dependence for cross-section of inelastic scattering of neutrons, fault of bound energy of biphonon. This inelastic scattering is going with fission of biphonon on unbound, but interacting due to anharmonicity one-phonon vibrations. The scheme of uniform surface filled with noninteracting 1D crystals was used for investigation of energy and angular dependence of neutron crossection. The main difficulty of calculations is necessity of using analytical form of dispersion dependence and wave functions both for bound states - biphonon and for unbound state of triphonons still interacting due to anharmonicity. The analytical presentation of energy and angular dependence for neutron fault crossection is of following form [3]

$$\sigma''(\varepsilon,\theta)=\sigma_0\frac{th\chi}{\sin k_0}\frac{\left[\alpha_0+T_0'\gamma_0'-T_0''\gamma_0''\right]^2+\left[T_0'\gamma_0''+T_0''\gamma_0'\right]^2}{\beta_0^2}, \qquad (1)$$

where χ is parameter of spatial damping for biphonon wave function, k is effective wave vector of two-phonon states, T is amplitude of scattering and α, β, γ are functions of ε,θ found in [3]. The $\sigma''(\theta)$ dependence for increasing (1,2,3,4,5) energy fault ε is shown on Fig.1. The breaks of curves in some points are caused by adopted for computation simplicity condition of normal to surface flight out of neutrons. The peculiarities of energy and angular dependence of neutron fault cross section, depicted on Fig.1 and by other curves in [3], may be used as crucial identificators of inelastic scattering of neutrons exactly on biphonon bound states. These peculiarities include particular shift of bands and sometimes nonuniform shift of resonance, special dynamics of resonance evolution.

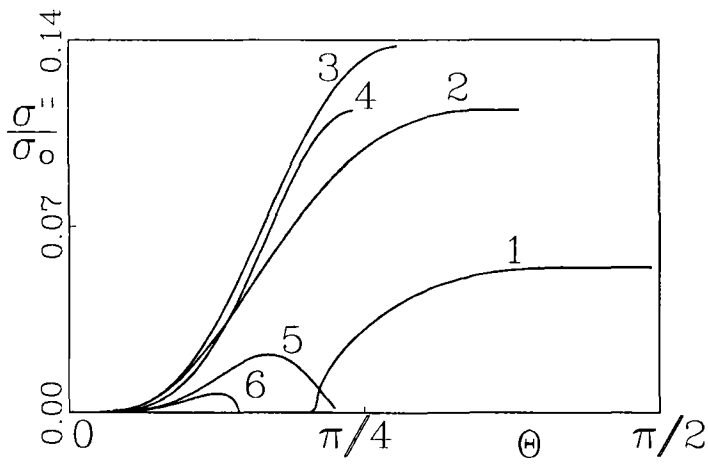

Fig.1

This work was carried out under the support of Russian State Science-technical Program "Actual directions in condensed matter physic" on the direction "Neutron research of matter".

References

1. A.I.Kolesnikov, M.Prager, J.Tomkinson, I.O.Bashkin, V.Yn.Malyshev, E.G.Ponyatovskii. J.Phys.: Cond. Matter **3**, *6*, 5297 (1991).
2. V.M.Agranovich, O.A.Dubovsky, A.V.Orlov. Phys.Lett. **A119**, *2*, 83 (1986).
3. O.A.Dubovsky, A.V.Orlov. Fizika tverdogo tela. **40**, *4*, 728 (1998).

The Dynamics of Hydrogen in $VO_{0.2}H_{0.05}$ β'-phase

S.I. Morozov

The objective of the present work was to trace by the INS method the effect of oxygen at high concentrations on the dynamics and position of hydrogen localization in the host lattice. To this end, samples of the alloys $VO_{0.2}$ and $VO_{0.2}H_{0.05}$ were prepared and measurements of the INS spectra were performed on a DIN2-PI spectrometer [1]. The result is displayed in Fig. 1.

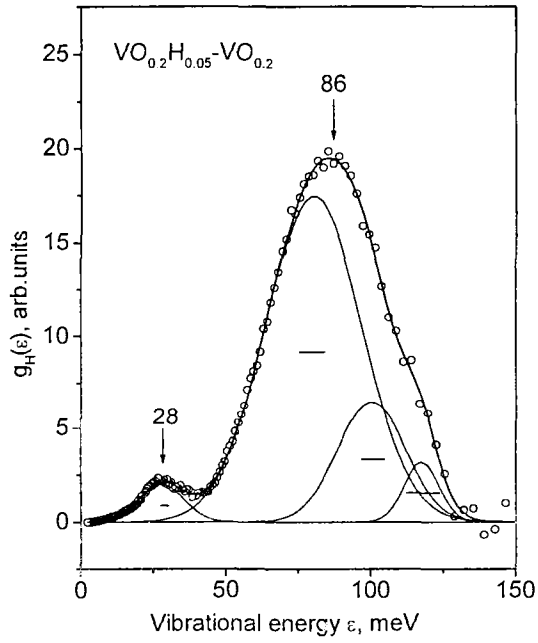

Fig.1. Vibrational spectrum of hydrogen atoms in the interstitial β' phase of $VO_{0.2}H_{0.05}$. The peaks shown by the fine lines were extracted from the spectrum by fitting Gaussian curves to the experimental data. The thick solid line shows the total result of the description. The positions of the features marked by arrows are given in meV. The horizontal bars show the half-width of the resolution function of the spectrometer.

Since interstitial atoms interact mainly with the nearest-neighbor metal atoms, the structure of the local vibrations (LVs) should be directly related with the symmetry of the interstitial position occupied by the interstitial atom. As one can see from Fig.1, the spectrum consists of a principal feature at ε=86 meV and a small feature at ε_1= 28 meV. The latter feature is due to the band modes of the hydrogen atoms in the $VO_{0.2}$ lattice. The fine lines in Fig.1 show the peaks identified in the spectrum by a best fit of Gaussian curves to the experimental data.

Such a structure is a typical of the vibration spectrum of light interstitial impurities in the fcc or ideal hcp lattice of the host atoms, where the *T* and *0* positions have T_d and O_h, point symmetry, respectively, while such a low vibrational energy of the H atoms is usually interpreted as evidence of octahedral coordination of hydrogen [2,3]

The character of the regular displacements of the vanadium atoms in the 16(*m*) positions in the $4V_{16}O_3$ superstructure [4], caused by the ordered arrangement of the oxygen atoms, is such that octahedral interstices with O_h symmetry (or weak tetragonal distortion) which are available to hydrogen do not form in it. At the same time, because

the vanadium atoms are displaced along the *z-axis* by δ=0.54Å some tetrahedral voids in this lattice, are appreciably larger in size than the TPs in pure vanadium and they possess the symmetry of an almost ideal tetrahedron. If light interstitial atoms occupy them, the spectrum of local vibrations should be either degenerate or weakly split. Therefore we arrive at the conclusion that the character of the local displacements of the vanadium atoms changes at a transition from the α to the β phase of V-O. Ordering of oxygen in the β'-phase results in regular displacements of a definite fraction of vanadium atoms. In the process, interstices with T_d local symmetry, which are most favorable for hydrogen atoms, are formed near the oxygen atoms. This result could also be important for interpreting the results of investigations of the vibrational spectrum of hydrogen in other ternary systems, for example, Ta-N-H and V-N-H, where the energy of the triply degenerate localized vibrations of the hydrogen atoms is ε=110 meV [5].

This work was supported by the Russian Fund for Fundamental Research, Project 95-02-04675-a, and the Russian State Program "Topical Problems in Condensed Matter Physics" in the subfield "Neutron Investigations of Matter."

References

1. Parfenov, P. S. Klemyshev. I. G. Morozov, and A. F. Pavlov. in Neutron Inelastic Scattering, Vol. 1, IAEA. Vienna, 1978, p. 81.
2. Morozov, V. V. Sumin. A. V. Belushkin. and I. Natkanets. Sov. Phys. Solid State (USA), 27. 1652 (1985).
3. Danilkin, V. V. Sumin. and V. P. Minaev. Sov. Phys. Solid State (USA), 28, 1592 (1986).
4. . Hiraga and M. Hirabayashi, J. Phys. Soc. Jpn. 34. 965 (1973).
5. Morozov. Physica B 234-236. 32 (1997).

2.6 MATEMATHICAL MODELING

Mathematical Modeling and Optimization of the Multi-Component Viscous Liquids Separation Processes Using Membrane Apparatus

A. Zinin, G. Zinina, M. Sotov

Membrane plasmapheresis is the kind of efferent therapy that is aimed at getting different pathology products out of the organism. The most efficient efferent therapy method is the removal of liquid fraction of the blood – the plasma. The creative group of engineers in the Center for membrane technologies of "Optika" enterprise (Saint Petersburg, Russia) has developed an original plasma-filter using flat porous track membranes (also known as "nuclear" membranes). The first Russian membrane plasma-filter, PFM, was authorized for clinical use in 1992. The core of the apparatus is 10 μm thick flat porous membrane with 0.5 μm diameter pores, which allows liquid fractions of the blood to pass while arresting formed components.

This work deals with the mathematical modeling of the PFM plasma-filter in order to optimize geometry and flow-rate parameters. The mathematical model and BLOOD3D computer program were developed for the non-stationary three-dimensional PFM hemofilter modeling. The geometry of the filter mathematical model is given on the Fig. 1.

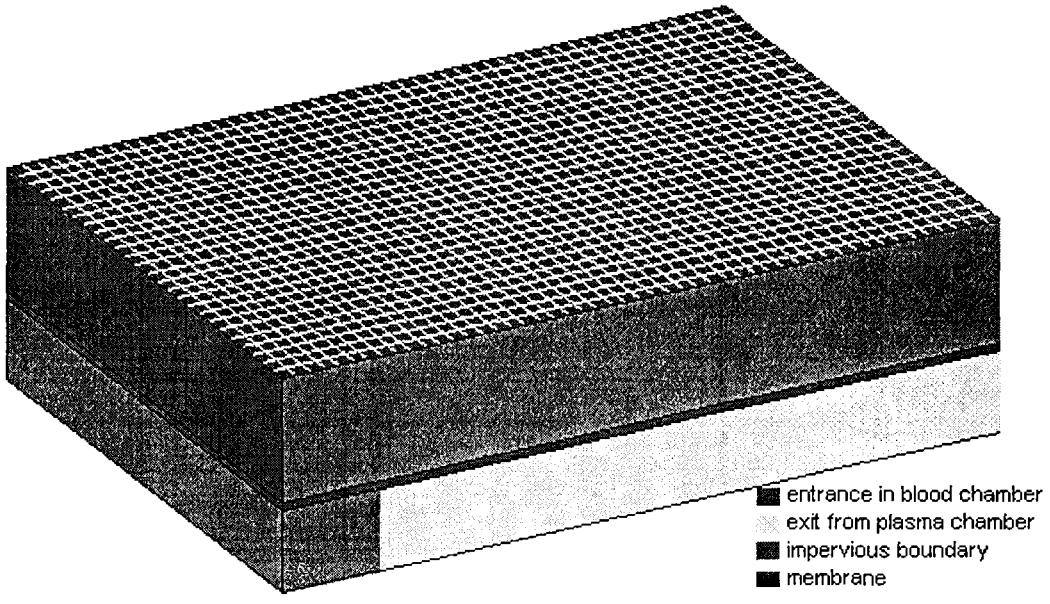

Fig. 1 The geometry of the plasma-filter mathematical model.

The estimations of the blood chamber permeability were acquired using two independent techniques, with results being close to each other. This is a considerable argument in favor of a view that flow macro-parameters in the blood chamber are in correspondence with the common laws describing liquid flowing through the porous matter. It is considered as the working hypothesis that the red blood cells transfer in the PFM filter can be described by the equation of convective-dispersion transfer with

anisotropic hydro-dispersion tensor. The main equation system for blood chamber flow includes: the equation of continuity; the Darcey's equation which defines the relation between filtration speed vector and pressure gradient; the convective-dispersion transfer equation describing the balance of red blood cells in the blood chamber. The equation system is accomplished by the equation of dependence of the blood viscosity on hematocrit. The condition of plasma flow proportionality to membrane pressure drop is adopted also.

The mathematical model's sensitivity to the variations in different input parameters was investigated using the BLOOD3D program code. It was shown that numeric viscosity doesn't lead to significant variations in modeling results. The strong non-linear behavior of the filter's hydrodynamics was demonstrated which is due to the variable liquid viscosity inside the blood chamber.

The numerical study of the hemofilter's non-stationary working regimes was held. The results of intercomparison analysis of regimes are given that can be used in optimized track membrane hemofilters. It was shown that in those cases where it's possible to neglect the contamination of the membrane's pores, the mean characteristics of periodic working regimes of a filter are close to stationary regime's ones with mean pressure drop between the membrane and the blood chamber. The difference in hemofilter's working regimes can be considerably determined by the differences in the membrane's contamination dynamics. So the importance of experimental and theoretical studies on kinetics of the membrane's contamination and clearing processes is implied.

The short guide on using the BLOOD3D computer program was developed. This program was used to conduct all the numerical study for the project.

References

1. V.Voinov. Efferent therapy. Membrane plasmapheresis (in Russian). St.-Petersburg, "Esculap", 1997.

Development of Benchmarks for Verification of Computer Programs Used in Burnup Calculations of VVER Type Reactors

D.M. Babanakov, I.R. Suslov, O.G. Komlev

The aim of the work carried out was to generate a set of benchmarks for verification of computer programs used in burnup calculations of VVER type reactors based on a microscopic model of the isotope kinetics in the core. Four types of reactor were considered: VVER-440 and VVER-1000 with uranium fuel as well as VVER-640 and VVER-1000 with MOX fuel, thus four benchmarks were generated. The input data for calculations were taken from [1].

The microscopic model includes a system of burnup equations where microscopic cross-sections and neutron flux are presented. The microscopic constants corresponding to the reactors considered were calculated on the basis of assembly-averaged macro cross-sections, nuclear densities, and reaction rates generated by the code WIMS. The computations were performed for each fuel type with taking into account the real geometry configuration of VVER assemblies (the cluster option of WIMS). The constants were generated for cases of both fresh and burned fuel loads.

The spatial distribution of neutron flux entering into the burnup equations was obtained as the solution of a 2D two-group diffusion equation. To provide reliable data for the benchmarks, two computer programs based on fundamentally different numerical methods were used to calculate this solution. The first of them named MAG [2] is based on the standard mesh center finite-difference scheme. The other program named HEXZ [3] is based on a nodal method using symmetry of the 3D hexagon with an analytical representation of neutron flux over the node. The solutions obtained were in good agreement, and it was concluded that the error resulting from approximation of the leakage operator in the diffusion equation was small enough to provide the accuracy acceptable for benchmark level data.

The burnup equations were solved by MAG and HEXZ using a standard Runge-Kutta scheme for each spatial mesh with the neutron flux recalculated at intervals of five Full Power Days.

The computation results presented in the benchmarks agree closely with the experimental data published in [1]. Thus the benchmarks developed seem to be a solid basis for verification of computer programs specialized in neutronics calculations of VVER type reactors.

References

1. In-Core Fuel Management Code Package Validation for WWERs, IAEA-TECDOC-847, Nov. 1995.
2. I.R.Suslov et al. MAG - Code for Fine Mesh VVER Calculations Proc. of 6th Symposium AER, 1996.
3. O.G.Komlev, Group Theory Nodal Method for the Diffusion Equation in 3-D Hexagonal Geometry, Proc. of Int. Conf. PHYSOR'96, 1996, A-60.

Spatial and Time-Dependent Calculation of Fast Reactor Transients

A. A. Bezborodov, A. V. Volkov, S. M. Ganina, V. P. Ginkin, I. A. Kuznetsov, N. M. Troyanova, Yu. E. Shvetsov

The GVA code complex was developed in the State Research Center - Obninsk Institute of Physics and Power Engineering for the calculation of spatial-dependent transients in fast reactors. This code complex is based on three independent codes, namely:

- GRIF-SM code for three-dimensional thermal hydraulics calculation of BN-like reactors with possibility to take into account two phases of sodium state;
- VOLNA code for three-dimensional Hex-Z calculation of reactor dynamics in multygroup diffusion quasi-static approximation;
- ARAMACO code for homogenized multygroup cross-sections preparation using typical fast reactor neutron spectrum.

The joining of these codes in one code complex allows to solve the main task - the direct numerical simulation of spatial and time-dependent behavior of reactor core parameters under accidental conditions. As primarily faults can be considered such events like the main coolant pump stopping and spontaneous movement of control rods.

Now the initial stage of accident can be only calculated by the GVA code complex when the fuel melting and destroying of reactor core do not occur. However there is no limitations to expand this approach for next stages of accident when the material replacement takes place. Moreover we suppose that the quasi-static approximation is the only acceptable and practicable for detail and complex description of accidents, which cause fuel melting and fuel assemblies destroying.

The GRIF-SM code solves the transient system of mass, impulse and energy conservation equations in the frame of porous body and the porosity, penetrability and other coefficients are the function versus spatial coordinates. Such approach permits to describe the boiling of sodium and its condensation in the upper part of reactor and to take into account the hydraulics interference of core channels. The input data of GRIF-SM are the spatial power distributions at each time moment. The output data are spatial distributions of pressure, coolant's velocity and density, temperatures of fuel, cladding, coolant and other materials.

The VOLNA code solves the spatial and time-dependent neutron transport equation in the diffusion approximation. The quasi-static approach of solution is applied in this code when the original equation is identically transformed to the system of two equations, one for spatial and time-dependent shape function $\psi(r,t)$ and another one for time-dependent only amplify factor P(t). The equation for P(t) is similar to point kinetics equation and the P(t) factor can be interpreted as reactor power. The neutron flux is the production of shape function by amplify factor.

The important feature of quasi-static approach is the possibility to use two different time mesh steps. The shape function $\psi(r,t)$ is recalculated with big time step and the amplify factor P(t) is recalculated with small time step.

The input data for VOLNA code are spatial distributions of cross-sections at each time moment and the velocities of control rods movement. These velocities are used indirectly, the code calculates the location of moving control rods ends and finds the averaged by volumes cross-sections in the cells containing these ends.

The output data of VOLNA code are the spatial power distribution in the reactor core, the group neutron flux and the group densities of precursors.

The group cross-sections for VOLNA code are calculated by ARAMACO code. The input data for ARAMACO are distributions of temperature and density of fuel, constructional materials and coolant found at each time moment by GRIF-SM code.

The initial state of reactor in GVA code complex is exact critical state. This state can be changed by change of cross-sections in any reactor cell. That means the introduction of reactivity due to any physical reason. The reactivity is calculated during solving of time-dependent diffusion equation as an integral by reactor volume of changes in cross-sections distribution and shape function and critical reactor fission neutron importance function are the weight functions.

The results of four different accidents calculations by GVA code complex are discussed. The considered accidents were as following:

- the stopping of all main coolant pumps (MCP) with simultaneous fault of control rods;
- 6 compensating rods are going up from the reactor core with the velocity 10 cm/s;
- 6 compensating rods are going up from the reactor core with the velocity 0.5 cm/s;
- 6 compensating rods are going up with the velocity 5 cm/s during 2 seconds, then they are stopped.

Resume:

1. The GVA code complex is developed for the joint solving of spatial and time-dependent dynamics equation and thermal hydraulics equations in three-dimensional geometry. The GVA can be used for transient and accidental calculations of fast reactors.
2. The ULOF and TOP accidents in the BN-800 reactor were calculated by GVA. These calculations are in good agreement with the results of calculations by the GRIF-SM code. However the calculations with GVA allow to take into account the shifts of spatial power distributions caused by the movement of reactor materials during accident and by movement of control rods (up to 10-15% of initial values).
3. It is desirable to provide detail verification of the GVA code for the applying of it in the practice of reactor calculations.

1-st Balakovo NPP Unit In 8-Th Fuel Cycle

Yu.I. Lihachev, V.P.Ginkin and other

Particularity of 8-th fuel loading of 1-st Balakovo NPP unit is a test operation of 54 Zirconium Fuel Assemblies (ZFAs) with different enrichments. Amongst them 24 fresh ZFAs, 24 one fuel cycle old ZFAs from the 7-th loading of 1-st Balakovo NPP unit and 6 two fuel cycle old ZFAs from 6-th and 7-th loading of 1-st Balakovo NPP unit.

The fresh FAs which used in 8-th fuel loading are as follows:

1 serial FA with enrichment 1.6 %, 12 serial FAs with enrichment 3.3 %,

12 serial FAs with enrichment 4.4%, with Burnable Absorption Rods (BARs) with g=0.036 g/sm^3,

6 serial profiled FAs with average enrichment 4.23 %, with BARs (g=0.065 g/sm^3),

6 ZFAs with enrichment 4.0% with zirconium Spacer Grids and Guide Tubes and diameter of central hole in fuel pellets 1.5 mm, with BARs (g=0.065 g/sm^3),

18 ZFAs with enrichment 4.0% with zirconium Spacer Grids and Guide Tubes and diameter of central hole in fuel pellets 2.4 mm, with BARs (g=0.036 g/sm^3).

As for serial FAs and ZFAs used staff profile scheme.

Accommodate scheme of 54-th ZFAs in the core is presented on the figure 1.1.

Calculations of boron fuel cycle are held with the code WIMS-VOLNA [1] for nominal parameters and 80% positions of Control Rods (CR) working group from the bottom of the core in four-group diffusion approximation for the sector of symmetry 60 degrees. On the figure 1.2 are presented changing of the Assembly Power Peaking Factor (Kq) and Volume Power Peaking Factor (Kv) during boron fuel cycle

The required data for thermo-mechanical calculations are:

- distribution of neutron flux with the energy above 0.1 Ìev on the corners of SFAs;
- distribution of heat generation rate ql per unit of SFA length on the corners of SFAs;
- distribution of fuel elements shell temperature on the corners of SFAs;
- distribution of Volume Power Peaking Factor in the core;
- distribution of the fuel burnup in the volume of the core.

These data are prepared by means of the code WIMS-VOLNA and will be sent in coordinated formats for further processing in thermo-mechanical code.

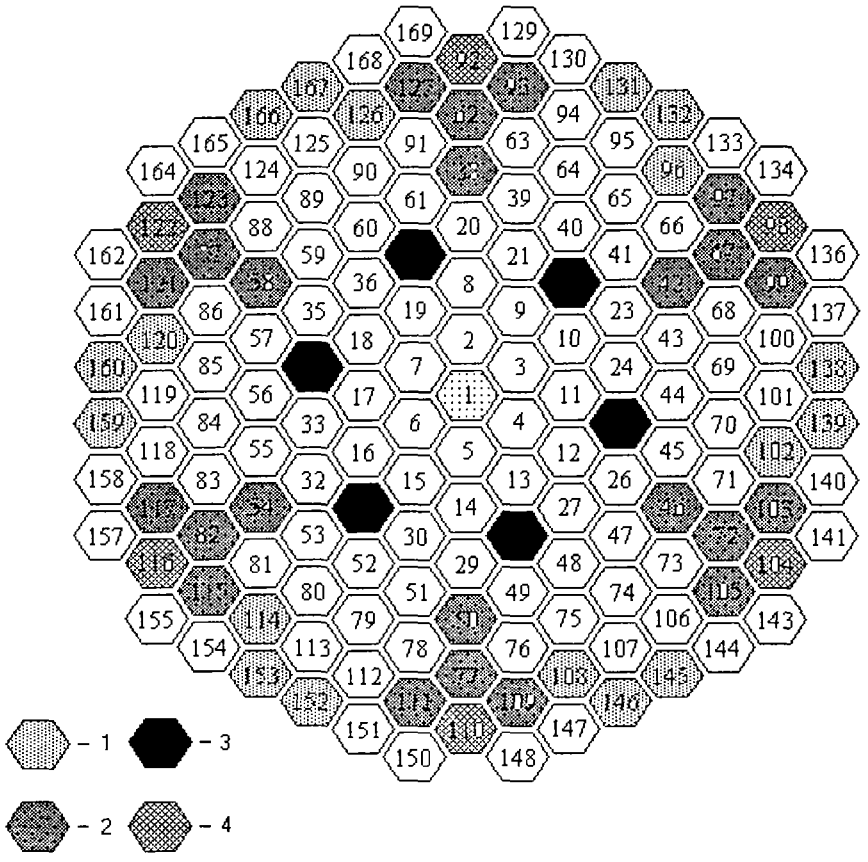

Fig. 1.1. Accommodate scheme of 54-th ZFAs in 8-th fuel loading 1-st Balakovo NPP unit:
1 - ZFAs with BAR (0.065), 1-st cycle old, 2 - ZFAs, 2-d cycle old, 3 - ZFAs,
3-d cycle old-, 4 - ZFAs with BAR (0.036), 1-st cycle old.

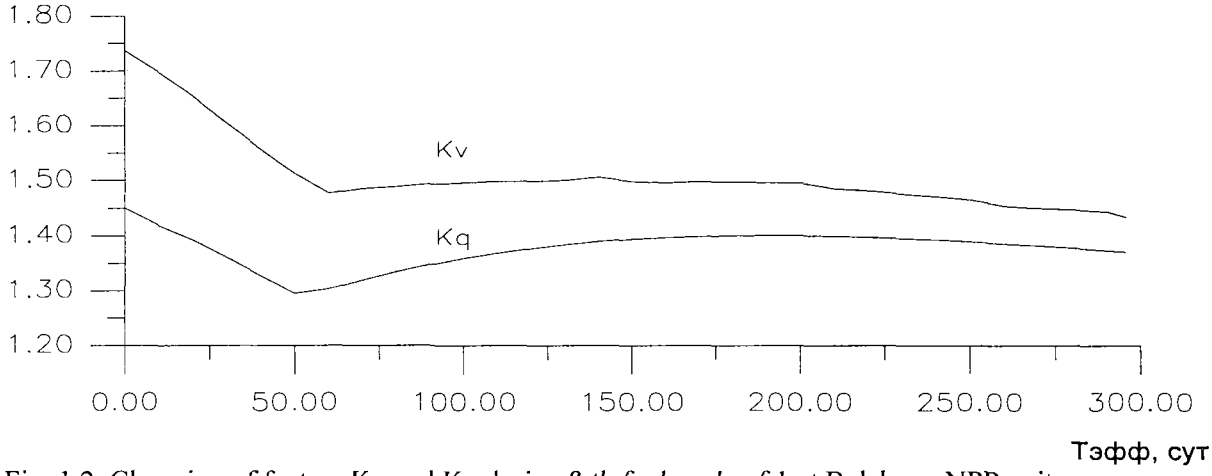

Fig. 1.2. Changing of factors Kq and Kv during 8-th fuel cycle of 1-st Balakovo NPP unit.

Reference

1. Проведение нейтронно-физических расчетов реальных состояний активной зоны реактора ВВЭР-1000. Отчет ФЭИ - 9258, Обнинск, 1996 г.

Modeling of Radioactive Contamination Migration in Underground Water

E.G.Drozhko[1], A.I.Zinin, G.A.Zinina, B.G.Samsonov[2], L.M.Samsonova[3]

[1] *PA "Mayak", Ozersk, Russia*
[2] *Russian Institute of Mineral Resources, Moscow, Russia*
[3] *State Geological Enterprise "Gidrospetsgeologia", Moscow, Russia*

Final disposal of radiochemical production wastes causes hydrodynamic, hydrochemical, radiation, and thermal impacts on underground waters. Mathematical modeling of radioactive migration processes is an important tool for substantiating safe operation of disposal sites. Mathematical models can contribute predictions of process development, define priorities for underground water monitoring, optimize the measures for rehabilitation of areas affected. However, creating numerical models involve considerable scopes of experimental information which is feasible provided that long-term monitoring is managed.

A large scale monitoring is available for Karachai lake, which is a major source of underground water contamination at PA "Mayak" site. The contamination spread has been under systematic observation since 1964. The monitoring data have been used as a basis for the development of three-dimensional model of non-stationary filtration and migration of radioactive contaminations from Karachai lake. Principle factors for the substance migration are convective transfer, dispersion, radioactive decay, and sorption. Vertical differentiation of solutions in the aquifer is determined by a high density of the technological solution. The mathematical model developed ensures prompt solutions for a wide scope of prediction problems.

Implicit Numerical Method for Solving of Fluid Mechanics, Heat and Mass Transfer Equations

V.K Artemyev

(Report for 11th International Heat Transfer Conference, august 23-28,1998, Kyondju, Korea)

Introduction

Present paper concerns major aspects of a numerical technique for solving fluid mechanics, heat and mass equations (Artemyev, [1-2]). A discretization of governing equations is carried out on the base of monotonous balance neutral (MBN) difference schemes, which allow keep some important integral properties of differential operators. A difference equation for pressure is derived from difference continuity and momentum equations. The discrete equations obtained are nonlinear so linearizing is introduced and implicit iterative procedure is developed for yielding converged solution. Explicit incomplete factorization method is employed for solving linearized momentum, heat and mass transfer difference equations and a variant of the method using Tchebyshev acceleration - for solving pressure equation. Results of numerical studies are presented.

Implicit numerical procedure. Monotonous balance neutral (mbn) discretization

A derivation of monotonous balance neutral (MBN) difference scheme is based upon joint consideration of transfer equation of a substance φ (φ may be a velocity component, an enphalpy, a concentration, etc.) and continuity equation in a bounded domain. The system can be written as follows

$$\rho \frac{\partial \varphi}{\partial t} + L(\varphi) = f \quad , \tag{1}$$

$$\frac{\partial \rho}{\partial t} + \frac{\partial \rho u^i}{\partial x^i} = 0 , \tag{2}$$

$$L(\varphi) = \rho u^i \frac{\partial \varphi}{\partial x^i} - \frac{\partial}{\partial x^i} \eta^{ii} \frac{\partial \varphi}{\partial x^i} \quad . \tag{3}$$

A monotonous schemes simulate important property of a fluid flow as a downstream transfer of some disturbance due to a convection motion. A balance (conservation) property is a discrete analog of the Ostrogradski-Gauss theorem. Another important relation can be obtained as the result of multiplication (1) by φ and integration over domain Q and over the time interval. The terms describing convection transfer are neutral relatively to the energy dissipation law or have null contribution.

A discretization of governing equations is carried out in a way, which allows keep above-mentioned important integral properties of differential operators. Obtained difference scheme is called as monotonous balance neutral (MBN) difference scheme. A difference equation for pressure is derived from difference continuity and momentum equations. Equation (2) is not directly included in the implicit iterative procedure but it becomes the main criterion of convergence.

Pressure, temperature, concentration are computed in the centres of grid cells, components of velocity vector - in the centres of faces. Both the MBN-scheme and a displacement of coordinates of grid functions enable to obtain physically realistic fields of computed values.

Implicit numerical procedure for prediction pressure and velocity field developed involves method of stabilization and incomplete factorization method (the subject method is related to a class of explicit incomplete factorization methods developed by Buleev (Buleev, [3]). Taking into account self-adjoint property of pressure equation it is suggested to employ incomplete factorization method with Tchebysev acceleration [4].

Results of numerical studies

Practical employment of the developed technique is connected with numerical study of transient accidental vapour-air flow in a containment, natural turbulent convection in a volumetrically heated pool, jet flow in a blind alley and others. Mathematical model may involve transient two--dimensional continuity, momentum, heat transfer equations, vapour transfer equation, equation of vapour-air mixture state, initial and boundaries conditions, other relations (full mathematical formulation is given in the paper (Artemyev, [2]).

Implicit method has been realized for a three-dimensional case and numerical investigation of natural convection of air in a cubical enclosure has been carried out (Fig.1-2). This problem is regarded as a bench mark test for numerical methods (Bessonov et al., [5]).

Implicit method is able to handle a wide variety of situations including complicated correlations between hydrodynamics and heat, mass transfer.

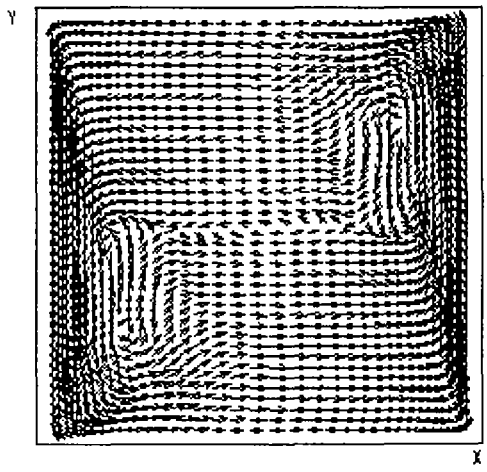

Fig.1. Natural convection in the unit cubical enclosure, flow patterns in the plane z=0.5.

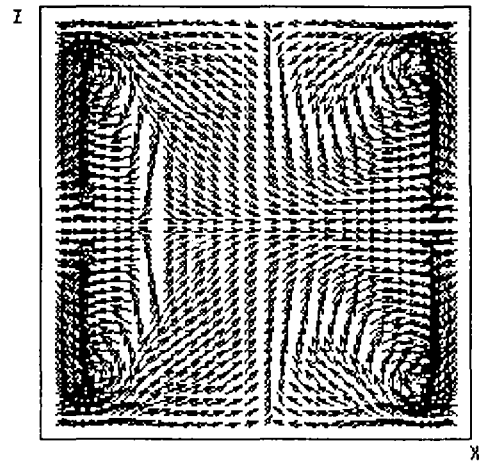

Fig.2. Natural convection in the unit cubical enclosure, flow patterns in the plane y=0.5.

References

1. ArtemyevV.K, 1992, Implicit Method for Solving Navier-Stokes Equations in Natural Variables, Modeling in Mechanics, Novosibirsk, vol. 6(23), N 1, pp.17-22.
2. ArtemyevV.K., 1997, Development of Numerical Methods for Solving Fluid Dynamics Problems, thesis, Institute of Physics and Power Engineering, Obninsk, Russia.
3. Buleev N.I., 1960, A Numerical Method for Solution of Two-Dimensional and Three-Dimensional Equations of Diffusion, Mat. Sb., 51, N 2, pp.227-238.
4. Artemyev V.K., 1990, Incomplete Factorization Method with Tchebyshev Adapted Acceleration, Preprint IPPE, N 2095, Obninsk.
5. Bessonov O.A., Brailovskaya V.A., Nikitin S.A. and Polezhaev V.I., 1997, Three-Dimensional Convection in a Cubical Enclosure: a Bench Mark Numerical Solution, Book of Abstracts. Int. Symp. On Advances in Computational Heat Transfer, Cesme, Izmir,Turkey, pp.6-8.

Development of the Analytical Closure Relationships Descriptions for One- and Two-Phase Wall Friction, Heat and Mass Transfer Coefficients for Subchannel Analysis

Y. Kornienko

The purpose of this paper is to describe the suggested approach of constructing generalized closure relationships for subchannel wall friction, heat and mass transfer coefficients, with taking into account not only axial and transversal parameter distributions, but an azimuthal substance transfer effects as well. These constitutive relations who are primordial in the description of one- and two-phase one-dimensional flow models can be derived from the initial 3-D drift flux formulation. The approach being based on the Reynolds flow, boundary layer and substance transfer generalized coefficient concepts. The one more aim is to illustrate the validity of the "conformity principle" for the limiting cases. The method proposed in this paper is founded on the similarity theory, boundary layer model and a phenomenological description of the regularity of the substance transfer (momentum, heat, and mass) as well as on an adequate simulation of the flows structure forms by a generalized approach to build (an integrated in form and semi-empirical in maintenance structure) analytical relationships for wall friction, heat and mass transfer coefficients.

A simple and descriptive approach to construct generalized three-dimensional integral relationships for the subchannel wall friction, heat and mass transfer coefficients is suggested in the paper. With help of this approach one can create integral analytical forms for the wall friction factor, heat and mass transfer coefficients accounting for the contribution of the various complementary effects. It is precisely these transversal varied profiles those are complementary effects for one-dimensional model. There are not only density (in the mixed convection problem), but also other components at the momentum, heat and mass transfer processes as well as their sources and sinks in the channel flow cross section.

Unlike the well known Kutateladze-Leont'yev (1985) relationships for the limiting friction, heat and mass transfer laws and also unlike Petukhov-Popov's relationship (Petukhov, 1987), the integral forms deduced in this paper have more generalities and they are characterized by an additive form of notation of the effects under consideration. This is significant for the criteria assessments of the contribution of the effect in question. Besides, important is not the absolute value of this effect, but the difference between a weighted value and its mean integral value.

The developed general integral relationships are recommended as a basis for the development of new phenomenological models of subchannel wall friction factor, heat and mass transfer coefficients.

Improvement and Verification of Relap5/Mod3.2 Wall Friction and Heat Transfer Models for Low Mass Flux Bubble Flow

P. Balakin, Y. Kornienko

The monotone and uniform void fraction profile two-phase flow pressure drop and heat transfer are predicted available approaches (like Lockhart-Martinelli and others) rather well. The present improvement of the friction factor and heat transfer concerns only saddle-shape void fraction effect on these integral flow characteristics. Such two-phase flows with pronounced and sharp void fraction peak in a wall region are characterized by a multiple shear stresses increasing (up to 9-10 times) on comparison with single-phase and homogeneous flows.

In the paper it is introduced the brief analytical derivation of the friction factor for improvement of the shear stresses and heat transfer with saddle-shape void profile two-phase flow on the bases of previous ICONE5-2433 two-zone model. This two-zone model taking into accounts the wall void peaking with assumption of the step-wise uniform void fraction distribution. The method suggested provide an analytical description of the abnormal wall friction and heat transfer processes that are most directly involved in effects of Archimedean forces. The developed empirical correlation for the excess wall above core average voids uses the file of being available Russian and Japanese and USA experimental data. The above mentioned improvements were introduced into the appropriate subroutines of RELAP5/MOD3.2 code.

For RELAP5/MOD3.2 calculation of the abnormal shear stresses the subroutine **fwdrag** was modified, and for calculation of the heat transfer coefficients the changes are implemented into the subroutines **dittus** and **petukv**. The two-zone model uses as the reference friction factor and heat transfer coefficient the Poiseuille-Zigrang-Sylvester and Petukhov formulas, possessed by RELAP5/MOD3.2 code. In this paper it is shown the insufficiency pseudo-grid (by bubble with Marie model) turbulization of a flow correction for the friction factor and heat transfer coefficient for adequate description for small Reynolds numbers ($Re' < 2 \div 4 * 10^3$) two-phase flows. The results of RELAP5/MOD3.2 code calculations with our abnormal models for shear stresses and heat transfer coefficients were compared for available low mass flux Russian experimental data.

These comparisons show that in most cases the original RELAP5/MOD3.2 predictions are well below corresponding experimental data. Whereas the predictions with RELAP5/MOD3.2 our modified models are more realistic description of the experimental data at low mass flux two-phase gas-liquid flows with saddle-shape void fraction a profile. Therewith, the more the excess wall above core average voids is nearer to experimental one, and the more agreement between two-zone model and the data is better.

Numerical Simulation of Crystal Growth by Floating Zone Method

V.P. Ginkin, V.K. Artemyev, N.V. Gusev, T.M. Luhanova,
I.L. Ozernyh, V.P. Shishulin, I.P.Sviridenko*

* *Scientific Investigating Centre of Cosmic System Technique,*
Koroleva 6, Obninsk, Kaluga region, Russia, 249020

Introduction

Extensive series of experiments on crystal growth by the floating zone method have been conducted aboard the FOTON satellite and aboard the MIR space station. The ZONE facilities were used for this purpose. As a result, crystals of germanium, indium antimonide, gallium antimonide 15-20 mm in diameter and 60 mm in length have been produced. The technological experiment is implemented in the following manner: a bar 15-20 mm in diameter and 110 mm in length is placed into a 30 mm quartz ampoule; the specimen is held inside the ampoule by means of 60mm long graphite inserts of intricate shape. The specimen is heated up until a melt-down zone is formed and kept for some time. After that, the ampoule starts to travel with a certain velocity relative to the heater.

The space conditions substantially extend the capabilities of the floating zone method, because the surface tension forces allow a melted zone of much larger diameter than that under terrestrial conditions, e.g. for accelerations equal to 10^{-4} g crystal diameters can be increased by a factor of 100. The experiments referred to show, however, that quality crystals could only be obtained if we develop a system for monitoring, diagnostics and control of the temperature fields and crystallization front parameters. This is where numerical simulation comes into play, considering the fact that opportunities to experiment are not unlimited.

A comprehensive numerical technique [1] for simulating conductive-radiational heat transfer in arbitrary domains in two-dimentional (r-z)-geometry was used to calculate melting and crystallization processes by the Bridgeman method [2]. The present paper employs this approach to calculate melting and crystallization processes in the floating zone method.

The paper presents a mathematical statement of the 2D nonstationary Stephen problem to simulate the process of growing crystals by floating zone method. The discretization method we used and the method for solving the problem considering conductive and radiational heat exchange are described.

Mathematical Statement of the Problem

The main mechanism that should be considered in modelling the growth process of the crystal is the heat-mass transfer in all the installation including the conductive and radiational heat exchange. A 2D- model of the process of crystal growth by the floating zone method is described in the paper. The calculational domain is a finite aggregate of physically homogeneous zones that may intersect along their boundaries only. The boundaries of the zones are cylindrical, conical surfaces; circles and rings perpendicular to the Z-axis. The domain may have cavities where heat is transferred by radiation. Two types of boundary problems for the calculational domain zones are distinguished: the heat conduction problem and the Stephen problem. The heat conduction problem describes nonstationary heat transfer in one-phase medium. It is a boundary problem for the quasilinear equation:

$$\frac{\partial(\rho h)}{\partial t} = q_v(t) + \nabla\lambda(h)\nabla T(h), \qquad (1)$$

where h stands for enthalpy, $\rho=\rho(h)$ is density, T(h) is the temperature, $\lambda(h)$ is the thermal conductivity coefficient, $q_v(t)$ stands for the density of a voluminous heat source. The functions $\rho(h)$, $\lambda(h)$, T(h) in the equation (1) are assumed to be smooth.

The Stephen problem describes nonstationary heat transfer under phase transition conditions. The statement of the problem includes two nonstationary thermal conductivity equations for different phases separated by a movable interfacial boundary subject to the Stephen condition

$$c(\vec{V}, \vec{n}) = Q^+ - Q^-, \qquad (2)$$

where c stands for phase transition specific heat, $\vec{V}$ stands for the velocity of a point on the interface, Q^+ is the normal heat flux from the phase with the lower specific enthalpy, Q^- is the normal heat flux to the phase with the greater specific enthalpy.

The interface may be multiconnected. In general the type of the boundary problem for each individual zone is actually dependent on time. The number of connected pieces of the interface in the Stephen problem may also depend on time. There is a natural relation of neighbourhood among the zones. Two zones are said to be neighbouring if they share an interzonal boundary. Transitive closure of the neighbourhood relation is the equivalence relation, which breaks the set of zones into equivalence classes. Each equivalence class is a connected piece of calculational domain that can be regarded as a united region where the equation (1) and the temperature continuity condition hold. Heat fluxes are continuous except for the interfaces between different phases where we have the equation (2). The enthalpy also has a discontinuity of the first kind on the interfaces. Heat exchange between the regions is by radiation.

References

1. Ginkin V.P., Artemyev V.K., Gusev N.V., Zinin A.I., Ozernyh I.L., Numerical Simulation of the Process of a Crystal Growth from the Melt, Proceeding of the ISSDT'95, Berg-en-Dal, Kruger NationalPark, South Africa, 15-17 November, 1995, pp 228-232.
2. Ginkin V.P., Zinin A.I., Balakin I.P. The Method of Global Calculation of Heat Transfer in Numerical Simulation of Crystal Growth. The Third International Seminar on Simulation of Devices and Technologis. Obninsk, Russia, July 5-7, 1994.

Problems of Numerical Simulation of the Single Crystal Growth Process

V.P.Ginkin

There are many papers on the numerical simulation of the SINGLE CRYSTAL growth process (see, for example, [1] and all the references presented there). At the same time, there is no established notion to single out the most efficient approach or algorithm for solving this problem now. An approach developed at the Institute of Physics and Power Engineering in Obninsk is described in the paper. The approach was originally proposed within the framework of a 2D conductive-radiative heat transfer problem in [2] and was further developed in [3]-[5].

The essential features of the process simulated are its nonstationary character and the presence of phase changes. Therefore, considering the heat transfer problem, one has to solve the Stefan problem. Different approaches for solving the problem are known presently [6], each of them having its advantages and disadvantages. We develop the enthalpy approach under which the nonstationary heat transfer equation is formulated and solved in variables of enthalpy. This approach provides a stable and efficient numerical algorithm for solving the Stefan problem.

To describe the radiation heat transfer, the method of angular coefficients is used. The main difficulties here are caused by calculation of the angular coefficient matrix for irregular forms of the radiation surfaces including heat shields situated inside of cavities. However, this problem is purely geometrical one, and we will not touch upon it in the paper. It should be noted only that the problem is solved by a scanning technique: a ray scans the visible region, then the generated image is projected on a special plane, and the projections obtained are integrated numerically.

The convective heat mass transfer is described by the Navier-Stockes equations under the Boussinesq approximation. Our approach presupposes that the Boussinesq equations are solved in the natural variables by the control volume method according to the implicit monotone conservative scheme. The equations are previously transformed to exclude the convective terms and to bring them into the divergence form by a method proposed in [7].

The outcomes of calculations of the crystal growth process by the floating zone method in conditions of a lack of a gravitation are reduced The space distributions of temperatures and velocities of a Marangony convection in a melt are obtained.

The described technique for calculating heat transfer in growing crystals from the melt has the following distinctive features:

1) heterogeneity of the domain;
2) the presence of radiation;
3) the presence of convective heat-mass transfer;
4) nonlinearity of properties, i.e. dependence of the thermophysical parameters on enthalpy;
5) nonstationarity stipulated by the time dependence of the heat generation source and the domain geometry configuration;
6) taking into account the heat of phase change;
7) validity of the model for 3D calculations;
8) possibility to increase the complexity of the model (e.g. by introduction of control magnetic field and vibration impact).

The calculational stability of the technique proposed is provided by the use of enthalpy variables in solving the heat transfer equation, by the use of natural variables and

the Patankar scheme in calculation of velocities and pressures, by the use of the Newton iteration process to solve the nonlinear system, and by the use of balanced monotonic neutral finite-difference schemes to discretize the space variable and the implicit scheme to discretize the time variable.

A high efficiency of the technique is basically provided through the use of a special organization of calculations and through performing the inner iterations by the conjugate direction method with preconditioning of initial operators by the incomplete factorization method.

References

1. Polezhaev V.I., Bune A.V., Verezub N.A., Glushko G.S., Gryaznov V.L., Dubovik K.G., Nikitin S.A., Prostomolotov A.I., Fedoseev A.I., Cherkasov S.G. Matematicheskoe modelirovanie konvektivnogo teplomassoobmena na osnove uravnenii Navie-Stoksa. M., Nauka, 1987, 271c.
2. Ginkin V.P., Zinin A.I., Balakin I.P. The Method a Global Calculation of Heat Transfer in Numerical Simulation of Crystal Growth. The Third International Seminar on Simulation of Devices and Technologies: Abstract. Obninsk, 1994, p.85.
3. Artemyev V.K., Ginkin V.P., Gusev N.V., Zinin A.I., Ozernyh I.L. Chislennoe modelirovanie protsessov teploperenosa pri vyrashivanii kristallov metodom Bridzhmena. III-i Minskii mezhdunarodny forum «Teplomassoobmen MMF-96»: tezisy dokladov, Minsk, 1996, pp.3-6.
4. Artemyev V.K., Ginkin V.P., Ozernyh I.L. Numerical Study of Convection Flow Influence on Dopant Distribution for Bridgman and Floating Zone Methods Under Microgravity. The Fifth International Conference on Simulation of Devices and Technologies - ICSDT'96: Abstract. Obninsk, 1996, p.126-127.
5. Ginkin V.P., Artemyev V.K., Gusev N.V., Luhanova T.M., Ozernyh I.L., Shishulin V.P., Sviridenko I.P. Numerical Simulation of Crystal Growth by Floating Zone Methods. International Symposium on Advances in Computational Heat Transfer. Cesme, Izmir, Turkey, 1997.
6. Vabshievich P.N. Chislennye metody resheniya zadach so svobodnoi granitsei. Moskva, izd-vo MGU, 1987, 164p.
7. Buleev N.I., Timukhin G.I. O sostavlenii raznostnykh uravnenii gidrodinamiki vyazkoi neszhimaemoi zhidkosti. Chislennye metody mekhaniki sploshnoi sredy. SO RAN, т.3, №4, 1972, c.19-26.

Monte-Carlo Methods for Solving Heat-Mass Transfer Problems under the Conditions of Non-Homogeneous Geometry

A.I. Kudryavtshev, P.A. Androsenko

1. Introduction

A new Monte Carlo technique is applied to solve mathematics physics boundary-value problems for equations of elliptic and parabolic kind under the conditions of complicated non-uniform geometry. Such equations describe wide sphere of physics problems, such as heat conduction, electrostatics, diffusion of ingredient and some other tasks. Classical method of walk by spheres is extended to the method of walk by some non-homogeneous figures, which most efficiently inscribes into limits of specific geometry.

It is well known that application of deterministic methods are limited by possibilities to describe the real geometry. It is may be useful to apply Monte Carlo methods, if employment of deterministic methods is difficulty.

Monte Carlo method based on the organization of walk process by net is universal ability for solving boundary-value problems with large dimension under conditions of irregular geometry. But, realized by this method estimate approximates the decision of difference task, don't original. Moreover, this method strongly yields to the method of walk by spheres in calculation efficiency.

In its turn, walk by spheres method, permitting successfully solve the tasks of point estimation of the decision, significantly loses calculation efficiency for the problems under the conditions of non-homogeneous geometry. It's happened because we are forced design walk by spheres process at each homogeneous subfield, and consider boundary of division as passing-repulsing barrier. This reason leads to sharp increase of computing expenditure, if even insignificant complication of internal structure is doing.

Marked considerations lead to mind about design new Monte Carlo method, that permitting to solve boundary-value problems under conditions of irregular non-homogeneous geometry. Algorithm of walk by some non-uniform figures is introduced in this paper, and walk methods by non-homogeneous spheres and parallelepipeds are described in detail. The essence of offered method is based on founding of integral presentation of the decision by Green function for some elementary forms. This technique may be called as generalizing to the non-homogeneous occasion of process of walk inside field. Note, this method enables to avoid epsilon - displacing of decision estimates by means of combining the part of external boundary with part of face of walk figure.

For example, the decision of the task with plane boundary, estimated by method of walk by parallelepipeds, will be non-displaced.

Dynamic Structure of Oxygen in Liquid Potassium Studied by MD Method and Statistical Geometry

I.Yu. Shimkevich, V.V. Kuzin, A.L. Shimkevich

Results of the molecular-dynamics simulation of K-O system in three-component approximation: $(1-\frac{2+q}{q}x)\mathrm{K}+\frac{2x}{q}\mathrm{K}^{q+}+x\,\mathrm{O}^{2-}$ where $0.25 < q \leq 1$ are presented. For calculating the MD model, a charge, q, is chosen equal to 1 on the basis of statement that dissolved oxygen in potassium melt forms clusters, $(\mathrm{K_2O})_n$ [1-3]. The MD simulation was conducted for the temperature of 550K as NVT ensemble of 2000 particles (N_K = 1490, N_{K^+} = 340, $N_{O^{2-}}$ = 170) in a cubic cell with periodic boundary conditions. The cube edge length, L= 54.004 Å, has been selected according to the oxide mass density, ρ_{K_2O} = 2320 kg·m^{-3}, at the given oxygen atomic concentration of 8.5% for unsaturated solution at 550 K [4] and the mass density of liquid potassium, ρ_K = 777 kg·m^{-3}.

Born-Mayer's potential without dispersion terms [5] is used for describing (K^+,K^+), (K^+,O^{2-}), (O^{2-},O^{2-}) and (K,O^{2-}) interaction with parameters $Z_{O^{2-}} = -2$, $Z_{K+} = 1$, Pauling's coefficients: $C_{K^+K^+} = 1.25$, $C_{K^+O^{2-}} = 1.0$, and $C_{O^{2-}O^{2-}} = 0.75$, the ionic sizes: σ_{K^+} = 1.39Å and $\sigma_{O^{2-}}$ = 1.33Å, the repulsive parameter: B = 0.21098 eV, the softness parameter: A = 3.45Å^{-1}, and the number of electrons in the outer shell, $n_{K^+} = n_{O^{2-}} = 8$. For (K,O^{2-}) interaction $Z_K = 0$ and $n_K = 1$.

The potential for describing interaction between the neutral potassium atoms (K,K) and ions (K,K^+) is common for two runs. In the first case, it is Lennard-Jones' (*n-m*) potential [6] with parameters: ε = 0.0614 eV, n = 6.5, m = 4.5, r_0 = 4.8359 Å. In the second one, the potential evaluated for treating the electron-ion coupling in the frame of the pseudo-potential concept (*ps*) and linear screening theory [7] with k_f = 0.7076Å^{-1}, R_c = 1.1854Å, and ν = 1.8253 .

The potassium/oxygen ternary system was simulated in the condition of charge exchange between each potassium ion and a nearest potassium atom over the 50 time steps. As realizing the charge exchange, the system relaxed to equilibrium. Then, such characteristics as the partial radial distribution function, $g_{\alpha\beta}(r)$, structure factor, $S_{\alpha\beta}(k)$, velocity auto-correlation function, $\Psi_{\alpha\beta}(t)$, frequency spectrum, $f^n_{\alpha\beta}(\omega)$, and self-diffusion coefficients, $D_{\alpha\beta}$, were calculated in given time moments $t \leq 1.05\cdot10^{-10}$ s. An addition investigation of cluster configurations has been conducted by statistical geometry method [8].

The influence of both (*n-m*) and (*ps*) potentials is small and not change the main conclusion about the system behaviour. The function, $g_{KK}(r)$, has the same form as, $g_{KK^+}(r)$, the function, $g_{KO^{2-}}(r)$, has a weekly oscillating form, and $g_{K^+O^{2-}}(r)$ has a narrow peak. The function for ions characterised by widened first peak of $g_{K^+K^+}(r)$ and small splitting the first one for $g_{O^{2-}O^{2-}}(r)$. The $\Psi_{K^+K^+}(t)$, $\Psi_{K^+O^{2-}}(t)$, and $\Psi_{O^{2-}O^{2-}}(t)$ are strong oscillatory. The diffusion coefficients of D_{KK}, D_{KK^+}, and $D_{KO^{2-}}$ are in the range of 0.8 to 1.2 10^{-1} [Å^2/ps], $D_{K^+K^+}$, $D_{K^+O^{2-}}$, $D_{O^{2-}O^{2-}}$, in the range of 0.3 to 0.05 10^{-1} [Å^2/ps]. The spectra including potassium partial have dominating frequency of atom vibration at ε_{max}

in the range of 3.5 to 11.0 meV (Fig. 1a), where ε denotes $\hbar\omega$. Otherwise the oxygen spectrum, $f^{n}_{O^{2-}O^{2-}}(\varepsilon)$, has the main peak of $\varepsilon_{max} \approx 50$ meV (see Fig. 1b).

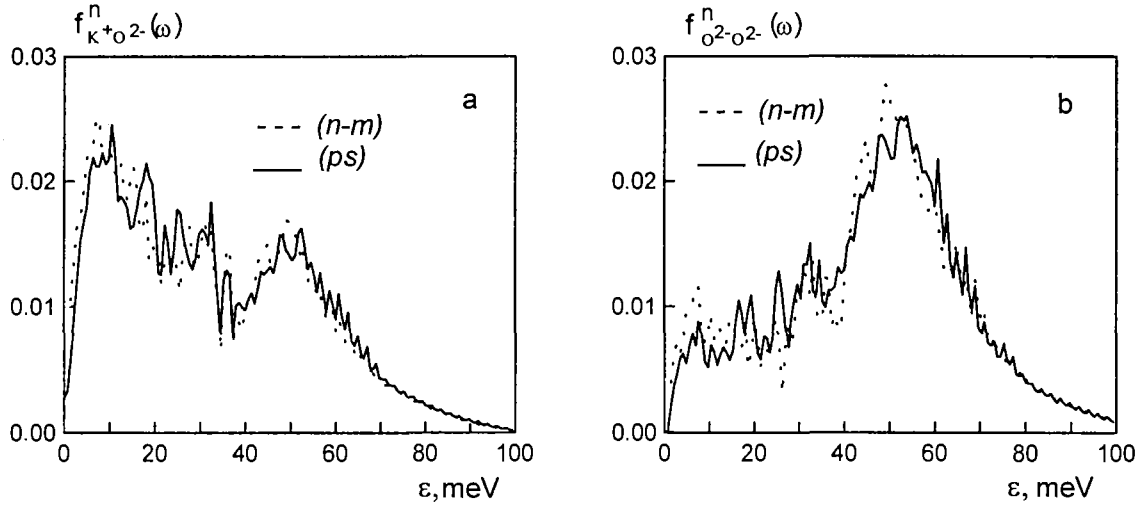

Fig. 1. The partial frequency spectrum for $K^{+}O^{-}$ (a) and $O^{2-}O^{2-}$ (b) at t=1.05·10^{-10} s.

The low values of partial diffusion coefficient for ionic pairs, $D_{K^+K^+}$, $D_{K^+O^{2-}}$, $D_{O^{2-}O^{2-}}$, and strong oscillatory modes of oxygen frequency spectrum reflect the formation of clusters in the unsaturated solution of oxygen in potassium melt [9]. The dominant values of high frequencies in oxygen spectrum, $f^{n}_{O^{2-}O^{2-}}$, and the low ones in partial potassium spectra indicate to oxygen clusterization in potassium melt where such the clusters exchange lightly potassium ions with the melt. This is consistent with the experimental data [10] that oxygen forms in liquid potassium microinclusions of $(K_2O)_n$ type which has the molten cation sublattice. The analysis of atomic configurations in the MD cell by means of the statistical geometry confirms the formation of such the clusters (see Fig. 2), in where big circles are oxygen anions and small circles are potassium cations.

So, the proposed simulation model allows the process of impurity behavior to study as an atomic clusterization in liquid alkaline metals.

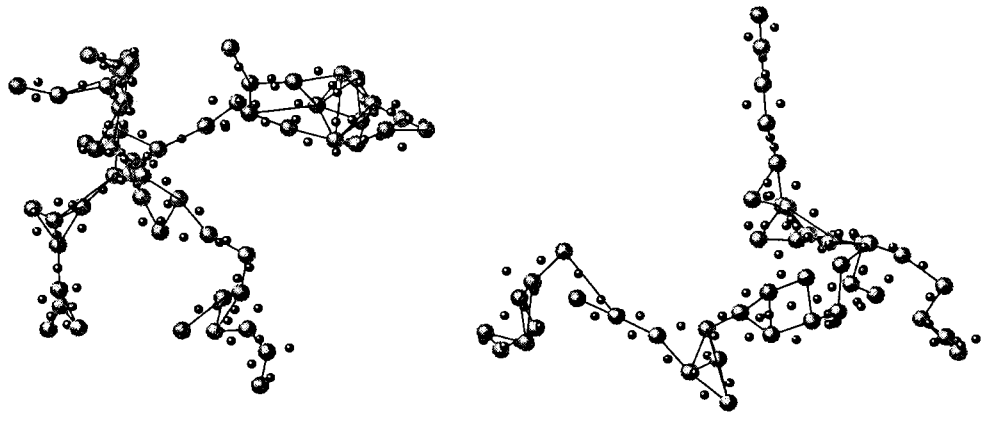

a) b)

Fig. 2. The greatest oxygen clusters in the MD run of 1.05·10^{-10} s for (*n-m*) potential (a) and for (*ps*) potential (b).

Acknowledgments
This work was supported by grant from the Russian Foundation for Basic Research (Project #96-02-1631a).

References

1. M.N. Ivanovsky, V.A. Morozov, N.N. Ponomarev-Stepnoi, and A.L. Shimkevich, Atomnaya Energia (Atomic Energy), V.65, N.5, 1988, P.319.
2. M.N. Ivanovsky, V.A. Morozov, A.L. Shimkevich, and B.A. Shmatko, (Liquid Metal Eng. and Technology, London, BNES, 1984) V. 3, P.15-22.
3. M.N. Ivanovsky, V.A. Morozov, A.L. Shimkevich, and B.A. Shmatko, Teplofizika Vysokikh Temperatur (J. High Temperature), V. 21, N 5, 1983, P.909.
4. M.N. Ivanovsky, A.G. Novikov, V.V. Savostin, A.L. Shimkevich, and M.V. Zaezjev, High Temperature, V. 32, N 5, 1994, P.701.
5. J.T.W.M. Tissen and G.J.M. Janssen, Mol. Phys. V.71, N.2, 1990, P.413
6. Shu Zhen and G.J. Davies, Phys. Stat. Sol. 78A, 1983, P.595.
7. K.C. Jain, N. Gupta, N.S. Saxena, Phys. Stat. Sol. 162B, 1990, P.395.
8. V.V. Kuzin, V.A. Morozov, A.L. Shimkevich, I.Yu. Shimkevich, Preprint IPPE–2415, Obninsk, 1994.
9. A.L. Shimkevich, Fluctuation Theory for Non-Homogeneous Melts, Workshop on Condensed Matter Physics, Lviv, May 21-24, 1998.
10. A.G. Novikov, V.V. Savostin, A.L. Shimkevich, and M.V. Zaezjev, (Tenth International Conference on Liquid and Amorphous Metals, 1998, LAM 10, Dortmund, UNI DO, LM27).

2-nd Kalinin NPP Unit in 10-th Fuel Cycle

Yu.I. Lihachev, V.P.Ginkin and other

Specific feature of 10-th fuel loading of second Kalinin NPP unit is an usage of 42 Serial Fuel Assemblies (SFAs) of different enrichments with modified heads.

The fresh SFAs which used in 10-th fuel loading are as follows:

1 SFA with enrichment 3.0%

36 SFAs with enrichment 4.4%, with Burnable Absorbtion Rods -BARs- (g=0.036 g/sm^3),

24 profiled SFAs with average enrichment 4.23%, with BAR (g=0.036 g/sm^3).

For SFAs used staff profile scheme.

Accommodate scheme of 42 SFAs with modified heads is presented in the figure 1.1.

Calculations of boron fuel cycle are held with the code WIMS-VOLNA [1] for nominal parameters and 80% positions of Control Rods (CR) working group from the bottom of the core in four-group diffusion approximation for the sector of symmetry 60 degrees. On the figure 1.2 are presented changing of the Assembly Power Peaking Factor (Kq) and Volume Power Peaking Factor (Kv) during boron fuel cycle.

Calculations have shown that during 10-th fuel cycle Kq and Kv are accepted to design restrictions.

The required data for thermo-mechanical calculations are:

- distribution of neutron flux with the energy above 0.1 Ìev on the corners of SFAs;
- distribution of heat generation rate ql per unit of SFA length on the corners of SFAs;
- distribution of fuel elements shell temperature on the corners of SFAs;
- distribution of Volume Power Peaking Factor in the core;
- distribution of the fuel burn-up in the volume of the core.

These data are prepared by means of the code WIMS-VOLNA and will be sent in coordinated formats for further processing in thermo-mechanical code.

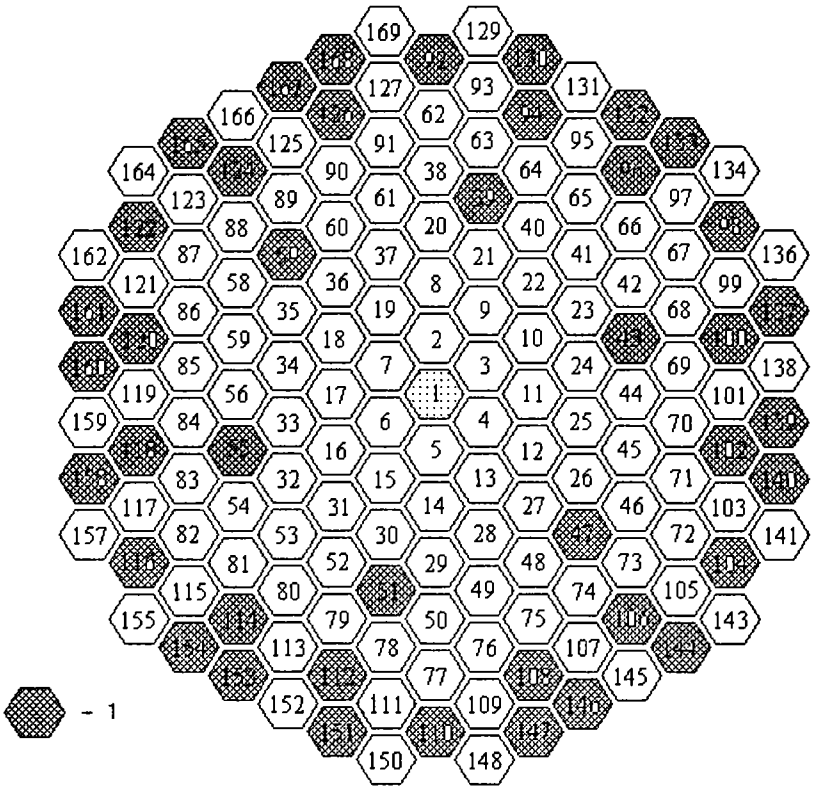

Fig. 1.1. Scheme of accommodation of SFA in the 10-th fuel loading of 2-nd Kalinin NPP unit (1 - SFA with modified heads).

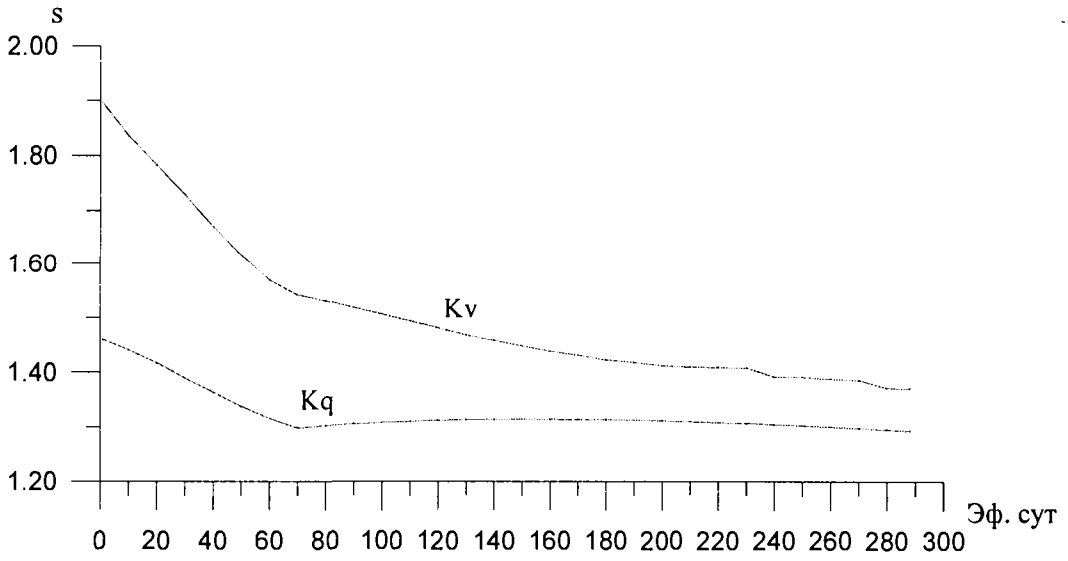

Fig. 1.2. Changing of factors Kq and Kv during 10-th fuel cycle of 2-nd Kalinin NPP unit.

Reference

1. Проведение нейтронно-физических расчетов реальных состояний активной зоны реактора ВВЭР-1000. Отчет ФЭИ - 9258, Обнинск, 1996 г.

3-d Zaporogie NPP Unit in 10-th Fuel Cycle

Yu.I. Lihachev, V.P.Ginkin and other.

Particularity of 10-th fuel loading of 3-d Zaporogie NPP unit is the test operation of 12 Zirconium Fuel Assemblies (ZFAs).

Only Serial Fuel Assemblies (SFAs) entered in the 9-th fuel loading of 3-d Zaporogie NPP unit composition.

The fresh SFAs which used in 10-th fuel loading are as follows:

24 profiled SFAs with average enrichment 4,23 %,

12 SFAs with enrichment 4,4% ,

12 ZFAs with average enrichment 3,92%, with zirconium Spacer Grids and Guide Tubes and diameter of central hole in fuel pellet 1.5 mm. Guide Tubes and Central Tube have an external diameter 13 mm, internal - 11 mm and made from the alloy Ý635.

For SFAs and ZFAs used staff profile scheme.

The Burnable Absorption Rods (BARs) with the natural boron concentration g=0.036 g/sm^{3}set in the fresh SFAs, and BARs with g=0.065 g/sm^3 set in ZFAs.

Accommodate scheme of 12-th ZFAs is presented on the figure 1.1.

Calculations of boron fuel cycle are held with the code WIMS-VOLNA [1] for nominal parameters and 80% positions of Control Rods (CR) working group from the bottom of the core in four-group diffusion approximation for the sector of symmetry 60 degrees. On the figure 1.2 are presented changing of the Assembly Power Peaking Factor (Kq) and Volume Power Peaking Factor (Kv) during boron fuel cycle.

Calculations have shown that during 10-th fuel cycle Kq and Kv are satisfied to design restrictions.

The required data for thermo-mechanical calculations are:

- distribution of neutron flux with the energy above 0.1 Ìev on the corners of SFAs;
- distribution of heat generation rate ql per unit of SFA length on the corners of SFAs;
- distribution of fuel elements shell temperature on the corners of SFAs;
- distribution of Volume Power Peaking Factor in the core;
- distribution of the fuel burnup in the volume of the core.

These data are prepared by means of the code WIMS-VOLNA and will be sent in coordinated formats for further processing in thermo-mechanical code.

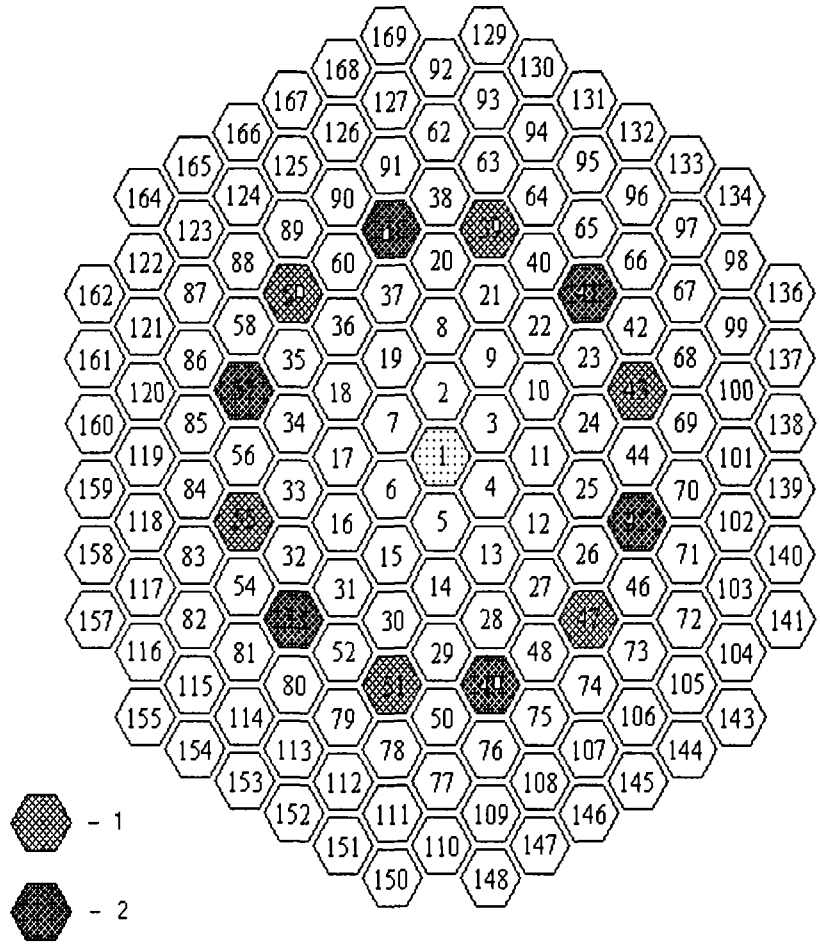

Fig. 1.1. Accommodate scheme of 12-th ZFAs in 10-th fuel loading of 3 Zaporogie NPP unit:
1 - ZFAs of AOO MC3's production,
2 - ZFAs of AOO H3XK's production.

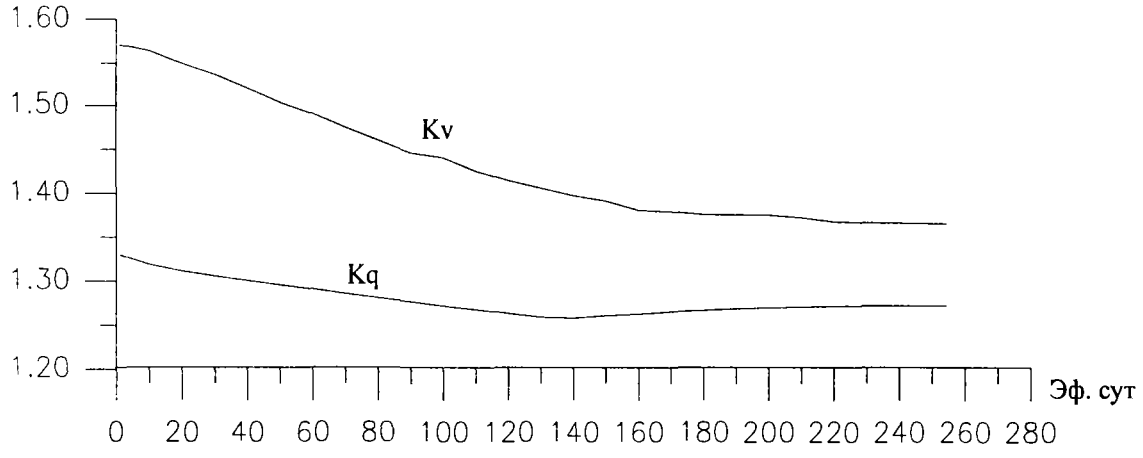

Fig. 1.2. Changing of factors Kq and Kv during 10-th fuel cycle of 3-d Zaporogie NPP unit.

Reference

1. Проведение нейтронно-физических расчетов реальных состояний активной зоны реактора ВВЭР-1000. Отчет ФЭИ - 9258, Обнинск, 1996 г.

2.7 APPLIED RESEARCH

New Construction of Plasmafilter with Track Membranes

B.I. Fursov, M.I. Sotov, V.P. Timokchovitch

The original design and technology for membranes plasmafilters (MPF) production have been developed recently at JSC "Optica" (St-Petersburg). The MPF are used in procedure of plasmapheresis - the process of plasma separation from human blood. The thin lavsane film (10μm) used for the MPF production provides some advantages in compare with another filters: a correct cylinder shape with diameter ~0.5μm, smooth surface, small thickness, low absorption and others. This allow us to increase transmembrane pressure (up to 250 Hg mm) and reduce of the erythrocites trauma. In an addition, in the MPF blood moves as a flat flux that provide optimal hydrodynamic.

However, developed device has a disadvantage which limited their application. It is low strength of junction of track membranes (TM) with hermetization materials, that connected with production technology (block production) and peculiarity of the construction (the junction of TM with hard cassette used for fixation).

We developed new construction (patent application "Plasmapherisator PMP-IPPE", output number 98115103 from 04.08.1998) that overcome this problem.

The test experiment with water allow us to conclude that this construction provide hermitezation of the junction with pressure 0.2MPa between blood and plasma chambers.

New Method of Water Purification with Track Membranes Filters

M.I. Sotov, G.S. Zhdanov, V.P.Timokchovitch

For the first time the track membrane (TM) have been applied for water purification in the device named as "Kriskaia rosinka", which is known now as "NEROX" filter. The diffusion of water due to capillary effect without an additional pressure provides the filtration process in this device. The yield of pure water is $(1.5\text{-}2.3)10^{-3}$ l/h from square centimeter of the TM.

Our recent investigation demonstrated that it is possible use the TM in pressure filters applied for water purification. The TM with pore diameter 0.4μm may provide:

- water yield 0.1 l/h/cm^2 for pressure 0.2MPa;
- operation resource of TM is 70 l/cm^2 with the regeneration after each 0.5 l/cm^2.

The operation resource depends on the method and regeneration interval of its surface. The tangent cleaning of the surface is more effective process that should be repeated after 50% reduction of the water yield.

The beginning yield is rather high. For example, for the TM with pore diameter 1μm it is ~60m^3/h/m^2/ata. However, the yield reduces very much to the quasistationary level ~5m^3/h/m^2/ata which is the same for pore diameter 1μm and 2μm.

The effectiveness of the TM for pressure filtration is demonstrated for "NEROX" filter element (FE). The standard "NEROX" FE may produce ~15 l/day of pure water. The same FE with pressure filtration with proper regeneration gives ~55l/h.

The several pilot samples for wide application have been developed. They may provide low water yield (0.01-0.1) m^3/h, middle water yield (0.1-1) m^3/h and high yield (1-10) m^3/h.

The component price for low yield FE are:

- vessel - 4 USD (100 units);
- TM - 30 USD/m^2 (~11 USD per FE, Dubna production);
- production (handle operation of FE) - 3 USD.

The total cost ~18 USD.

However, it is possible to reduce the cost.

- vessel ~2 USD (>1000 units);
- TM - 8 USD/m^2 (~2.5 USD per FE, IPPE production);
- production ~1 USD (less of handle operation).

The total cost ~5.5 USD.

The cost of another FE types may be estimated in the same way.

Structural and Selective Properties of Track Membranes "REATRECK-IPPE"

B.I.Fursov, G.V.Anikin, V.I.Bolshov, G.S.Zdanov, T.A.Krasavina, V.G.Nesterov, A.A.Tumanov, P.A.Abramov[1)], D.L.Zagorski[1)], A.N.Netchaev[1)], B.V.Mchedlishvili[1)], A.V.Sergeev[1)]

[1)] - *Institute of Crystallography RAS*

Structural and selective properties of the nuclear track membranes mainly depend on the following characteristics:

- angular pore distribution in the bulk of a polymeric matrix;
- calibration of the pore shape and size;
- homogeneous distribution of the pores on the surface of a track membrane.

These essential characteristics make the nuclear track membranes superior to conventional items with the tracks produced by accelerated ions.

Geometry of the pore distribution is determined by absolutely isotropic space distribution of the fission fragments emitted from uranium targets. All heavy ions, when accelerated, have parallel trajectories. To achieve angular distribution of the tracks in a single plane, the film is irradiated using "on-the-drum" effect. All attempts to achieve simultaneous angular distribution in another plane, i.e., in the polymer bulk, have been hardly possible so far because of insoluble technical problems.

It is well known that fission fragments greatly vary in mass, charge and kinetic energy. It is significant for production procedure, that almost all fragments are composed of the elements with a high effective charge and an average mass from krypton to xenon. Therefore, a destructive effect of these elements is the highest in the whole range of heavy accelerated ions used for production of the track membranes. The rate of the core track etching of any fragment in polyethylene terephthalate is (1-3)104 times higher that of undamaged polymer. That is why all pores of the nuclear track membrane have a cylindrical shape and calibrated size.

Homogeneous distribution of the pores on the surface of a nuclear track membrane is (3-5)%, which is due to uniform target thickness, stable speed of film irradiation inside the facility and control of the reactor power.

At high pore density imposition of the tracks on the membrane surface will be similar irrespective of irradiation technique because the number of impositions increases with increasing pore density. Selective properties of the membranes drastically depend on whether a pore imposition pattern at a certain section of one surface can be projected on the reverse side. If pores have parallel trajectories (acceleration method), track imposition causes the formation of through holes with uncontrollably large diameter, and thus significantly decreases selectivity of the membranes. In nuclear membranes angular distribution of the tracks in the polymer bulk is perfectly isotropic. In this case pores intersect membranes at random angles and have a statistically homogeneous distribution in any plane and direction. As a result, each pore contained in any association imposed on the membrane surface has an exit to a different pore association on the reverse side. This microstructure of the nuclear track membranes decreases the probability of forming the pores of uncontrollably large size by several orders of magnitude.

Thus, the attractive features successfully combined by the method of reactor irradiation give rise to a new perfect quality structure of the track membranes, i.e., isotropic angular distribution of the tracks in space, equal diameters of the cylindrical

pores and uniform density of the pores on the membrane surface. It is a perfect structure that ensures a reliable sterilizing effect for nuclear track membranes, and thus, makes them promising for such application as liquid and gas filtration.

The Table gives a list of performance characteristics for tested microfiltration track membranes "REATRACK-IPPE". Selectivity was determined on the rigid and calibrated ball-shaped particles of 0.3 (m in diameter, which are close in size to bacterium Pseudomonus diminuta. The calculations were made by equation $\varphi+(1-C_f/C_0)100\%$, where C_0 is the initial concentration of latex, is C_f the concentration of latex in a filtrate, φ is the selectivity.

Sample number	Porous diameter, μm	G_{sp}, $m^3/m^2 \cdot h \cdot Atm$	C_0, particles/ml	C_f, particles/ml	φ, %
1	0,16	2,7 ± 0,2	$2 \cdot 10^8$	0	100
2	0,18	5,6 ± 0,5	$2 \cdot 10^8$	0	100
3	0,21	8,4 ± 0,7	$2 \cdot 10^8$	$1,3 \cdot 10^6 \pm 5\%$	99,4
4	0,23	10,5 ± 0,8	$2 \cdot 10^8$	$2,7 \cdot 10^7 \pm 5\%$	86,5
5	0,26	13,8 ± 0,9	$2 \cdot 10^8$	$5,2 \cdot 10^7 \pm 5\%$	74,0

Reactors Track Membanes "REATRECK-IPPE": Technology, Characteristics, Properties

B.I.Fursov, G.V.Anikin, V.I.Bolshov, G.S.Zdanov, T.A.Krasavina, V.G.Nesterov, A.A.Tumanov

The industrial production of polymer track membranes was created in the IPPE. The technology is based on the irradiation of polymeric films (polyethylene terephtalate) by fission fragments in nuclear reactor BR-10 and on the advanced methods of physico-chemical treatments. The manufactured articles represent new generation of track membranes and these one have more high selectivity, productivity and resort of filtration process than existing analogs (COSTAR-NUCEPORE, USA). Developed track membranes can be used in the purification, separation and sterilizing filtration processes of liquids and gases.

The equipment for irradiation of polymeric films in nuclear reactor includes stainless steel cylindrical vacuum chamber of 3 m length and 0,5 m in diameter. This chamber is placed in graphite thermal column of the nuclear reactor. High flux of thermal neutrons ($\sim 10^{12}$ $cm^{-2} \cdot s^{-1}$) produce fissions in uranium-235 target, which contain two thin (0.3 mg/cm^2) fissile layers on aluminum backing with linear dimensions 300×500 mm^2. Bombardment of polymer films by fission fragments is produced isotropically into certain solid angle interval 0^0 - 35^0. Large size of uranium target of regular thickness and constant speed of film movement provide high (3-5%) homogeneity of pore density.

The statistically distributed pores on the track membrane surface can be partially overlapped, but nonparallel tracks isotropically distributed in solid angle exclude large through pores. This principal factor of reactor track membranes provide fine microstructureis and high selectivity of reactor track membranes.

Main shortcoming of the method based on the bombardment with fission fragments in nuclear reactor is the fission fragment radioactivity. But conditions of polymer films irradiation (thin uranium fissile layer, special collimator system) and the following chemical treatment make the radioactivity of track membranes extremely small. During pause about two months after irradiation the reactor track membranes with the pore density of 10^8 cm^{-2} have specific radioactivity less than 0.01 Bq/cm^2. Thus reactor track membranes in accordance with Standard of Radiation Safety (SRS-96) are not radiation source and can be used without any limitations.

Technological regulations of the reactor track membrane manufacturing provide six months of storage. It gives supplementary quarantee of lack reactor track membranes radioactivity. The radiation safety of reactor track membranes was confirmed by results of examination by independent experts of some specialized organizatoins. Toxicology safety of track membranes was confirmed by control of organizations of Ministry of Public Helth.

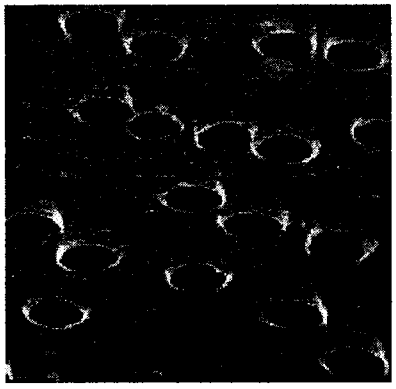

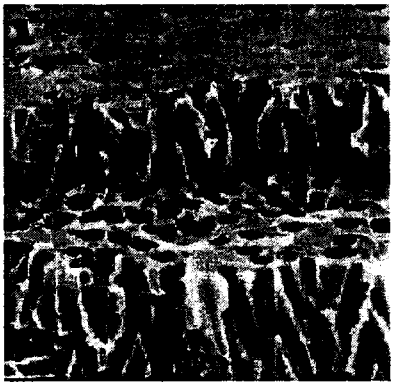

In conclusion let us list the basic properties of reactor track membranes manufactured in IPPE:

- band width 320 mm, band length up to 3 000 m;
- film thickness from 8 to 12 μm;
- diameter of cylindrical pores from 0,05 to 5 μm;
- pore size dispersion ~5 %;
- pore density from 10^5 to $5 \cdot 10^9$ cm^{-2};
- pore density uniform ~5 %;
- porosity from 7 to 20 %.

Low-Activation Materials with Isotopic Tailoring for Future NPPs

G.L. Khorasanov, A.P. Ivanov, A.I. Blokhin,
V.A. Apse[+], A.N. Chmelev[+], A.A. Glazkov[+], A.D. Koljaskin[+]

[+]*Moscow State Engineering Physics Institute.*

Presently, a great attention is devoted to the problem of materials with low level of induced radioactivity. For fusion devices the possibility of low-activation ferritic and martensitic, and vanadium steels creation using isotopic tailoring has been considered by several authors [1,2]. The goal of present paper is to recognize such perspectives for nuclear power facilities. Challenges of construction of two type low-activation materials for NPP will be analyzed.

The first considered material to be improved by isotopic tailoring is a zirconium alloy. It is known that such alloys are widely used in LWR. After decommissioning its mined geologic disposal is required due to accumulation of long-lived zirconium isotope Zr-93, which is generated in natural zirconium Zr-nat by Zr-92(n,γ)Zr-93 reaction. The possibility to avoid the Zr-93 accumulation by the enriching of natural zirconium with his stable isotope Zr-90 is considered.

The following calculations were carried out:

- an estimation of isotopic composition of a product and dump during natural zirconium enrichment;
- an estimation of Zr-nat and Zr-90 radioactivities induced by irradiation in the VVER-1000 reactor fission neutron spectrum;
- an estimation of enrichment required for the fast decay of radioactivity;
- an estimation of energy costs to be spent to achieve the required enrichment.

The calculations performed show that Zr-nat enriching by Zr-90 up to 99% of its composition permits the tailored material to decrease its radioactivity to hands-on level after 3 years irradiation time and 5 years cooling time.

The another our example of isotopic tailoring usefulness is concerned with a heavy liquid metal coolant in a fast reactor. Last time, a new safe fast reactor with a lead coolant was proposed in Russia [3]. Our main concern is with the way for the low induced activity of this coolant after its irradiation by the fast reactor fission neutron spectrum. It might be supposed that enriching of natural mixture of lead isotopes Pb-nat by his stable isotope Pb-208 gives such a possibility. Indeed, reactions of (n,γ) and (n,xn) types are of the great importance for a fast reactor. Thus, if the lead coolant consists of 100% of Pb-208, its products will be mainly stable isotopes Bi-209, Pb-207 and Pb-206 after irradiation by the fast neutron spectrum.

Calculations of the transmutation of elements and the induced radioactivity were performed using the FISPACT-3 inventory code [4], activation cross-section library FENDL-2/A and decay data library FENDL-2/D [5]. The analysis of time-dependent radioactivity and contact dose rate after shutdown were carried out under following conditions:

- the neutron spectrum is taken as for central zone of the BOR-60 fast reactor;
- total flux of fission neutrons is equal 5.0·10+15 n/cm2/s;
- irradiation time is equal 1 year;
- mass of material irradiated is equal 1 kg;
- cooling time after shutdown is equal 10-8 - 10+3 years.

Some results of induced dose rate and activity at several cooling time up to 1000 years for Pb-nat, Pb-208, Bi-209 and Na-23 are presented. According to these results, it might be concluded that radiotoxicity of Pb-208 coolant decays essentially faster than one of Pb-nat or Na-23, that is very important for the problem of reactor decommissioning and accidents connected with coolant losses.

References

1. Kohayama et al. Low activation ferritic and martensitic steels for fusion application. - J.Nucl.Mater., v.233-237, p. 138-147 (1996).
2. N.P. Lyakishev et al. Prospect of development and manufacturing of low-activation metallic materials for fusion reactor. - J.Nucl.Mater., v.233-237, p. 1516-1522 (1996).
3. V.V.Orlov. Nuclear power of the next stage: profitable U-Pu breeding, safety, radwastes, nonproliferation. - Yadernaya Energetica, N5, p. 57-59 (1997).
4. R.A. Forreset, J.Ch. Sublet. FISPACT-3 user manuel. - Report AEA/FUS/227 (1993).
5. A.B. Pashchenko. Summary report on the IAEA advisory group meeting on completion of FENDL-1 and start of FENDL-2, Del Mar, California, USA, 1995, Report IAEA/INDC(NDS)-352 (1996).

Method and Set-Up for Measurements of Trace Level Content of Heavy Fissionable Elements Based on Delayed Neutron Counting

V.M. Piksaikin, A.A. Goverdovski, G.M. Pshakin, S.G. Isaev

Experimental method and set-up for content determination of fissionable elements in samples

Experimental set-up primarily was designed and successfully used for the investigations of the delayed neutron yields from neutron induced fission of heavy nuclei [1]. The set-up was installed at the electrostatic accelerator KG-2.5 and has the following main parameters: ion (proton and deuteron) current - up to 500 μA, pneumatic sample delivery system - 150 ms and 1 s for 'fall down' sample delivery system, high voltage - up to 2 MV, neutron flux monitor - calibrated fission chamber, neutron detector - 30 boron counters embedded in the polyethylene moderator. Neutron detector efficiency is 0.084 with very low sensitivity to gamma-ray background of the sample under investigation. The intensity of the neutron background during delayed neutron counting period is about 0.008 counts/s per 1 μA of deuteron current in case of the (d,n) neutron production reactions.

The value of parameters of the set-up allow to estimate the (detectable concentration) detection limit of fissionable elements (as well as minimal detectable amount) in the samples for the neutron source based on the $^{9}Be(d,n)^{10}B$ reaction and deuteron ion current of 500 μA [2]. It was assumed that for the reliable analysis one needs to register one hundred delayed neutron counts above the background. The result of the estimation for thorium, uranium and plutonium elements are presented in the Table 1.

Table 1.

Sensitivity of delayed neutron counting technique in the analysis of the content of fissionable elements in the samples.

Nuclide	Minimal detectable amount*, g		Detectable concentration*, g/g	
	Fast neutron flux	Thermal neutron flux**	Fast neutron flux	Thermal neutron flux**
^{235}U	$6.3 \cdot 10^{-6}$	$1.5 \cdot 10^{-6}$	$1.3 \cdot 10^{-8}$	$3 \cdot 10^{-9}$
^{238}U	$1 \cdot 10^{-5}$		$2 \cdot 10^{-8}$	
^{239}Pu	$1 \cdot 10^{-5}$	$2.6 \cdot 10^{-6}$	$1.9 \cdot 10^{-8}$	$5 \cdot 10^{-9}$
^{232}Th	$1.7 \cdot 10^{-5}$		$3.3 \cdot 10^{-8}$	

*) amounts which were obtained at the experimental conditions indicated in the text,
**) degradation of the neutron flux in the neutron slowing down process was taken into account.

Ten cycles of irradiation and delayed neutron counting were taken into consideration. The sample irradiation time was 100 s and the delayed neutron counting time was 25 s starting at 1 s after the end of irradiation. The total time spent for analysis was 1260 s. The estimation was made both for the fast neutron flux from the $^{9}Be(d,n)^{10}B$ reaction at 2 MeV deuteron energy and for the thermal neutron flux which can be easily obtained by slowing down the neutrons from the neutron target. Degradation of the neutron flux during the neutron slowing down process was accounted for.

The combination of the fast neutron flux and the thermal neutron flux analysis allows to make the identification of the isotopic content of the sample.

Method of identification of isotopic content of sample

Until now the identification of isotopic content of the sample in the frame of the DN counting technique was based on the difference between the values of relative abundances of the definite DN group for different nuclides [3]. This method requires a high statistical accuracy of DN decay curve [4] and reliable data base for the DN group parameters (decay constants and relative abundances). The first condition is difficult to reach because of small amount of fissionable elements in the sample.

We propose another approach for the identification of isotopic content of sample, which is based on the new systematic of the delayed neutron parameters [5]. According to this systematic the average half-life of the delayed neutron precursors for the isotopes of thorium, uranium, plutonium and americium elements can be presented by the following expression

$$\langle T_i \rangle = a_{1i} \cdot \exp\left[(a_{2i}(-(A_c - 3Z) \cdot A_c / Z)\right], \qquad (2)$$

where index i is related to the certain fissioning systems (thorium, uranium, etc.), A_c and Z - the mass number and atomic number of the fissioning nuclei respectively. The experimental data on the average half life parameters were obtained using the formula

$$\langle T \rangle = \sum_{i=1}^{6} a_i t_i ,$$

where a_i and t_i are the relative abundance and period of the i-th DN group.

Thus all of the known isotopes can uniquely be identified by only one parameter - the average half life of the delayed neutron precursors. Therefore for the identification of the isotopic content of the sample one needs to make measurements and the least squares analysis of DN decay curve with the purpose to obtain the value of average half life parameter (for the mixture of nuclides). As compared with the six group parameters analysis [4] such analysis can be done using decay curves with much less statistical accuracy. In the case of presence of two nuclides in the sample the obtained value $\langle T_{1,2} \rangle$ is connected to unknown value of the fractional amount of the number of atoms of nuclides 1 and 2 by the following expressions

$$\langle T_{1,2} \rangle = (\nu_1 \sigma_1 \varphi m_1 \langle T_1 \rangle + \nu_2 \sigma_2 \varphi m_2 \langle T_2 \rangle)/(\nu_1 \sigma_1 \varphi m_1 + \nu_2 \sigma_2 \varphi m_2),$$

$$m_1 + m_2 = 1,$$

where ν_1 , ν_2 - the total delayed neutron yields related to nuclide 1 and 2, σ_1 , σ_2 - the fission cross section of nuclides 1 and 2, $\langle T_1 \rangle$, $\langle T_2 \rangle$ - the average half life of DN precursors of nuclide 1 and 2, m_1 , m_2 - the fractional amount of the number of atoms of nuclide 1 and 2 respectively, φ - the neutron flux through the sample.

References

1. V.M. Piksaikin, Yu.F. Balakshev, et al. Measurements of periods, relative abundances and absolute total yields of delayed neutrons from fast neutron induced fission of ^{237}Np. Proc. Inter. Conf. on Nuclear Data for Science and Technology, Trieste, Italy, May 19-24, 1997, p.
2. N.A. Lose. Nuclear data for industrial neutron sources. Proc. Inter. Conf. on Nuclear Data for Science and Technology, Julich, 13-17 May, 1991, p.678-680.
3. B.P. Maksjutenko, Yu.F. Balakshev, et al. Determination of percentage content of ^{235}U and ^{239}Pu mixture using delayed neutrons, Atomic energy (in Russian), 1975, v.39, N.6, p.420-422.
4. G.R. Keepin. Physics of Nuclear Kinetics, Addison-Wesley Pub. Co., 1965.
5. V.M. Piksaikin, S.G. Isaev. Correlation properties of delayed neutrons from fast neutron induced fission. Report INDC(CCP)-415, IAEA, Vienna, 1998.

Insulating Material Activation in Fusion Reactor Spectrum

G.L.Khorasanov, A.I.Blokhin and M.V.Mikhailyukova

Insulating materials will be required for numerous components of fusion reactor including RF windows, MI cables and wire insulation. The main candidate material for these applications is Al_2O_3, both in the polycrystalline alumina form and as single crystal sapphire.

It is known that irradiation of natural aluminum, Al-27, with fast neutrons leads to the formation of its isotope, Al-26, due to the (n,2n) reaction. For 14 MeV neutrons this reaction cross-section is of 3 orders of magnitude more than that for fission neutrons. Thus, the activity of Al-26 which is accumulated in irradiated alumina and sapphire can be high enough, despite the long half-decay time of Al-26, $T_{1/2}=7.16\cdot10^5$ y.

The analysis of induced radioactivity was carried out for 1 kg aluminum, Al-27, irradiated by the DEMO reactor spectrum with neutron fluence up to $1\cdot10^{23}$ n/cm^2 (10 y of irradiation for neutron flux $3.3\cdot10^{14}$ n/cm^2/s) and decay time up to 10^3 y. Calculation of aluminum transmutation and radioactivity induced were performed using FISPACT-3 code, activation cross-section library FENDL-2/A and decay data library FENDL-2/D.

The calculation results give a complete picture about the time dependent values of induced radioactivity and dose rate. It is shown that total dose rate of 1 kg aluminum after 10 y irradiation in the DEMO spectrum reaches the value of 10^5 Sv/h. In a month after shutdown this dose rate decreases to the level of $2.5\cdot10^{-2}$ Sv/h which is kept for a long time, $7.16\cdot10^5$ y. Accordingly, total induced activity of aluminum is equal $1\cdot10^{14}$ Bq/kg after 10 y irradiation time and the activity of Al-26 is equal $3\cdot10^7$ Bq/kg which is much higher than the clearance level for Al-26, $1\cdot10^4$ Bq/kg. This fact has to be taken into account for using of alumina and sapphire in fusion reactors.

2.8 HIGH-VOLTAGE ACCELERATORS

Calculation and Preliminary Analysis of Optical Characteristics of the Ion Beam Injection System into Accelerating Tube of Tandem Accelerator

S.V.Bazhal, V.A.Romanov

Efficiency of charge particles transport through the low–energy stage of tandem accelerator is in many respects defined by the capability of injection system to compensate the uncontrolled effect of the strong aperture lens formed by an open entrance to the acceleration tube on ion beam. There are several approaches to the solution of the problem of strong lens, one of them being discussed in this work (EGP–15 accelerator operated at IPPE as an example). Considered is the feasibility of using the zoom electrostatic lens in injection system for beam matching with optical channel of the low–energy acceleration stage. Based on the numerical solution of Laplace equation, geometry and potentials of electrodes are defined providing a fixed position of optical image of the entrance crossover at the terminal stripper. The absolute value of magnification of the optical system under consideration has been shown to remain close to 1 in the change of terminal potential from 2.0 to 8.0 MV. Beam envelopes have been calculated for different energy modes of the accelerator. Efficiency of the injection system proposed is discussed.

Systematic Error Estimation of an Electric Field Strength for High-Voltage Devices

K.A.Rezvykh, V.A.Romanov

Abstract

A set of systematic errors of a potential and a normal derivative for finite-difference method and numerical differentiation is considered. Methods for estimating errors based on the simulation of real gaps are described. The complete compensation of an error increases an accuracy and an efficiency of an numerical analysis.

Contents

Breakdown Voltage Calculation for Gases with Nonuniform Fields of an Accelerator by Base Method

K.A.Rezvykh, V.A.Romanov

Abstract

The method for calculating the breakdown voltage of gas insulating the gaps in accelerator has been developed. A new model of insulation system element is proposed according to the results of tests for the EG-2.5 Van de Graaff accelerator, IPPE (Fig. 1). Complete enough set of causes (factors) for the gas breakdown has been defined based on the experimental and calculated study. The calculation method includes the combination of some analytical equations coupled with the results of a special experiment with breakdown. A conclusion is made based on the comparison of experimental and calculated findings for the EG-2.5, MP and FN accelerators and other insulation structures that the accepted element model and the used dependencies of the breakdown voltage on the main factors are adequate to the gas discharge nature of different gases. Since the calculation error is within of the limit for the input data, the method described allows to predict the breakdown voltage for insulation gaps of accelerator with accuracy of 1-5%.

The breakdown voltage is calculated accurately enough if the value of the breakdown gradient is obtained from the procedure described above and relates to the given special conditions. It can be stated that the element model accepted for the insulation system and the set of the breakdown factors considered are adequate for the nature of the gas discharge. The old concept according to which the breakdown gradient can be found from generalized data obtained by other experiments seems to be not satisfactory, since it involves different surface conditions and uses an incomplete set of the breakdown parameters. The method is valid for different gases. As a rule the total error of calculations does not exceed the error limits of the input data. So the calculation accuracy is achievable within some per cent for the high-voltage accelerators.

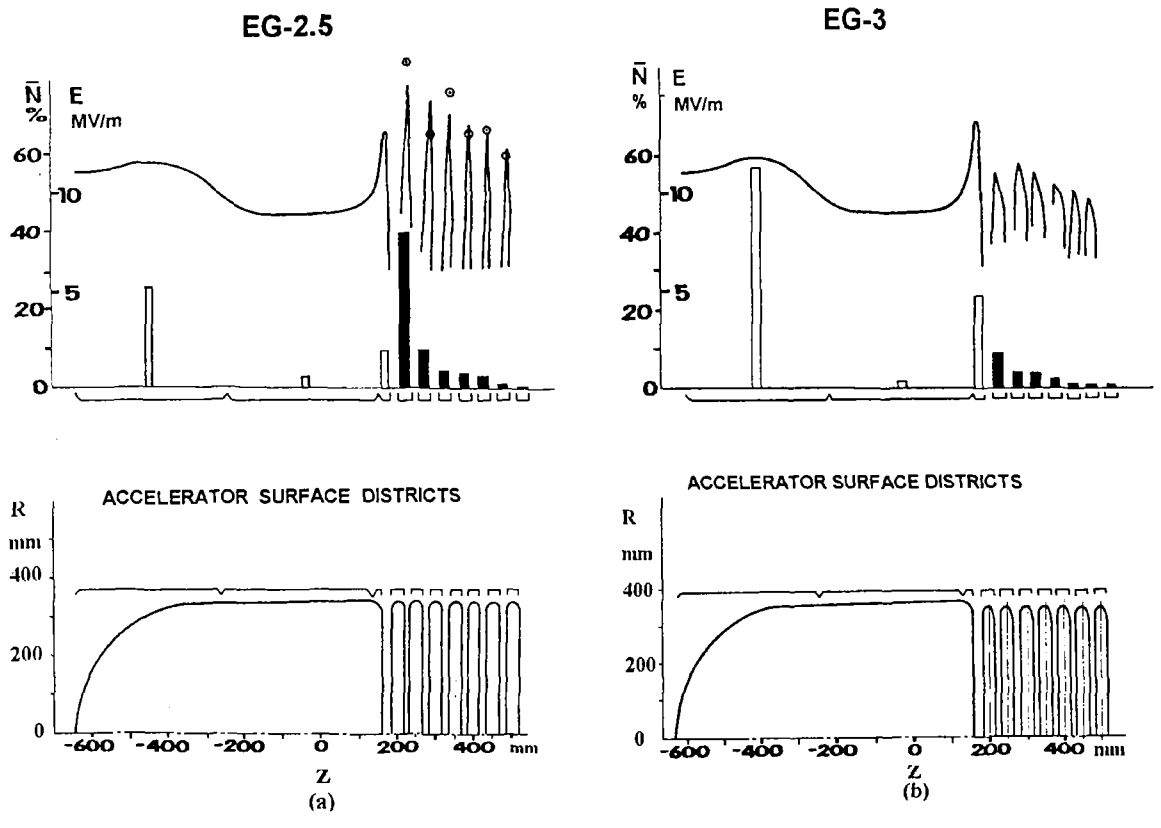

Fig. 1. The distribution of the potential gradient E (full line) and the mean number $\overline{N}$ of the breakdown marks (□) along the electrode surfaces for two modifications of the EG-2.5 accelerator [13]. (a) EG-2.5 with hoops of the circular cross section, (b) EG-3 with hoops of the twice oriented oval cross section. Both insulating systems consist of two elements: the terminal top ($z \leq -250$ mm) and the junction of the terminal and the column ($z > 112$ mm). Accelerator dimensions in mm. The terminal potential (U_{calc}) is equal to 2,5 MV at the field calculation.
° – the potential gradients corresponding to the variation (within ± 3 mm) of the 350 mm external radius for the first, second, etc. hoops;
– the terminal number of spark marks on the surface districts;
■ – the hoop number of spark marks on the surface districts

Substantiation of Breakdown Voltage Calculation for High-Voltage Accelerators, Insulated by Binary Mixtures N_2 - Co_2

K.A.Rezvykh

Abstract

The main grounds of a rather accurate calculation of accelerator gas gaps breakdown voltage for variable electrode geometry are given. On the 2nd stage of the calculation technique development a variable composition of binary mixture N_2 / CO_2 is considered.

Contents

Table. The calculation error estimation for the N_2 / CO_2 mixture

Structure of h-v. accelerators	Terminal EG-3[3]	Column EG-3 [3]	Tandem MP [25]	Tandem MP [25]	Column EG-2,5[3]
χ_{CO_2}, %	20	20	20	50	20
S_{eff}, m^2	1.0	0.08	1.42	1.42	0.16
E_{max}/U_{calc}, 1/m	4.64	5.52	2.422	2.385	2.307
R_{av}, i	0.35	0.0476	0.0373	0.0373	0.0251
L, i	0.45	0.45	1.8	1.8	0.45
k_{non}	2.088	2.484	3.83	3.83	2.75
$(\sigma / \overline{U})_{calc}$, %	3.9	3.9	3.9	3.90	3.9
U_{calc}, MV	3.50	base	2.417	2.393	2.574
δU_{calc}, %	–0.3	–	–1.7	–10.4	–1.6

It can be seen that the error of the method of the base equals 0.3÷1.7 % for the atmospheric air and about 0.3÷1.6% for N_2 / CO_2 mixtures. The high accuracy of the method of the base is explained by the fact that conception "inherent electrical strength – asymptotic breakdown field intensity E_{asm} for the gas-electrodes combination" was taken as the foundation of the calculation. The element model accepted for the insulation system is adequate for the nature of the gas discharge.

The Obninsk EGP–15 Tandem (Status and Development)

V.S.Bashmakov, S.V.Bazhal, A.I.Glotov, V.K.Debin, A.S.Feigin, B.V.Kuprijanov, E.I.Lobanov, A.A.Malygin, V.A.Nikitin, V.A.Romanov, K.A. Rezvykh, V.I.Spirin, V.I.Volodin

Abstract

The main parameters of EGP-15 tandem are presented and some trends of its future modernization are discussed.

1. Main characteristics of accelerator

EGP–15 accelerator was designed and constructed by the SSC RF IPPE on the basis of the well known EGP–10 accelerator design developed at D.V. Efremov Institute of Electrophysical Facilities [1]. The accelerator is of vertical design. Diameter of the accelerator column is 1350 mm, its height (including high voltage electrode) being about 11 m. The column consists of six sections, each section 1.6 m long. High voltage terminal is 1450 mm in diameter and 1100 mm high. Vessel of about 12 m total height consists of 3 sections. The height of the upper and lower sections is respectively 3.5 m and 4.5 m; their inner diameter being 3 m. Height and inner diameter of the intermediate section are respectively 4.4 m and 4 m. N_2 and CO_2 insulation gas mixture is currently used. For the purpose of mass analysis of accelerated ion beams unilateral 90° analising magnet (1.5 m radius, peak magnetic intensity $1.5\ 10^4$ Oersted, $ME/Z^2=200$) is installed at the accelerator outlet. Magnetic analyzer is located on the rotating device, providing 180° slewing about vertical axis for its connection to three ion channels. During operation vacuum at the exit of the accelerating tube is $5\ 10^{-6}$ Pa with optimum stripping target thickness.

2. Charging system

Two types of charging systems are possible to use: induction system and transport belt. Induction system was used to provide short circuit current up to 300 μA at the chain velocity of 15 m/s, but now it is out of operation. The charge transport belt was designed in co-operation with some other Russian institutions on the base of Kapron cloth of 0.2 and 0.5 mm thickness. In the process of the belt development the main attention was paid to its mechanical and dielectric strength and wear resistance. Raw rubber for the rubber mixture was chosen from the requirement of its appropriate wear resistance, strength and elasticity. Chosen materials were used for manufacturing 1.3 mm thick two–layer and 1.6 mm thick four–layer belts. Strength of the interlayer connection in these belts is 3.2÷3.4 kg/cm. Four–layer belt of this type is now used on the accelerator. Lifetime of the belt is over 8 thousand hours.

On the stage of new charge transport belt installation much attention was paid to the uniformity of charge distribution over the belt, since this parameter has a strong influence on the stability of the accelerated beam energy and position.

3. Negative ion injector

Only shortened horizontal section of the injector is currently used [2] with one sputter negative ion source of MISS 483 type designed by the Rossendorf Center, Germany.

For nuclear physics studies intensive light ion beams were needed. In particular it was necessary to have continuous and pulsed beams of hydrogen isotopes. Application of the

sputter source for this purpose becomes inefficient. In this connection it was decided to make partial modification of the injector, i.e. to install beam buncher and hydrogen negative ion source of duoplasmatron type in vertical injection line.

The next stage of the injector modification will be the installation of several ion sources with the switching magnet.

4. Optimization of high voltage structure of accelerator

In order to increase operating voltage and improve the accelerator reliability it is suggested to replace round equipotential rings of 30 mm diameter on two column sections by the elliptical equipotential rings. The shape and dimensions of equipotential rings were determined using computer code for calculation of electrostatic field characteristics [3]. Shielding electrode, which is common for three column sections, provides high electric strength of the column in both lateral and axial directions and increased operating reliability of the accelerator. Figs. 1 and 2 show respectively field pattern for the initial structure of EGP–15 accelerator and the new field pattern with changed equipotential rings. As a result of new design the column gradient decreased from 19 to 14.8 MV/m. In this case high–voltage terminal becomes a vulnerable element, and the energy dissipated over one insulation section W_{dsp} decreases by two times after the break–down to the vessel occurs. This leads to the increase of the operating reliability of the internal structure of the column and accelerating tube.

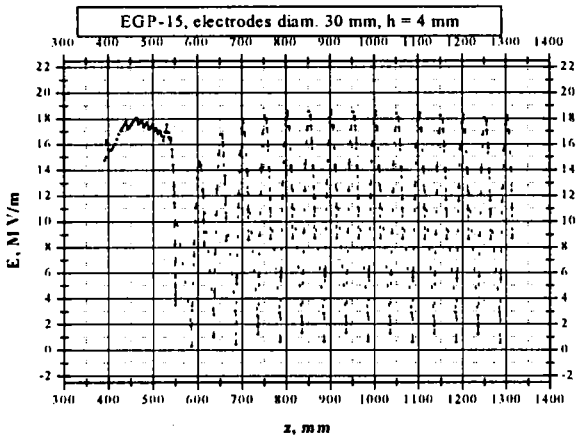

Fig. 1

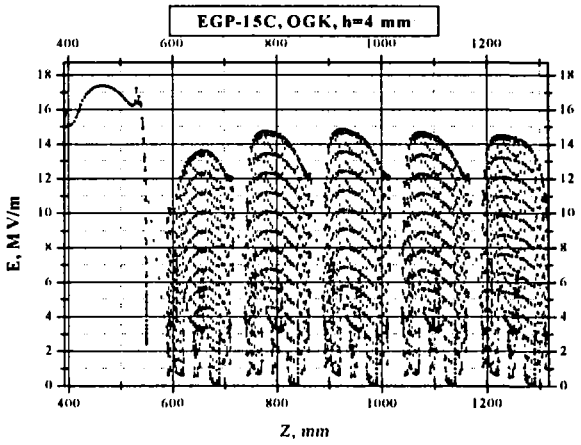

Fig. 2

5. Accelerating tubes

The EGP–15 accelerator was designed for acceleration of wide range of ions. There are some features concerning multiple charged ion beam transport through high–energy accelerating tube. Ion charge variation occurring in the terminal results in dependence of the ion tracks in the stationary electric field on the charge state [4]. In order to increase electric strength of the tube it is equipped with the electrodes having lateral components of accelerating field (i.e. inclined fields are applied). However, it is well known that the ion tracks dependence on the charge state proves to be most strong just in such accelerating structures [3], resulting under some conditions in the total loss of the beam [5].

Evaluation of the effect of dissipation processes in the stripper on the beam transport, previously made for the EGP–15 tandem accelerator, has shown, that even if additional optical elements are installed in the terminal the increase of Br^{+9} ion beam cross section

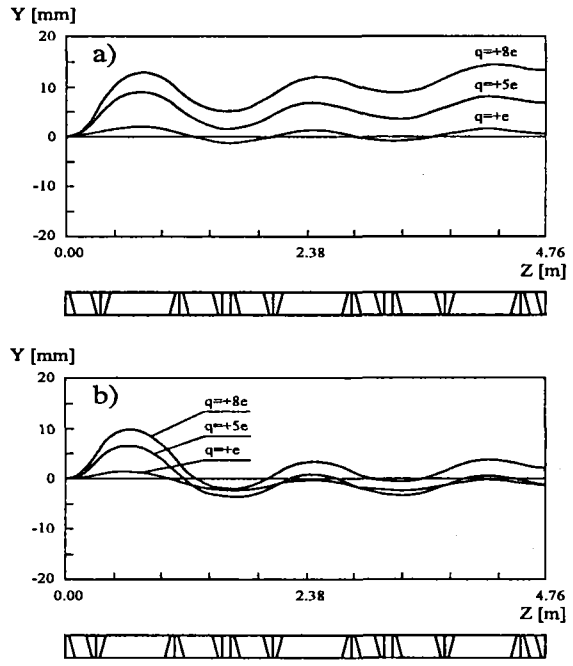

Fig. 3

with the energy of 75 MeV at the exit of the accelerating tube, may reach 10 mm and more [6].

Therefore it was important to choose such inclined electrode structure, which should not impact multiple charged beam, the electric strength of the tube being kept. Fig. 3 presents particles trajectories for different charge states in the EGP–15 accelerating tube adjusted for the single charged ions (3a) and multiple charged ions (3b). As it can be seen from the Fig. 3b, the displacement of multiple charged ions is about 2 mm, this value being quite acceptable.

The tube electrodes were made of stainless steel and the insulating rings were made of glass and porcelain. The tube was cemented using PVA adhesive.

6. Ion–optical system for beam matching

Unrestricted impact on the beam caused by the strong aperture lens, formed by the equipotential surfaces of the electric field at the entrance of low–energy section of the accelerating tube, is a serious problem concerning tandem ion optics [7]. In order to solve this problem there are widely used injection systems, in which metallic grid is provided in the plane of the tube entrance electrode [8]. It is to be admitted that undoubtedly improving ion–optical characteristics of the low–energy accelerator section, the grided accelerating tube injection has some significant drawbacks.

Therefore, within the framework of activities aimed at the increase of maximum voltage of the EGP–15 tandem accelerator studies were made on the possibility of application in the existing low–voltage injector of an optical system having open tube entrance. It is free from the above mentioned drawbacks and provides reliable matching of the beam characteristics with the accelerator channel. In order to eliminate the dependence of the open tube entrance first order optical properties from the accelerating voltage, at least the proportionality of the accelerating tube entrance/exit particles energies should be maintained for the fixed position of the aperture lens object plane. These conditions can be met using three–electrode zoom lens. We have proposed and calculated the optical system for the beam matching on the basis of this lens [9]. It was demonstrated that optical magnification module of the proposed device is close to one, while the matching voltage changes almost linearly with particles energy under the terminal. Fig.4 shows

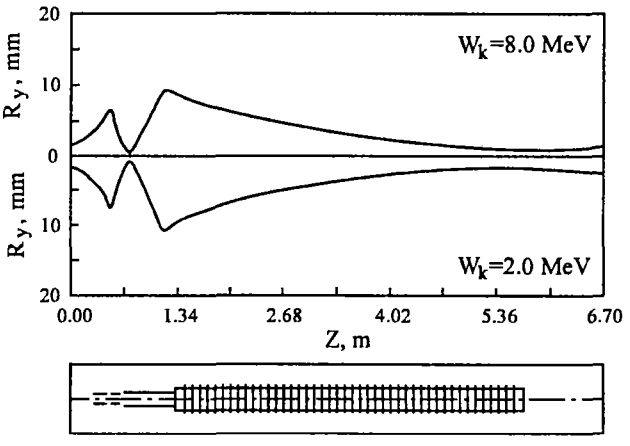

Fig. 4

the beam envelope in the optical channel of low–energy stage of the EGP–15 tandem, obtained for two energy modes, corresponding to 8.0 and 2.0 MeV particles energies in the terminal. The evaluation was made in the assumption that the beam was transformed in the object diaphragm plane into a crossover with $r_0 = 1.5\ 10^{-3}$ m, its normalized emittance was 3 π mm mrad $(MeV)^{0.5}$, and the particles energy at the entrance of the zoom lens is 30 keV. As it can be seen from the Figure, the shape of the beam is slightly influenced by the terminal voltage, and its cross section dimensions at the tube entrance are sufficient for passing the stripping target channel (6 mm in diameter).

7. Irradiation of film materials on the EGP–15

Considerable attention was paid to design, manufacture and adjustment of technological film materials irradiation system for track membranes production. By now the works are completed. Test Irradiation of 10, 20 and 30 μm thick Lavsan films were carried out. They were irradiated by oxygen and silicon ions. In the nearest future 10 μm Lavsan film will probably be irradiated for the purpose of the track membranes commercial production.

Fig. 5

In order to assure high quality of the track membranes, the following modifications were made:

- ion beam stabilization at the inlet of irradiation chamber;
- ion beam monitoring in the process of adjustment works;
- improvement of vacuum in the irradiation chamber;
- monitoring and stabilization of the film movement speed;
- system for ion beam distribution monitoring in the process of irradiation, etc.

Fig. 5 shows the system for irradiation of film materials.

References

1. Ivanov A.S., Kirshin G.F., Latmanizov V.M., et al, EGP–10 type charge–changing electrostatic accelerator, Atomnaya Energiya, v.34, No.5, p.p.401–403;
2. Bashmakov V.S., Glotov A.I., Kupriyanov B.V., Matveyev V.M., Sarytchev S.A., Low–voltage injector of EGP–15 accelerator, Proceedings of X Workshop on electrostatic accelerators, Obninsk, 1992, p.p.195–206;
3. Rezvykh K.A., Romanov V.A., EGP-15 tandem high voltage structure optimization experience. Proceedings of XV Workshop on charged particles accelerator, Protvino, 1996, v.1, p.p.192–195;
4. Larson J.D., Beam transport through electrostatic accelerator and matching into post accelerator, N.I.M., 1986, v.A244, p.p.192–200;
5. Friedrich M., Ion–optical studies on acceleration of heavy ions in the EGP tandem generator, PTE, 1983, No.3, p.p.25–27;
6. Bazhal S.V., Burushkin O.S., Romanov V.A., On application of the envelope method for evaluation of multiply charged ions optics in the charge–changing accelerators, IPPE preprint No.2332, Obninsk, 1993;

7. Larson J.D., Resolving beam transport problems in electrostatic accelerators, Rev. de Physique Appliquee, 1997, 12, p.p.1551–1561;
8. Purser K.H., Heavy ion injection for tandem accelerators, Nuclear Instrument Methods, 1977, v. 146, p.p.115–119;
9. Bazhal S.V., Romanov V.A., On application of zoom electrostatic lens for matching ion beam to the optical channel of low–energy stage of charge–changing accelerator, Proceedings of XV Workshop on accelerators of charged particles, Protvino, 1996, p.p. 201–205.

High-Voltage Structure Development for The EGP-15 Tandem (Project)

K.A.Rezvykh, V.A.Romanov

Abstract

A comparatively accurate method for breakdown voltage calculation allows to optimize the accelerator geometry for obtaining maximum operating voltage. Due to complex approach, the breakdown voltage can be increased up to 1.5 times or more relative to usual structure. In addition to the EGP-15 project the paper studies how much variation of forms and dimensions of accelerator electrodes is powerful as to the increasing of an insulation gap breakdown voltage.

1. Methods

For simplicity one can consider an insulation structure breakdown voltage as the main function and search its maximum. In IPPE there was developed a procedure of breakdown voltage calculation based on the analysis the insulation system (similar to a high-voltage accelerator) into separate elements and considering all principle breakdown parameters [1-3]. It has made available to compare some accelerators of the same 6–9 MV class.

This algorithm is called the "base" technique, as it supposes performing an experiment at the standard base gap. If the input information of the base breakdown voltage and electrostatic field strength is accurate within 1–2%, then our approach allows to compare different high-voltage structures with the same accuracy.

Electrostatic field is calculated by a special code REP, used the method of finite-differences, the axial symmetry and an accurate description of curvilinear boundaries by Shortley–Weller method. Besides, a special estimation procedure was developed for the systematic error caused by numerical calculation of accelerator weakly nonuniform fields [4,5]. Six factors of net nodes potential errors are considered. Then another six factors inducing error of calculation of electrostatic field strengths are considered. The main factors are the distance between the net nodes and the curvature of field boundaries. The compensation of the 100% of systematic error increases precision and efficiency of numerical calculation.

2. The EGP-15 project

The EGP-15 tandem has the same internal structure as the EGP-10-1 tandem except the tube length (4.8 m counter 4.2 m). The equipotential rings have circular profile with diameter of 30 mm. The EGP-15 tank has a 4 m ID middle part. Diameter of the tank at one-third of the column from the terminal decreases to 3 m (Fig. 1,2).

The calculated breakdown voltage of this structure is equal to 7 MV at 1.1 MPa of gas mixture N_2–CO_2 pressure, CO_2 volume concentration of 20%, humidity of 50 ppm. A conditioning degree k_{cntn} is proposed to equal

$$k_{cntn} = U_{unstbl}/U_{stbl} = 0.85,$$

as a complete conditioning is difficult to reach and is dangerous for solid insulation. (Here U_{stbl} denotes a mean breakdown voltage which doesn't depend on a breakdown number, U_{unstbl} is a low unstable breakdown voltage).

On the first stage of modernization a *common equipotential ring* of the OGK-type (Fig. 3) shields three elements of support column. The common ring profile is conjugation of two half-ellipses. The profile inclines to the accelerator axis at an angle of 15°.

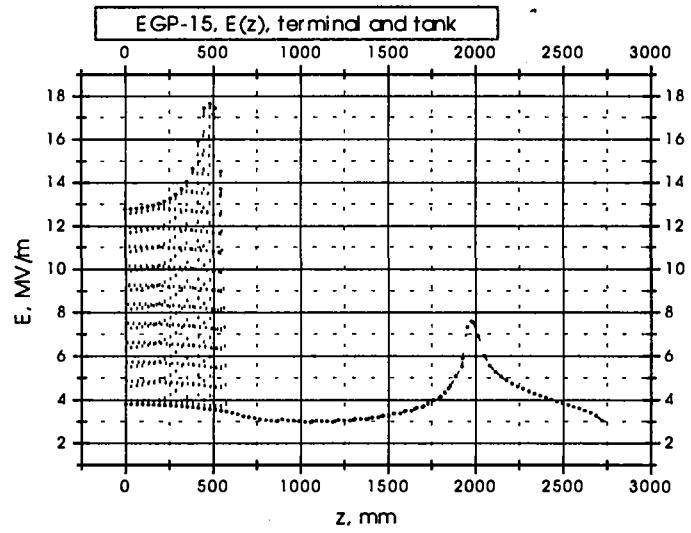

Fig. 1

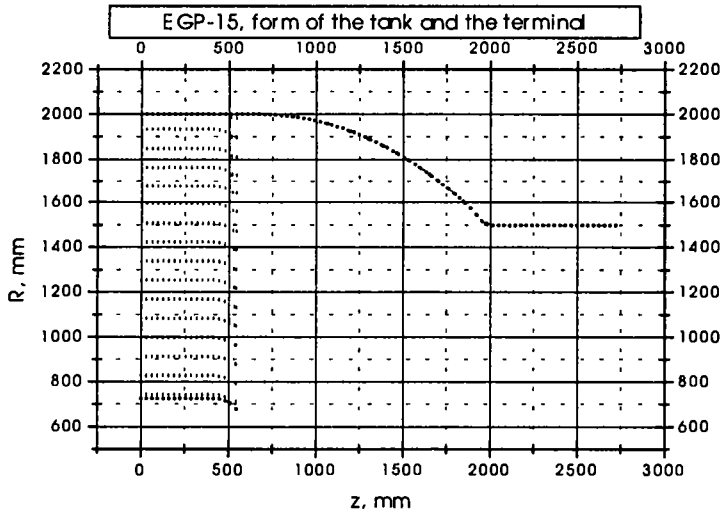

Fig. 2

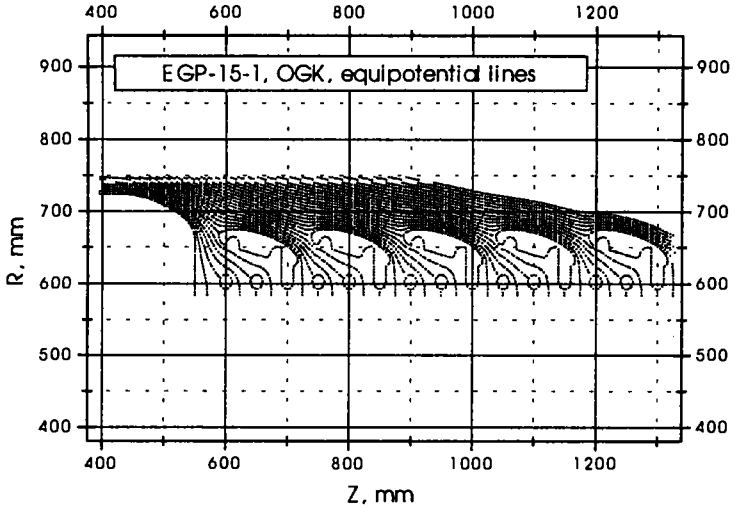

Fig. 3

As a result the column field strength decreases from 19.0 MV/m to 14.8 MV/m [7, Fig.3,4]. However, a breakdown voltage of this insulation system even decreases because the terminal has lower breakdown strength, than a 30 mm OD equipotential ring profile. A notable increasing of a breakdown voltage was obtained only after the terminal profile variation (structure EGP-15CT).

Common equipotential ring forms four insulation gaps: one is outer and three are inner. When the inner insulation is stronger, then

$U_{syst} = U_{br.term} < U_{br.inn} \times n_{ser}$.

Relative electrical strength $k_{strn.inn}$

$$k_{strn.inn} = \frac{U_{br.inn} n_{ser}}{U_{syst}}$$

for the EGP-15CT structure is for instance equals 2.1. Here U_{syst} denotes minimum breakdown voltage to tank, $U_{br.inn}$ is that between neighboring rings, n_{ser} denoted a quantity of gaps connected seriesly along the column.

The additional increase of radial breakdown voltage due to common ring inclined oval profile causes decrease of axial one, giving rise to form spark gaps between the equipotential rings. That is why the EGP-15CT column can be made stronger than terminal in the case that $k_{strn.inn} \leq 1$. As it was pointed in Ref. [6], the small probability of the "column–tank" breakdown means lowering of overvoltages and lower energy dissipated on the solid insulators of the column and the tube after the tank breakdown occurs. The operation reliability rises.

Table 1: Efficiency of electrode geometry variation for the purpose of increase the insulation gap breakdown voltage

Structure	R_{tank} (m)	L (m)	E_{max}/U(1/m)	L/L_{EN}	E_{EN}/E_{max}	U_{br}/U_{EN}	U_{br}(MV)
EN[8]	1.2	0.7	3.4	1.0	1.0	1.0	5.03
EGP-10-1[9]	1.5	0.775	2.75	1.1	1.24	0.99	5.00
FN[8]	1.83	1.33	2.556	1.9	1.33	1.31	6.61
EGP-15	2/1.5	1.35	2.19	1.93	1.55	1.39	7.00
EGP-15C	2/1.5	1.35	2.04	1.93	1.67	1.35	6.8
EGP-15CT	2/1.5	1.35	1.75	1.93	1.94	1.53	7.71
Sh6[10]	1.8	1.193	1.78	1.70	1.91	1.45	7.29

The manufacture technology of the OGK-type common rings and the KRF-type terminal profile was developed at IPPE. Similar terminal is prepared for the EGP-8 tandem.

3. Breakdown voltage of some accelerators without tubes

Breakdown voltages have been calculated at mentioned above in section 2 conditions. In Table 1 EGP-15C (EGP-15-1) has the modernized column, EGP-15CT has both the column and the terminal modernized. R_{tank} denotes a tank radius, L is a terminal–tank distance, E_{max}/U denotes a field strength and an applied potential difference ratio at the field calculation.

It is seen that the geometry optimization increases the breakdown voltage up to 1.5 times. The gap increase not always gives a positive effect (EGP-10-1), as well as decrease E_{max}/U (for example EGP-15C). The EGP-15CT structure has some reserve of electrical strength and reliability.

Conclusion

1. An electrode geometry optimization must be complex.
2. A geometry optimization of a column and of a terminal is competitive with using SF_6 gas and, maybe, is the cheapest way for increasing operation voltage.

References

1. K.A.Rezvykh, V.A.Romanov, Voltage Tests and Breakdown Voltage Calculation of High-voltage Accelerator Gas Insulation, //Electricity(1988)no.12,10-19 (in Russian).
2. K.A.Rezvykh, V.A.Romanov, Gases Breakdown Voltage Calculation for the Case of Accelerator Nonuniform Fields by Method of the Base // Nucl. Instr. Meth., ser. A, (in print).
3. K.A. Rezvykh, The Main Grounds of Breakdown Voltage Calculation for High-Voltage Accelerators Insulated by Binary Mixtures N2 – CO_2 // Proceedings of XII Intern. Conf. on Electrostatic Accelerators ,Obninsk, November 25-28, 1997, IPPE,1998, in print (in Russian).
4. K.A.Rezvykh, V.A.Romanov, Calculated Systematic Error Estimation of an Electric Field Strength at Accelerator Structure Optimization, // Proceedings of XIV Workshop on Charged Particle Accelerators ,Protvino, IPHE, 1994, v. 3, 55-59 (in Russian).
5. K.A.Rezvykh, V.A.Romanov, Systematic Error Estimation of an Electric Field Strength for High-voltage Devices, // Electricity, in print (in Russian).
6. K.A.Rezvykh, V.A.Romanov, High-voltage Structure Optimization Experience for the EGP-15 Tandem, // Proceedings of XV Workshop on Charged Particle Accelerators, Protvino, IPHE, 1996, v. 1, 192-195 (in Russian).
7. V.S.Bashmakov, S.V.Bazhal, A.I.Glotov et al., The Obninsk EGP-15 Tandem (Status and Development), This Conference Proceedings.
8. I.I. Rabinowitz, Comparison of calculated Electrostatic Field Distributions in Tandem Van de Graaff Accelerators, Proceedings of the Intern Conf. on the Technol. of Electrost. Accel., Daresbury, DNPL/NSF/R5,1973, 179-184.
9. R. Günzel, SCAPOT, BAHN und FELDS, Ein Programmsystem, ZfK–372, 1978, S.21.
10. W. Lai, H. Si, J. Zhu and M. Li, The Shanghai 6 MV Tandem, //Nucl. Instr. Meth., A 382 (1996)89-96.

Fission Rate Determination in Delayed Neutron Emission Measurements with T(p,n) and D(d,n) Neutrons

V.M. Piksaikin, V.S. Shorin, G.Ya. Tertychny

The purpose of the present work is to create a method of determination of fission event rate in a sample irradiated with quasimonoenergetic neutrons from the $T(p,n)^3He$ and $D(d,n)^3He$ reactions. The consideration is given for the case of the measurements of DN yields from neutron induced fission of ^{237}Np.

Fission rate in samples

In general the calculation of fission rate in the sample is a quite complicated problem [6] connected with solving the neutron transport kinetic equation taking into account neutron multiple scattering in a sample and construction materials of the experimental setup. It is necessary to account for a composite nonmonoenergetic spectrum of accelerator-based neutron source as well. In the general form the value of $R(E_n)$ can be presented as the functional of the following type:

$$R(E_n) = <\Sigma(E)\cdot\Lambda(r)\cdot\varphi(E,E_n,r)>_{E,r} \qquad (1)$$

where $\Sigma(E)$ is the effective macroscopic fission cross-section for neutrons with energy E, $\Lambda(r)$ is the neutron path length in the sample in the direction of radius-vector r of the interaction point, $\varphi(E,E_n,r)$ is the neutron flux on the sample with average neutron energy E_n, the sign $<>_{E,r}$ denotes the averaging over all coordinates r and neutron energies E. The value of $\varphi(E,E_n,r)$ is associated with a spectrum of accelerator-based neutron source φ_0 by the relation

$$\varphi(E,E_n,r) = \Phi_0(E_n)\cdot<\varphi_0(E',E_n\Omega)\cdot G(E'\rightarrow E,\Omega\rightarrow r)>_{E',\Omega}, \qquad (2)$$

where Ω is the unit vector of an outgoing neutron direction, $\Phi_0(E_n)$ is the total neutron yield from an accelerator target

$$\Phi 0(En) = <\varphi 0(E',En\Omega)>_{E',\Omega}, \qquad (3)$$

$G(E'\rightarrow E,\Omega\rightarrow r)$ is the Green function (scattering indicatrix) of the system which is taking into account the features of neutrons transport for the given geometry of experiment. The normalization constant $\Phi_0(E_n)$ can be determined by the comparison of the calculated value with the count rates $R_i(E_n)$ of two monitor fission chambers (with fissile layers made of the same material ^{237}Np, i is the chamber's number) located directly in front of and behind the researched sample in the same neutron flux.

Results

The test of the method (to estimate the $R_s(E_n)$ value properly) was carried out by measuring the count rate $R_i(E_n)$ in the fission chambers placed at different distances from the neutron target and by comparing the results with calculated values W_i (Fig.1).

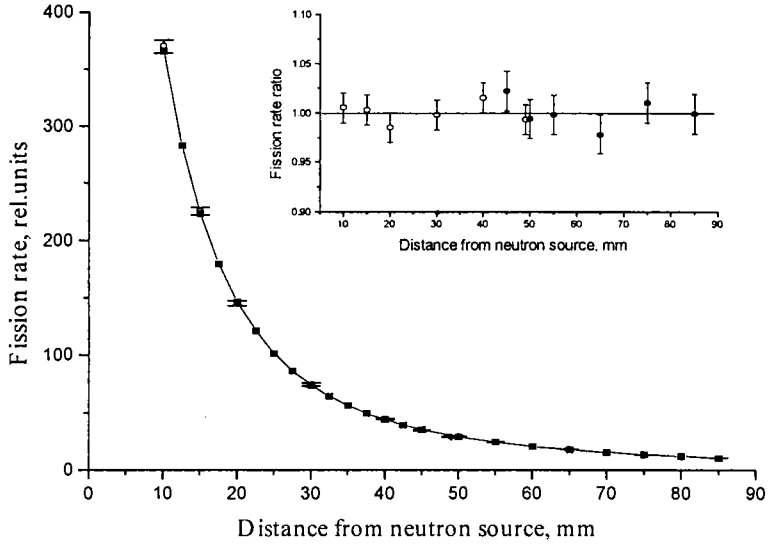

Fig. 1. Comparison of fission rates in the fission chambers at different distances from a neutron source T(p,n) obtained by measuring $R_i(E_n)$ and on the basis of W_i calculations. The energy of primary protons is 1.974 MeV.

In Fig.2 the results of calculations of the values $(W_i \cdot W_s^{-1})$ for the ^{237}Np sample obtained for two cases of neutron flux monitoring (by one and two fission chambers) are presented.

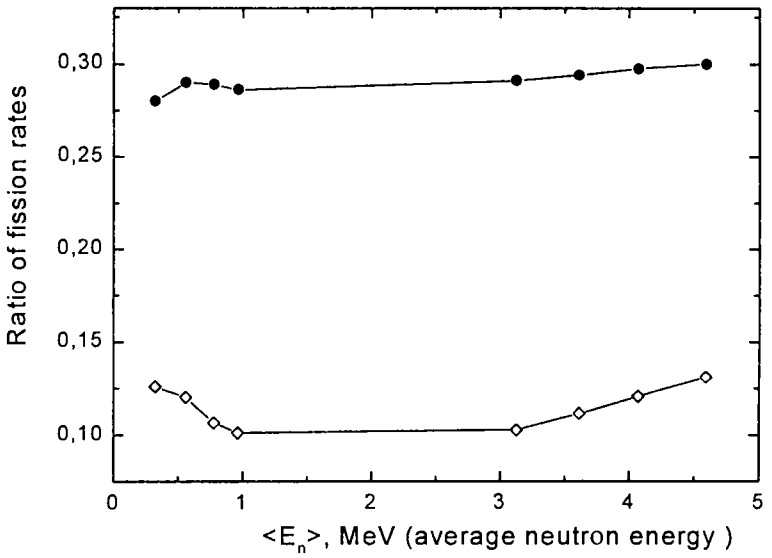

Fig. 2. The ratio of fission rates in a layer of fission chamber and ^{237}Np sample $W_i \cdot W_s^{-1}$. Open circles are related to "one fission chamber" geometry. Black circles are related to "two fission chambers" geometry. The points are connected by straight lines for visualization.

The Code for Calculation of Accelerator-Based Neutron Sources Properties

V.S. Shorin, G.Ya. Tertychny

The code for calculation the yields and spectra of neutrons generated in (p,n) and (d,n) -nuclear reactions on some light nucleus targets is described. The specific features of stopping processes of charged projectiles (with incident energy less than 15 MeV) in multilayer (not more than 6 layers) and multicomponent (not more than 6 components) targets are taken into account. Inside each layer the element concentration function was supposed to be a constant. This approximation allows to operate with both solid and gas targets. A small scattering angles approximation was used for the ion multiple scattering problem. The case of normal incidence of a wide ion beam is considered. All calculations were based on the ions stopping data dE/dx in matter obtained with the help of the well-known code TRIM. The relativistic kinematic formulas for two-particle nuclear reactions and the atomic masses table Audi-93 were used. The code operates with the following neutron production reactions: T(p,n), D(d,n), T(d,n), ^{7}Li(p,n)^{7}Be and ^{7}Li(p,n)^{7}Be* (and the inverse to them). The data on the neutron production cross-sections were taken from Drosg-87 evaluation and some extrapolation was used near threshold range for (p,n) – reactions.

The code version is made in terms of the "SOURCE" subroutine for MCNP4a code. The code is written in "Fortran–77" for compiler f77L-EM/32. This subroutine generates such random variables as the neutron energy, the neutron weight (number of neutrons per 1 μKl) proportional to the differential reaction cross-section and the outgoing neutron direction angles in the LS system. The code takes into account the presence of two groups of outgoing neutrons for threshold reactions. Some results of calculations for most popular accelerator-based neutron sources are given. The results demonstrate the effects of neutron multiple scattering on target assembly matter.

The Tritium Admixture in Solid Target Backing and Neutron Spectrum from "Monoenergetic Source"

N.V. Kornilov, A.B. Kagalenko, S.V. Poupko, P.A.Androsenko

In fast neutron physics the most frequently used tool is the accelerator-based neutron source with solid tritium target. Such targets consist of very thin tritium absorber layer (as a rule Ti) deposited onto metallic backing and they are very convenient for practical applications. In spite of all efforts, the real neutron sources always have an admixture of non-monoenergetic low energy neutrons. There are a lot of papers devoted to (or at least, discussed) this problem [1-4]. The three most frequently discussed sources of these "additional" neutrons are: 1) (p,n)-reactions in target construction materials, 2) neutron scattering on the target assembly, 3) neutron scattering on the shielding collimator. The neutron yield from (p,n)-reactions on target construction materials may be effectively reduced with the proper choose of the target material and incident proton energy. In an addition these neutrons may be measured with 'blank' target (i.e. the same Ti layer deposited onto backing, but without adsorbed tritium). As a rule experimenters used low-mass target assembly to reduce neutron scattering. However, in some cases even the low amount of the scattered neutrons may distort the measurement effect significantly.

In our experiment [5,6] we investigated the neutron inelastic scattering on the ^{237}Np with NpO_2 sample. In spite of the share of the background neutrons (due to target scattering) is rather small, however, being elastically scattered by the sample nuclei (Np, O, Fe) they may produce the contribution comparable with inelastic scattering on ^{237}Np. So, the detail investigation of the energy-angular distribution of the source neutrons is the crucial point of this experiment. It was found that the experimental neutron spectrum from the solid target can not be explained only by neutron scattering. Some experimental peculiarities allow us to conclude that there exists some amount of tritium inside the target backing which produce neutrons with the broad energy distribution (less than E_0 that corresponds to the monoenergetic neutron peak). Due to importance of this fact for neutron data measurements we presented these experimental results and their analysis in this paper.

The neutron spectra from reaction T(p,n) in solid tritium target were measured by time-of-flight (TOF) technique with the EG-1 accelerator spectrometer of the IPPE. The measured spectra were compared with results of full-scale Monte Carlo simulation. It is shown that low-energy part of neutron spectrum can not be described by scattering of monoenergetic neutrons on target assembly. The conclusion was made that the observed spectra can be explained by presence of some amount of tritium in a target backing material.

References

1. Kegel G.H.R., Ciarcia C., Couchell G.P., Shao J., Proc. Intern. Conf. on Nuclear Data for Science and Technology, Antwerpen, 1982, NDST pp.897-899, (1983).
2. Kagalenko A.B., Kornilov N.V , Proc. Advisory Group Meeting on Properties of Neutron Sources, Leningrad, June 1986, Report IAEA-TECDOC-410, Ed. K.Okamoto, Vienna,1986, p.115
3. Baba, M., Matsuyama, S., Ishikawa, M., Chiba, S., Sakase, T. and Hirakawa, N. NIM, A366, 1995, page 354-365.
4. Kornilov N.V., Kagalenko A.B., NSE, 120, (1995).
5. Kornilov N.V., Kagalenko A.B., Dubna 1997, ISINN-5, 297.
6. Kornilov N.V., Kagalenko A.B., Baryba V.Ya.,Pupko S.V., Androsenko P.A., Proc. Intern. Conf. on Nuclear Data for Science and Technology, Trieste, 19-24 May 1997, p.577.

Nonmonoenergety of Neutron Source Based on the Solid Tritium Target

S.P. Simakov, G.N. Lovchikova, A.M. Trufanov, V.A. Vinogradov, M.G. Kobozev

The accurate measurements of neutron-nuclei interaction cross sections needs exact knowledge of the parameters of neutron source used in experiment. In precision measurements usually mono-energetic neutron sources are used for generation of the neutrons with specific and well-defined neutron energy. Typically the T(p,n), Li(p,n), T(d,n) reactions are used for production mono-energetic neutrons in keV – MeV energy range. Even in this case, the source will inevitably produce the neutrons (we will designate them as "nonmonoenergetic") with energies usually less the energy of the neutrons from main reaction. It is rather important to know the absolute yield and energy distribution of these neutrons. In the present work we experimentally and theoretically investigated the contribution of the nonmonoenergetic neutrons from the solid tritium-titanium-molybdenum target under the bombardment of the proton beam with energy varied from 4 to 9 MeV.

The measurements of neutron spectra from tritium solid target have been made by time of flight technique at angles from 0° to 150° at fast neutron spectrometer based on tandem accelerator EGP-10M of IPPE. The solid target, as specified by manufacture, was a titanium layer (∅11 mm by 0.96 mg/cm^2 or 2.1 μm thickness) on molybdenum backing (∅11 by 0.3 mm thickness), the ratio of absorbed tritium to titanium atoms - 1.97. It was found that, besides the T(p,n) neutrons, there are low energy neutrons, which contribute 4% to 3000% compare to the main monoenergetic neutrons as proton energy increases from 4 to 9 MeV. The energy spectra of these neutrons are shown in Fig. 1 for the case of proton energy 4 MeV.

The theoretical analyses have shown that there are two physical reasons of these low energy neutrons: neutron scattering on the target assembly and the (p,n) reactions on titanium and molybdenum. Besides on the way to the detector the part of the T(p,n) neutrons inelastically scatters on the detector shielding (collimator). For description of these process the theoretical calculations have been made with Monte-Carlo (MCNP 4.a) and Hauser-Feshbach statistical theory (TNG) codes.

The analyses of the (p,n) reaction thresholds have shown that for some titanium and molybdenum isotopes they are very close to the T(p,n) threshold. It means that titanium absorber and molybdenum backing produce neutrons practically in the same proton energy range as T(p,n) reaction. The calculated by TNG code the energy distribution of the neutrons from the ^{49}Ti(p,n)^{49}V reaction is shown in Fig.1. It demonstrates prominent peaks corresponding excited levels of residual nucleus.

The calculation made with Monte-Carlo technique have shown that neutron scattering on the target materials also results to the structure in the neutron spectra. It turns out that neutrons flying along molybdenum backing and bottom of the target holder gives two neutrons groups with energies of 1.4 and 0.65 MeV (see Fig. 1) resulted from the elastic and inelastic scattering of source neutrons.

The approach tested in the present work could be used for estimation of the nonmonoenergetic neutrons contribution for other neutron producing reactions and target assemblies.

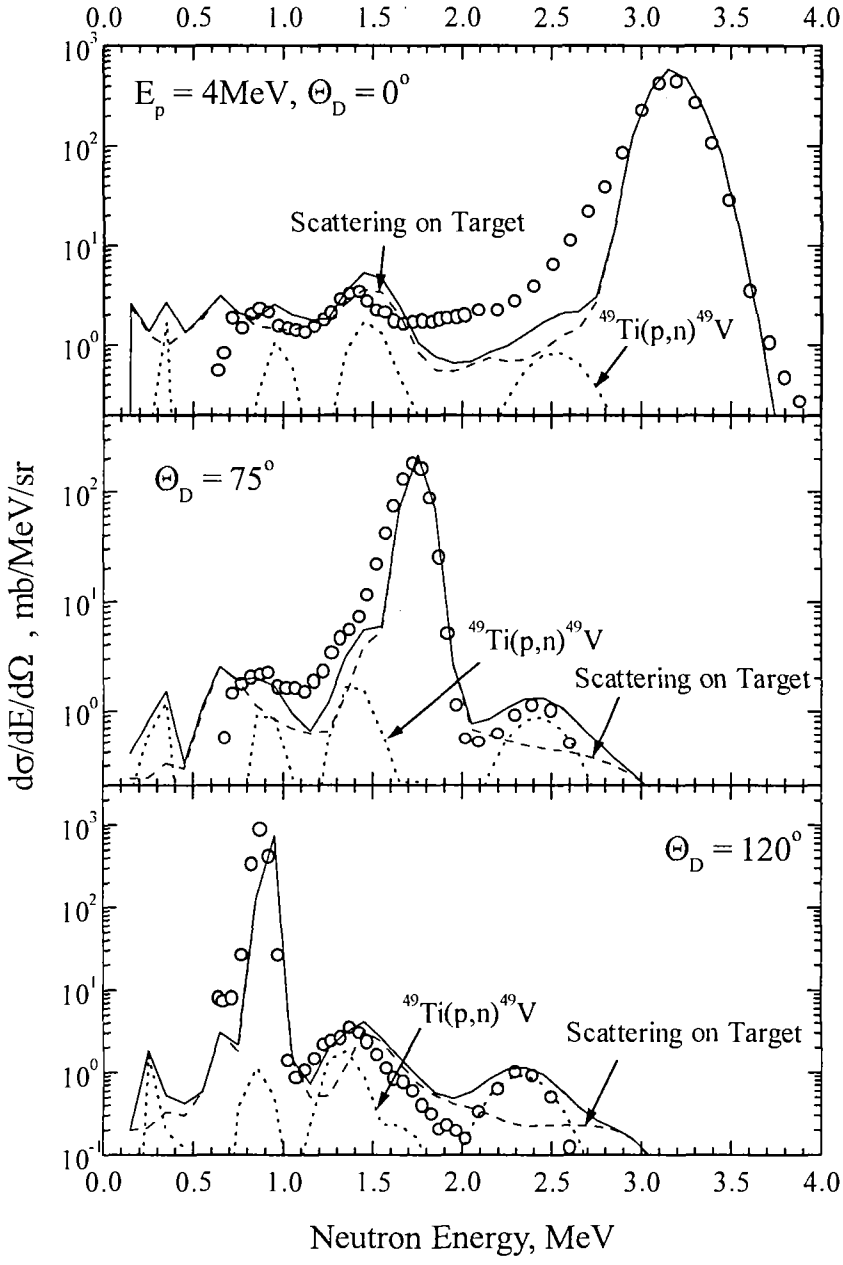

Fig. 1. Energy differential cross-sections from TiT-Mo target at E_p = 4 MeV and detector angles Θ_D = 0°, 75°, and 120°. Points – experiment. Curves: dashed – neutrons scattered by the target assembly and collimator, dotted – energy differential cross section for $^{49}Ti(p,n)^{49}V$ reaction, solid – their sum.

3. ACCELERATORS COMPLEX

During 1998 four accelerators were operated providing the necessary experimental base for researches in the Nuclear Physics Department. The main parameters of accelerators are given in Table.

Accelerator type	*Singly-charged ion energy (MeV)*	*Ions type*	*Operation conditions*	*Ion beam parameters at a physical target*	*Operation time (h)*
EG-1	1.9...4.,0	H, D	pulsed	Pulse duration - 2 ns Pulse beam current –2.,5 mA Pulse-repetition - 1; 2 MHz	1580
KG-2,5	0.25...2.1	H, D	continuous	beam current 10...50 μA	2380
EGP-10M	4.0...9.2	H	pulsed	Pulse duration - 1 ns Pulse beam current –0.2 mA Pulse-repetition – 2.5 MHz	450
EGP-15	11...12	Si^{+5}, Si^{+6}	continuous	beam current 10...200 nA	50

During 1998 accelerator EGP-15 was operated for the development of membranes preparation technology with their irradiation by silicon multicharged ions. Other accelerators operation was directed towards nuclear physics tasks fulfillment.

4. PUBLICATIONS

THEORETICAL NUCLEAR PHYSICS DIVISION

1. S.Kamerdzhiev, J.Speth. On the nuclear gap eqquation accounting for the quasiparticle- phonon interaction; IKP Annual Report 1997
2. S.Kamerdzhiev, A.Avdeenkov. Distribution of single- particle strength in odd non-magic nuclei. To be published in Proc. of the 6th Int. Spring Seminar on Nucl.Phys. "Highlight of modern nuclear structure" Italy, May18-22
3. S.Kamerdzhiev, J.Speth, G.Tertychny. Effects of the quasiparticle- phonon interaction in magic and non-magic nuclei. Acta Phys. Pol. 29(1998)2231 Invited talk at the Int.Workshop "Structure of mesons, Barions and Nuclei" Cracow, May 26-30.
4. S.Kamerdzhiev, A.Avdeenkov, The role of ground state correlation in the single- particle strength of odd non- magic nuclei. Submitted to Phys.Lett.B
5. S.Kamerdzhiev, J.Speth, G.Tertychny, F.Osterfeld. Microscopic analysis of the breathing mode in ^{58}Ni. Submitted to Phys.Rev.Lett.
6. S.Kamerdzhiev, J.Speth, G.Tertychny, F.Osterfeld., There is no missing isoscalar monopole strength. IKP Annual Report – 1998.
7. A.I.Blokhin, V.N.Manokhin, S.M.Nasyrova, Discrepancies in (n,2n) reaction excitation functions of rare earth isotopes. Recommendations for selection of more reliable curves. Report INDC(CCP)-411, 1998, Vienna.
8. Блохин А.И., Чернов В.М., Завяльский Л.П. Активация и накопление продуктов в сплавах (V-Ti-Cr) и (Cr-Ni-Mo) и сталях 316LN-IG и EPM-450 под действием нейтронного термоядерного спектра: Препринт ФЭИ-2706, Обнинск, 1998.
9. Блохин А.И., Чернов В.М. Активация и накопление газообразных продуктов в сплавах (V-Ti-Cr) и (Cr-Ni-Mo) и сталях 316LN-IG и EPM-450./ Труды VIII Межнационального совещания "Радиационная физика твердого тела". Севастополь, 29 июня-4июля 1998.
10. Хорасанов Г.Л., Иванов А.П., Коробейников В.В., Блохин А.И., Шимкевич А.Л. Свинцовый теплоноситель для быстрого реактора-выжигателя с жестким спектром нейтронов. // Труды Международного совещания «Тяжелые жидкометаллические теплоносители в ядерных технологиях». Обнинск, октябрь 1998. Будет опубликовано.
11. A.I.Blokhin, V.N.Manokhin, S.M.Nasyrova. Comparison of threshold Reaction Cross Sections for the Ti,V,Cr,Fe,Ni,Cu and Zn isotopes from Evaluated data Libraries. Report INDC(CCP)-412, Vienna,1998.
12. Manokhin V.N., Blokhin A.I., Systematical trends in the behaviour of fission and (n,2n) reaction cross sections of fissile isotopes. // Вопросы атомной науки и техники, Сер. Ядерные константы, 1998, №2. См. Также Препринт ФЭИ-2715, 1998, Обнинск.
13. Золотарев К.И., Тертычный Г.Я., Лунев В.П. Сечение гамма-производства на Bi-209 в диапазоне энергий налетающих нейтронов 0,5-20 МэВ. // Вопросы атомной науки и техники, Сер. Ядерные константы, 1998, №2, с.52.
14. K.I.Zolotarev. Development and testing of the helium production data base for main structure materials. Report INDC(CCP)-414, IAEA, Vienna, 1998.

15. K.I.Zolotarev, N.V.Kornilov, A.B.Kagalenko. On contradictions between microscopic and macroscopic data for the U-235 fission neutron spectrum at the thermal energy. In: Proc. VI Seminar on Interaction of Neutron with Nuclei (Dubna, May 1998). To be publ.
16. A.V.Ignatyuk, A.I.Blokhin, V.P.Lunev, V.N.Manokhin, V.A.Tolstikov, G.Ya.Tertychny, K.I.Zolotarev. New evaluations of neutron cross sections for Am-241 and Am-243. VANT, Ser. Nuclear Constants. 1998, to be publ.
17. Лунев В.П., Проняев В.Г., Симаков С.П., Шубин Ю.Н. Анализ сечений и механизма реакций (n,xn) и (n,xγ) на ядрах свинца и висмута. / Доклад на 48 конф. по ядерной спектроскопии и структуре атомных ядер. Москва, 1998.
18. Солдатов А.С., Блохин А.И., Игнатюк А.В., Стороженко А.Н. Фотоделение Pu-238, 240, 242 в области энергий 5 - 10 МэВ. Статья в ЯФ, 1998.
19. Ignatyuk A.V. Collective enhancement in nuclear level densities. In: Proc. Workshop on «Nuclear Reaction Data and Nuclear Reactors (Trieste, March 1998). World Sci., Singapore, to be publ.
20. Ignatyuk A.V. Validation of nuclear level density parameters in calculations with ALICE and GHASH. In: Proc. Research Coordination Meeting on «Reference Input Parameter Library: Phase II», (Vienna, November 1998). Report INDC(NDS)-389, Vienna, IAEA, 1998, to be publ.
21. Forget F., Ignatyuk A.V. Junghans A.R., Schmidt K.-H. Pair breaking and even-odd structure in fission fragment yields. Submitted to Nuclear Physics A, 1998.
22. Бадиков С.А., Гай Е.В., Работнов Н.С. О влиянии корреляций экспериментальных данных на погрешности оцененных нейтронных сечений. Направлена в Атомную энергию, 1998.
23. Gay E.V., Ignatyuk A.V., Lunev V.P., Shubin A.Yu., Titarenko N.N. Neutron cross section evaluations for ^{232}Th up to 150 MeV. In: Proc. IAEA Consultancy Meeting on Accelerator Driven Systems Related Reseaches, (Moscow, July 1998), to be publ.
24. Игнатюк А.В., Шубин Ю.Н. Потребности в ядерных данных для управляемых ускорителем подкритических систем с жидкометаллическим теплоносителем. // Труды Международного совещания «Тяжелые жидкометаллические теплоносители в ядерных технологиях». Обнинск, октябрь 1998. Будет опубликовано.
25. M. Fassbender, Yu.N. Shubin and S.M. Qaim. Formation of Activation Products in Interaction of Medium Energy Protons with Si, P, S, Cl, Ca and Fe. Radiochimica Acta, 1998, to be publ.
26. V.P.Lunev, Yu.N.Shubin, A.Yu.Konobeyev, Semi-empirical systematics for (n,t) reaction cross sections at the energy of 14.6 MeV. Il Nouvo Cimento , Vol. 11 A, № 5, pp. 445-456, 1998.
27. Zhuravlev B.V., Titarenko N.N., Trykova V.I. et.al. Nuclear level densities and spin cutoff parameters for nuclei ^{59}Ni, ^{96}Tc, ^{118}Sb from the differential neutron emission cross-sections of (p,n) and (α,n) reaction. In: Proc. VI International Seminar on Interaction of Neutrons with Nuclei (Dubna, April 1998). E3-98-202, 1998, p.151.
28. Титаренко Н.Н., Титаренко В.Н. Специализированный пакет прикладных программ для численного решения задач с особенностями: Препринт ФЭИ-2738, Обнинск, 1998.
29. S.A.Fayans, S.V.Tolokonnikov, E.L.Trykov, D.Zawischa. Local energy-density functional and density-dependent pairing in nuclear systems. Pis'ma v ZhETF, 1998, vol.68, p.260,

30. S.A.Fayans, S.V.Tolokonnikov, E.L.Trykov, D.Zawischa. Density-dependent pairing in nuclei far from stability. Nuovo Cimento, A111, No.6-7, 1998, p.823.
31. A.V.Ignatyuk. Level densities of neutron rich nuclei. In: Proc. Symposium on Nuclear Astrophysics "Nuclei in the Cosmos V" (Volos, July 1998), to be publ.
32. I.N.Borzov, S.Goriely, J.M.Pearson. Large-scale calculations of the beta-decay rates and the r-peocess of nucleosynthesis. In: Proc. Workshop on Nuclear Astrophysics (Hirschegg, January 1998). Eds. M.Buballa et al., GSI, Darmstadt, 1998, p. 293.
33. I.N.Borzov, J.M.Pearson, S.Goriely. Theoretical beta-decay rates and their astrophysical applications. In: Proc. Symposium on Nuclear Astrophysics "Nuclei in the Cosmos V" (Volos, July 1998), to be publ.

EXPERIMENTAL NUCLEAR PHYSICS DIVISION

1. V.M. Piksaikin, S.G.Isaev. Correlation properties of delayed neutrons from fast neutron induced fission. Report INDC(CCP)-415, IAEA, Vienna, October 1998, p.1.
2. V.M.Piksaikin, A.A. Goverdovski, G.M. Pshakin. Method and set-up for measurements of trace level content of heavy fissionable elements based on delayed neutron counting. Report INDC(CCP)-415, IAEA, Vienna, October 1998, p.15.
3. Пиксайкин В.М., Исаев С.Г., Казаков Л.Е., Королев Г.Г., Кузьминов Б.Д., Проняев В.Г. Особенности энергетической зависимости полных выходов запаздывающих нейтронов при делении ^{235}U и ^{237}Np быстрыми нейтронами. Ядерная физика (принята к печати).
4. Пиксайкин В.М., Балакшев Ю.Ф., Исаев С.Г., Казаков Л.Е., Королев Г.Г., Кузьминов Б.Д., Проняев В.Г., Семенова Н.Н., Сергачев А.И., Тараско М.З. Экспериментальные исследования характеристик запаздывающих нейтронов при делении ^{235}U и ^{237}Np быстрыми нейтронами // Избранные труды Физико-энергетического института за 1997 г.
5. Пиксайкин В.М., Шорин В.С., Тертычный Р.Г. Метод определения скорости реакции деления в исследованиях характеристик запаздывающих нейтронов с использованием T(p,n) и D(d,n) источников нейтронов. Послано в NIM.
6. Пиксайкин В.М., Балакшев Ю.Ф., Исаев С.Г., Казаков Л.Е., Королев Г.Г., Мильшин В.И., Семенова Н.Н., Сергачев А.И., Тараско М.З. Измерения энергетической зависимости относительных выходов запаздывающих нейтронов и периодов полураспада их предшественников при делении ^{237}Np быстрыми нейтронами. // Атомная энергия, 1998. Т.85, вып.1, с.51.
7. G.D. Spriggs, J.M. Campbell, V.M. Piksaikin. An 8-Group Delayed Neutron Model Based on a Consistent Set of Half-Lives. Report LA-UR-98-1619, May 29, 1998.
8. Пиксайкин В.М., Исаев С.Г., Казаков Л.Е., Королев Г.Г., Кузьминов Б.Д., Проняев В.Г., Семенова Н.Н. An experimental studies of the absolute total delayed neutron yields from neutron induced fission of ^{237}Np and ^{235}U in the energy range 0.3. to 5 MeV. / XIV конференция по физике деления, Обнинск, Россия,12-15 октября, 1998 (в печати) (XIV International Workshop on Nuclear Fission Physics).
9. Пиксайкин В.М., Исаев С.Г. Систематика среднего периода полураспада предшественников запаздывающих нейтронов, образованных в реакции деления тяжелых ядер быстрыми нейтронами. / XIV конференция по физике деления, Обнинск, Россия,12-15 октября, 1998 (в печати) (XIV International Workshop on Nuclear Fission Physics).
10. Пиксайкин В.М., Исаев С.Г., Казаков Л.Е., Королев Г.Г. Энергетическая зависимость среднего периода полураспада предшественников запаздывающих нейтронов при делении ядер ^{235}U и ^{236}U быстрыми нейтронами. / XIV конференция

по физике деления, Обнинск, Россия, 12-15 октября, 1998 (в печати) (XIV International Workshop on Nuclear Fission Physics).
11. K.Wisshak, F.Voss, F. Kappeler, L.Kazakov, G.Reffo. Stellar neutron Capture Cross section of the Nd isotopes, Phys.Rev. C. V.57, No.1, 1998, P.391-408.
12. F.Voss, K.Wisshak, C.Arlandini, F. Kappeler, L.Kazakov, T.Rauscher. Stellar neutron Capture Cross section of Pr and Dy isotopes, Report FZKA and Phys.Rev. (to be published).
13. K.Wisshak, F.Voss, F. Kappeler, L.Kazakov, G.Reffo. Stellar neutron Capture Cross section of the Yb isotopes, (to be published in Report FZKA and Phys.Rev.).
14. Тамбовцев Д.И., Козловский Л.К., Фурман В.И. и др. // Ядерная физика, 1999, вып. 5, принято к печати.
15. A.B.Popov, D.I.Tambovtsev, W.I.Furman et. al, // in Proc. of II-d Intern. Workshop on Fission and Fission Fragment Spectroscopy, Seyssins, France, Apr. 21-24, 1998, to be published.
16. Yu.N.Kopach, D.I.Tambovtsev, A.B.Popov et. al, //in Proc. of VI-d Intern. Seminar on Interaction of Neutron with Nuclei, Dubna, Russia, May 12-15, 1998, to be published.
17. D.I. Tambovtsev, L.K.Kozlovsky, W.I.Furman et. al, // in Proc. XIV-d Intern. Meeting on Physics of Nuclei Fission, Obninsk, Russia, Oct. 12-15, 1998, to be published.
18. Yu.N.Kopach, D.I.Tambovtsev, W.I.Furman et. al, // in Proc. of IV-d Intern. Conf. on Dynamical Aspects of Nuclear Fission – DANF-98, Casta-Popernichka, Slovakia, Oct. 20-23, 1998, to be published.
19. Журавлёв Б.В. Плотность уровней ^{208}Bi и ^{209}Po из анализа дифференциальных сечений (p,n) реакции на ядрах ^{208}Po и ^{209}Bi. // Известия Академии наук, сер. Физическая, 1998. Т.62, №1, с.179.
20. Журавлёв Б.В., Титаренко Н.Н., Трыкова В.И., Чжоу Цзуин, Тан Хунцин, Чи Будзя, Чжоу Ченьвей, Ду Яньфен. Дифференциальные сечения эмиссии нейтронов из реакции ^{56}Fe(α,n)^{59}Ni и плотность уровней ядра ^{59}Ni. // Известия Академии наук, сер. Физическая, 1998. Т.62, №1, с.110.
21. B.V.Zhuravlev "Structure in energy dependence of nuclear level density." Proceedings of the 6 Inter. Seminar on Interaction of Neutrons with Nuclei, Dubna, May 13-16, 1998, JINR E3-98-202, p.161
22. B.V.Zhuravlev, N.N.Titarenko, V.I.Trykova, Zhou ZuYing et al. "Nuclear level density and spin cut-off parameter of ^{59}Ni, ^{96}Tc, ^{118}Sb from differential neutron emission cross-sections of (p,n) and (α,n) reactions." Proceedings of the 6 Inter. Seminar on Interaction of Neutron with Nuclei, Dubna, May 13-16, 1998, JINR E3-98-202, p.151.
23. Журавлёв Б.В. Структура в энергетической зависимости плотности уровней ^{165}Er в области малой энергии возбуждения. // Известия Академии Наук, сер. Физическая, 1999. Т.63, №1, с.154.
24. B.V.Zhuravlev, N.N.Titarenko, V.I.Trykova, Zhou ZuYing et al. "Nuclear level density and spin cut-off parameter for nuclei of ^{59}Ni, ^{96}Tc, ^{118}Sb from differential neutron emission cross-sections of (p,n) and (α,n) reactions." Report on Inter. Nuclear Physics Conference, France, Paris, August 24-28, 1998. Abstracts of Contributed Papers, v.1, p.467.
25. Журавлёв Б.В., Титаренко Н.Н., Трыкова В.И., Чжоу Цзуин и др. Плотность уровней и параметр спиновой зависимости ^{59}Ni, ^{96}Tc, ^{118}Sb из дифференциальных сечений эмиссии нейтронов в (p,n) и (α,n) реакциях. // Доклад на 48 Межд. конференции по ядерной спектроскопии и структуре атомного ядра, Москва, июнь 11-14, 1998 г. Будет опубликован в Изв. Ак. наук, сер. Физическая, 1999, №5.

26. Деменков В.Г., Журавлёв Б.В. Экспандер временных интервалов наносекундного диапазона. Послана в ''Приборы и техника эксперимента''. Исх.№64-03/317 от 14.10.98 г.
27. B.V.Zhuravlev, N.N.Titarenko, V.I.Trykova, Zhou ZuYing et al. "Nuclear level density and spin cut-off parameter of fragment nuclei from differential neutron emission cross-sections of (p,n) and (α,n) reactions." Report on 14 Inter. Workshop on Nuclear Fission Physics, Obninsk, 12-15 October, 1998.
28. Лунев В.П., Проняев В.Г., Симаков С.П., Шубин Ю.Н. Анализ сечений и механизма реакций (n,xn) и (n,xγ) на ядрах свинца и висмута. // Доклад на 48 совещание по ядерной спектроскопии (июнь 1998, г. Москва).
29. Девкин Б.В., Кобозев М.Г., Талалаев В.А., Симаков С.П., Синица В.В., U. Fischer, U. Von Moellendorff. Спектры нейтронов утечки из железных сферических сборок с ^{252}Cf источником нейтронов. // Доклад на VII Росс. научн. конф. по защите от иониз. излуч. ядерн.-техн. установок. (сентябрь 1998, Обнинск), с.134.
30. S.P. Simakov, A. Pavlik, H. Vonach, S. Hlavac - Status of experimental and evaluated discrete γ-ray production at E = 14.5 MeV - Report INDC(CCP)-413, Vienna, 1998
31. S.P. Simakov, B.V. Devkin, B.I. Fursov, M.G. Kobozev, V.A. Talalaev, U. von Moellendorff, M.M. Potapenko - Benchmarking of the evaluated data for vanadium by a 14 MeV spherical shell transmission experiment - Report FZKA-6096, Karlsruhe, 1998.
32. S.P. Simakov, G.N. Lovchikova, A.M. Trufanov, V.A. Vinogradov, M.G. Kobozev - Nonmonoenergety of neutron source based on the solid tritium target // ПТЭ, 1999, № 5.
33. S.P. Simakov, B.V. Devkin, M.G. Kobozev, U. von Moellendorff, D. Yu. Chuvilin - Benchmarking of the evaluated data for nickel by a 14 MeV spherical shell transmission experiment - Fusion Technology, 1999, v. 63, no 2.
34. Kornilov N.V., Kagalenko A.B., Baryba V.Ya., Demenkov V.G., Pupko S.V., Androsenko P.A. "Inelastic neutron scattering and prompt fission neutron spectra for ^{237}Np", submitted to Nuclear Science and Engineering.
35. Kornilov N.V., Kagalenko A.B., Zolotarev K.I., "On the contradiction between microscopic and macroscopic data for ^{235}U fission neutron spectrum at thermal energy", Proc. of ISINN-6, p.242.
36. Kornilov N.V., Kagalenko A.B., Poupko S.V., Androsenko P.A. "The tritium admixture in solid target backing and neutron spectrum from "monoenergetic source", preprint IPPE-2720, 1998.
37. A.F.Gurbich "Evaluation of non-Rutherford proton elastic scattering cross section for silicon" - Nucl. Instr. and Meth. v.145/4 (1998), p.578-583.
38. A.F.Gurbich "Proton elastic scattering cross section for carbon: Confrontation of theory and experiment" - Nucl. Instr. and Meth. (accepted for publication, in press).
39. Труфанов А.М., Ловчикова Г.Н., Свирин М.И., Поляков А.В., Виноградов В.А., Дмитриев В.Д., Бойков Г.С. Спектр нейтронов, сопутствующих делению ядра урана-238, вызванного быстрыми нейтронами: Препринт ФЭИ-2689, Обнинск, 1998.
40. Ловчикова Г.Н., Труфанов А.М., Свирин М.И., Поляков А.В., Виноградов В.А., Дмитриев В.Д., Бойков Г.С. Особенности формы спектров нейтронов и механизм эмиссии нейтронов при делении актинидных ядер // Доклад на 14 международной конференции по физике деления ядер. Обнинск, 12-15 октября, 1998.

41. Тертычный Р.Г., Шорин В.С. Программа для расчета характеристик ускорительных источников нейтронов: Препринт ФЭИ-2743, Обнинск, 1998.
42. B.I.Fursov, B.F.Samylin, V.S.Shorin, E.Yu.Baranov, E.S.Lavrov, V.I.Milshin, V.B.Pavlovich, S.V.Pupko, Yu.M.Turchin, V.N.Polynov "Fission Cross Section Measurements for Minor Actinides" Доклад (14-я международная конференция по физике деления ядер, Обнинск, 12-15 октября, 1998).
43. Детальная отработка и оптимизация технологии производства трековых фильтрующих мембран из полиэтилентерефталата: Отчёт ГНЦ РФ-ФЭИ, №9760, Обнинск, 1998, 24 с. - Исполн. А.А.Туманов, Г.С.Жданов и др.
44. Технология производства трековых мембран из полиэтилентерефталата и микрофильтрационных устройств на их основе: Отчёт ГНЦ РФ-ФЭИ, №9835, Обнинск, 1998, 28 с.-Исполн. А.А.Туманов, Г.С.Жданов и др.
45. Большов В.И., Жданов Г.С., Туманов А.А. Исследование сенсибилизирующей роли механических нагрузок на радиационно-химические и физико-химические процессы формирования пористой структуры трековых мембран // Сб. докладов Всероссийской научной конференции "Мембраны-98". 5-10 октября 1998, М., с.120.
46. Красавина Т.А., Махова Г.П., Жданов Г.С., Туманов А.А. Спектрофотометрический контроль при производстве трековых мембран. Там же, с.128.
47. Худяков А.В., Рыков В.А., Туманов А.А., Сумин Д.В. Измерение пористости трековых мембран с использованием тяжелых заряженных частиц. Там же, с.129.
48. Фурсов Б.И., Туманов А.А., Мчедлишвили Б.В. и др. Реакторные трековые мембраны "РЕАТРЕК-ФЭИ": особенности производства, характеристики, свойства. Там же, с.139.
49. Туманов А.А. Радиационно-гигиенические характеристики трековых мембран. Там же, с.145.
50. Сотов М.И., Жданов Г.С., Тимохович В.П. Применение трековых мембран в бытовых напорных фильтрах для очистки питьевой воды. Там же, с.117.
51. Подзорова Е.А., Сотов М.И., Жданов Г.С. Очистка подземных источников от окислов железа с использованием трековых мембран. Там же, с.118.
52. Radiation-induced chemical processes in polystyrene based scintillators. G.S.Zhdanov, V.K.Milinchuk, E.P.Klinshpont. 3-th International symposium on ioniting radiation and polymers. September 19-24, 1998, Waldhotel Weinbohla, Germany, p.6.
53. Жданов Г.С., Виленский А.И. Химические изменения в области треков ПЭТФ, облученных ионами ксенона // Химия высоких энергий, 1998. Т. 32, №2, с.112.
54. Терефталевая кислота. Спектрофотометрическое определение в водных растворах. Методика анализа. №48-03/42, Обнинск, 1998 г., 7 с.
55. Этиленгликоль. Спектрофотометрическое определение в водных растворах. Методика анализа. №48-03/41, Обнинск, 1998 г., 8 с.
56. Заявка на изобретение "Мембранное устройство на основе трековой мембраны для лечебного плазмафереза крови", регистрационный № 98115103 от 04.08.1998 г.

CONDENSED MATTER PHYSICS LABORATORY

1. A.G.Novikov, M.N.Rodnikova, O.V.Sobolev, «The comparative analysis of ionic and hydrophobic hydration effects», Submitted to J. of Mol. Liquids.
2. A.G.Novikov, M.N.Rodnikova, V.V.Savostin, O.V.Sobolev, «The study of hydration effects in aqueous solutions of LiCl and CsCl by inelastic neutron scattering», Submitted to J. of Mol. Liquids.
3. A.G.Novikov, M.N.Rodnikova, O.V.Sobolev, «Neutron scattering study of the 0.94 m tetrabutilammonium chloride aqueous solution» / Тезисы доклада на VII Международной конференции «Проблемы сольватации и комплексообразования в растворах», Иваново, 29 июня-2 июля.
4. A.G.Novikov, M.N.Rodnikova, O.V.Sobolev, «Investigation of hydrophobic hydration effects by inelastic neutron scattering», Annual report 1997, FLNP JINR, Dubna, p.107.
5. Новиков А.Г., Родникова М.Н., Соболев О.В. Эффекты гидрофобной гидратации из экспериментов по рассеянию медленных нейтронов. Статья направлена в Журнал физической химии.
6. M.V.Zaezjev, A.G.Novikov, V.V.Savostin, «Frequency spectrum and specific heat of liquid potassium from inelastic neutron scattering», Abstracts of Tenth International Conference on Liquid and Amorphous Metals, University of Dortmund, Germany, 1998, p. 48.
7. M.V.Zaezjev, A.G.Novikov, V.V.Savostin, «Isochoric specific heat and anharmonicity for liquid potassuim», статья направлена в J. of Non-Cryst. Solids.
8. A.G.Novikov, V.V.Savostin, A.L.Shimkevich, M.V.Zaezjev, «Oxygen microscopic dynamics in liquid potassium studied by inelastic neutron scattering», Abstracts of Tenth International Conference on Liquid and Amorphous Metals, University of Dortmund, Germany, 1998, p. 50.
9. A.G.Novikov, V.V.Savostin, A.L.Shimkevich, M.V.Zaezjev, «Oxygen microscopic dynamics in liquid potassium studied by inelastic neutron scattering», статья направлена в J. of Non-Cryst. Solids.
10. Заезжев М.В., Новиков А.Г., Савостин В.В., Шимкевич А.Л. Микродинамика расплава калий-кислород: Препринт ФЭИ-2713, Обнинск, 1998, 19 с.
11. Новиков А.Г., Соболев О.В., Селиверстов Д.И., Тихонов Г.В. Структурно-динамические особенности жидкой хлорокиси фосфора ($POCl_3$) из экспериментов по нейтронному рассеянию: Препринт ФЭИ-2723, Обнинск, 1998, 20 с.
12. M.Baeva, S.Danilkin, A.Beskrovni, E.Jadrowski, Lattice Dynamics of the Fe-Cr-Mn and Fe-Cr-Ni Nitrogen Steels with Different Cr Content, Report on V International Conference on High Nitrogen Steels, May 24 -28, 1998, Espoo-Finland, Stockholm-Sweden).
13. M.Baeva, A.Beskrovni, S.Danilkin, E.Jadrowski X-Ray and Neutron Diffraction Study of Fe-(15 to 29)Cr-11Ni-0.5N Steel, J. of Materials Science Letters, vol. 17 (1998) pp. 1169-1171.
14. S.Danilkin, H.Fuess, T.Wieder, H.Wipf , E.Yadrowski, Interstitial Atom Effect on the Structure and Lattice Dynamics of Nb and Fe-based Alloys, Proceedings of the German-Russian User Meeting, Condensed Matter Physics with Neutrons at IBR-2, Frank Laboratory of Neutron Physics, Dubna, Russia, April 2-4, 1998, p.111-116.
15. H.Wipf, S.Danilkin, E.Jadrowski, H.Fuess, T.Wieder, «X-ray and neutron scattering study of the Nb-O solid solutions», Annual report 1997, FLNP JINR, Dubna, p.109.

16. S.Danilkin, A.Beskrovni, E.Jadrowski, Nitrogen Effect on the Lattice Dynamics Of FCC Fe-18Cr-19Mn Austenitic Alloys, Report on V International Conference on High Nitrogen Steels, May 24 -28, 1998, Espoo-Finland, Stockholm-Sweden.
17. S.Danilkin, H.Fuess, E.Jadrowski, T.Wieder, H.Wipf X-ray and neutron scattering study of the α-NbO_x solid solutions. J. of Alloys and Compounds, 1998, v. 266, p. 230-233.
18. S.Danilkin, D.Delafosse, H.Fuess, V.Gavriljuk, A.Ivanov, T.Magnin, H.Wipf Hydrogen vibrations in austenitic stainless steels, ILL Experimental Reports and Theory Activities, 1998, to be published.
19. Морозов С.И. О локализации водорода в β'-фазе $VO_{0.2}$. // Письма в ЖЭТФ, 1998, Т.67, вып.5, с.326-328.
20. V.A.Semenov, «The inelastic neutron scattering in oxides with corundum structures», to be published in «Annual Report 1997, Nuclear Physics Department IPPE, Obninsk.
21. V.M.Agranovich, S.A.Darmanyan, K.I.Grigorishin, O.A.Dubovsky, A.M.Kamchatnov, Th Neidlinger, P.Reineker. "Fermi resonance of nonlinear vibrations on interfaces of anharmonic crystals". Phys.Rev.B, v.57, N26, p.2461-2472, 1998.
22. V.M.Agranovich, O.A.Dubovsky, "Repulsion induced Frenkel biexciton resonances in organic crystals". Phys.Lett.A, 1998, (in press).
23. Дубовский О.А., Орлов А.В. Идентификация бифононов по особенностям угловой и энергетической зависимости сечения неупругого рассеяния разваливающих бифононы нейтронов // ФТТ, 1998, 40, №4, с.728-734.
24. Дубовский О.А. Сверхсвечение поляритонов в ограниченных одномерных кристаллах с увеличивающейся длиной: переход от димера к бесконечному кристаллу // ФТТ, 1998, 40, №11,с.1132-1140.
25. Дубовский О.А. Кинематические квазивакансионные биэкситоны Френкеля в давыдовском мультиплете. Статья направлена в журнал ФТТ.
26. V.M.Agranovich, O.A.Dubovsky. "Frenkel biexcitons in crystals with two atoms in elementary cell". Статья направлена в журнал Phys.Lett.A.
27. Дубовский О.А., Орлов А.В. Локальные поляритоны нового типа на границе раздела гиротропных энантиоморфных кристаллов. Статья направлена в журнал ФТТ.
28. Дубовский О.А., Орлов А.В. Деление бифононов нейтронами. Направлено в журнал ФТТ.
29. Дубовский О.А., Орлов А.В. Солитоны в двумерных и трехмерных кристаллах при Ферми-резонансе оптических колебаний. Направлено в журнал ФТТ, исх.№64-03/260 от 08.07.98.
30. Дубовский О.А. Кроссовер от щелевых бифононов к щелевым биэкситонам Френкеля в давыдовском мультиплете при сильном ангармонизме в ограниченных кристаллах. Направлено в ФТТ, исх64-03/329 от 05.11.98.
31. K.H.Andersen, I.V.Bogoyavlenskii, V.G.Kolobrodov, A.V.Puchkov, A.N.Skomorokhov, «Study of the phonon-maxon region in liquid helium excitation spectrum», Annual report 1997, FLNP JINR, Dubna, p.94.
32. I.V.Bogoyavlenskii, A.V.Puchkov, A.N.Skomorokhov, «Analysis of liquid 4He neutron scattering data on basis of the Glyde-Griffin model,» Physica B241-243(1998)947.
33. Пучков А.В., Скоморохов А. // Исследование динамического структурного фактора жидкого гелия. // XXXI Совещание по физике низких температур (2-3 декабря, МГУ, Москва). Тезисы докладов, с.186.

34. Исследование конденсированных сред на импульсных быстрых реакторах ИБР-1(30) и ИБР-2: Отчет ФЭИ №9505, 1998. - Исполн. Пучков А.В., Семенов В.А.
35. Натканец И., Пучков А.В. Нейтронная спектрометрия на импульсном реакторе ИБР-2. // Поверхность (Рентгеновские, синхротронные и нейтронные исследования), 1998. Т.3, с.5-19.
36. S.N.Ishmaev, Y.V.Lisichkin, A.V.Puchkov, V.A.Semenov, Neutron study of dynamic atomic correlations in amorphous isotopic Ni-B alloys, Proc.of 6th European Powder Diffraction Conference EPDIC-6, Aug.22-25, Budapest, Hungary, 1998.
37. Губарева И.В., Лисичкин Ю.В. Расчет энергетического и временного спектров нейтронов за прерывателем двойного времяпролетного спектрометра: Препринт ФЭИ-2709, Обнинск, 1998, 28 с.

MATHEMATICS AND SOFTWARE DIVISION

1. V.M. Piksaikin, S.G. Isaev, L.E. Kazakov, M.Z. Tarasko. Energy dependence of average half-life of delayed neutron induced fission 0f ^{235}U and ^{236}U. //XIV International Workshop on Nuclear Fission Physics, 12-15 Oktober, 1998, Obninsk.
2. Пиксайкин В.М., Исаев С.Г., Казаков Л.Е., Тараско М.З. Измерение энергетической зависимости относительных выходов запаздывающих нейтронов и периодов полураспада их предшественников при делении Np-237 быстрыми нейтронами. // Ат. эн., 1998, Т.85, вып.1, с.51.
3. Пиксайкин В.М., Исаев С.Г., Казаков Л.Е., Тараско М.З. Экспериментальные исследования характеристик запаздывающих нейтронов при делении Np-237 и U-235 быстрыми нейтронами. // В сб. Избранные труды ФЭИ, 1998 г.
4. Расчет прогибов ТВС в процессе 10-й топливной кампании на блоке № 2 Калининской АЭС: Отчет ФЭИ - 9878, Обнинск, 1998. - Исполн. Лихачев Ю.И., Гинкин В.П. и др.
5. Расчет прогибов серийных и циркониевых ТВС в процессе 10-й топливной кампании на блоке №3 Запорожской АЭС: Отчет ФЭИ - 9879, Обнинск, 1998.-Исполн. Лихачев Ю.И., Гинкин В.П. и др.
6. Расчетный прогноз деформации всех ТВС активной зоны блока № 1 Балаковской АЭС в процессе перегрузки и 8-й топливной кампании: Отчет ФЭИ - 9880, Обнинск, 1998.-Исполн. Лихачев Ю.И., Гинкин В.П. и др.
7. Расчет поведения активной зоны ВВЭР-1000, работающего в маневренном режиме. Сравнение результатов расчётов деформирования ТВС Запорожской АЭС (блок № 3) для маневренного и базового режимов работы: Отчет ФЭИ - 9882, Обнинск, 1998.-Исполн. Лихачев Ю.И., Гинкин В.П. и др.
8. Балакин И.П., Гинкин В.П., Уваров А.А. Моделирование движения ОР СУЗ и компенсация численной неустойчивости при расчете переходных процессов в реакторах типа ВВЭР. // В сб. Интегрированные математические модели и программные комплексы в ядерной энергетике, М.,1998, с. 301-304.
9. Безбородов А.А., Волков А.В., Гинкин В.П. и др. Пространственно-временной расчет переходных процессов в быстрых реакторах. // В сб. Интегрированные математические модели и программные комплексы в ядерной энергетике, М.,1998, с. 304-307.

10. Безбородов А.А., Волков А.В., Ганина С.М., Гинкин В.П., Кузнецов И.А., Троянова Н.М., Швецов Ю.Е. Spatial and time-dependent calculation of fast reactor transients. Доклад на семинар Consulting Meeting of IAEA specialists on fast reactor problem, 4 June, 1998, Obninsk, Russia.
11. Безбородов А.А., Волков А.В., Ганина С.М., Гинкин В.П., Кузнецов И.А., Троянова Н.М., Швецов Ю.Е. Пространственно-временной расчет переходных процессов в быстрых реакторах. // Доклад на семинар "Нейтроника-98", Обнинск, 27 - 29 октября, 1998 г.
12. V.A. Khriatchkov, M.V. Dunaev, V.V. Ketlerov, N.N. Semenova, M.Z. Tarasko. Investigation of the CsJ(Tl) scintillator properties for registration low-energy charge particles. XIV International Workshop on Nuclear Fission Physics, 12-15 Oktober, 1998, Obninsk.
13. Разработка математической модели экспериментальной установки для анализа коэффициентов чувствительности: Отчет о НИР (промежуточный) ФЭИ. Инв. № 9722. Обнинск, 1998. 26 с.-Исполн. Комлев О.Г., Суслов И.Р.
14. Развитие программы MCCG3D решения уравнения переноса в трехмерной нерегулярной геометрии методом характеристик: Отчет о НИР (промежуточ-ный) ФЭИ. Инв. № 9723. Обнинск, 1998. 33 с.-Исполн. Комлев О.Г., Суслов И.Р.
15. Применение программы MCCG3D для расчетов экспериментов на критической сборке ZR-6. Часть I Математические модели критической сборки ZR-6 в регулярной геометрии: Отчет о НИР (промежуточный) ФЭИ. Инв. № 9774. Обнинск, 1998. 14 с.-Исполн. Комлев О.Г., Суслов И.Р.
16. Формулы теории возмущений для скоростей реакций и отношения скоростей реакций в подкритических и условно-критических системах. Часть I. Формулы теории возмущений в дифференциальной форме. Алгоритмы нахождения решения уравнения переноса со знакопеременным источником: Отчет о НИР (промежуточный) ФЭИ. Инв. № 9785. Обнинск, 1998. 15 с.-Исполн. Комлев О.Г., Суслов И.Р.
17. Решение нестационарного уравнения диффузии в нерегулярной геометрии методом разделения области. Формулировка краевых задач в подобластях и численные методы их решения: Отчет о НИР (промежуточный) ФЭИ. Инв. № 9827. Обнинск, 1998. 25 с.-Исполн. Комлев О.Г.
18. V.K. Artemyev, V.P. Ginkin, N.V. Gusev, T.M. Luhanova, I.L. Ozernyh, V.P. Shishulin, I.P. Sviridenko. Numerical Simulation of Crystal Growth by Floating Zone Method. CHT'97 Advances in Computa-tional Heat Transfer. Proceedings of a Symposium organized by International Center for Heat and Mass Trasfer f CESME, TURKEY, May 26-30, 1997, pp. 500-507.
19. Артемьев В.К., Гинкин В.П. Численное моделирование трехмерной естественной конвекции. // Вторая Российская национальная конференция по теплообмену, РНКТ2. Изд-во МЭИ, Москва, 1998. Т. 3, с.38-41.
20. Численная методика решения двумерных и трехмерных уравнений вынужденной и естественной конвекции. Верификация программ FLUID2D и FLUID3D: Отчет ФЭИ № 9842, 1998.-Исполн. Артемьев В.К., Изотов А.А.
21. V.K. Artemyev. Implicit Numerical Method for Solving of Fluid Mechanics, Heat and Mass Trasfer Equations. 11th International Heat Trasfer ConferenceKyongju, Korea, 1998.

22. Yu.N. Kornienko. "Quasi-Two-Dimensional Modeling of the Closure Relationships for Wall Friction, Heat and Mass Transfer in Channels and Rod Bundles." Proc. of Int. Conf. "Thermophysical Aspects of WWER-Type Reactor Safety", V.1, pp. 418-429, 1998.
23. P.P. Balakin, Yu.N. Kornienko. "Influence of the Saddle-Shape Void Fraction Profile on the Thermohydraulic parameters in RELAP5/MOD3.2" Proc. of Int. Conf. "Thermophysical Aspects of WWER-Type Reactor Safety",, V.1, pp. 442-455, 1998.
24. Yu.N. Kornienko. "Development of the Analytical Closure Relationships Descriptions for One- and Two-Phase Wall Friction, Heat and Mass Transfer Coefficients for Subchannel Analysis." Proc. of ICONE-6, Trac.7, CD-Room, 10-15 May 1998, Tokyo, Japan.
25. P.P. Balakin, Yu.N. Kornienko. "Improvement and Verification of RELAP5/MOD3.2 Wall Friction and Heat Transfer Models for Low Mass Flux Bubble Flow." Proc. of ICONE-6, Trac.7, CD-Room, 10-15 May 1998, Tokyo, Japan.
26. P.P. Balakin, Yu.N. Kornienko. "Improvement and Verification of RELAP5/MOD3.2 Wall Friction and Heat Transfer Models for Bubble Flow with Saddle-Shape Void Fraction Profiles." Proc. Int. Conf. " Thermohydraulics-98".
27. Yu.N. Kornienko. "Analytical Closure Relationship descriptions for Local Wall Friction, Heat and Mass Transfer Coefficients." Proc.Int.Conf. "Thermohydraulics-98".
28. Yu.N. Kornienko. "On development of Analytical Closure Relationships for Local Wall Friction, Heat and Mass Transfer Coefficients for Sub-Channel Codes." IAEA, International Working Group on Fast Reactors, Tech. Comm. Meeting on "Methods and Codes for Calculations of Thermohydraulic Parameters for Fuel, Absorber Pins and Assemblies of LMFBRs with Traditional and Burner Cores", Obninsk, Russia, 27-31 July, 1998.
29. E.V. Kornienko, Yu.N. Kornienko. "Estimation of the Density and Temperature Distribution Effects on the Errors of Wall Friction and Heat Transfer Coefficients for "Best Estimate" Codes." Information Exchange Forum on Analytical Methods and Computational Tools for NPP Safety Assessment, Obninsk, Russian Federation, 26-30 October 1998.
30. Бабанаков Д.М. Аналитическое решение неавтономной системы линейных уравнений точечной кинетики реактора // Математическое моделирование. 1998.Т.10, №11.
31. Шимкевич И.Ю., Кузин В.В., Шимкевич А.Л. Исследование тройной системы $K + K^{+q} + O^{-2q}$ методом молекулярной динамики и статистической геометрии: Препринт ГНЦ РФ ФЭИ-2724. Обнинск. 1998, 36 с.
32. I.Yu. Shimkevich, A.L. Shimkevich and V.V. Kuzin. Investigation of Triple $K+K^{q}+O^{-2q}$ system by MD Method and Statistical Geometry // INTAS-Ukraine Workshop on Condensed Matter Physics, Lviv, Ukraine, May 21-24 , 1998.
33. I.Yu. Shimkevich, A.L. Shimkevich, V.V. Kuzin. Dynamic Structure of Oxygen in Liquid Potassium Studied by MD Method and Statistical Geometry // Tenth International Conference on Liquid and Amorphous Metals, University of Dortmund, Germany, August 30 - September 4 , 1998.
34. V.V. Kuzin, I.Yu. Shimkevich, and A.L. Shimkevich. 1998, "Dynamic Structure of Oxygen in Liquid Potassium Studied by MD Method and Statistical Geometry", Journal of Non-Crystalline Solids (Accepted).

35. Проведение численных исследований на модельных задачах с целью оценки факторов всплытия при закачке отходов в горизонты с высокой плотностью пластовых вод и влияния слабопроницаемых включений на динамику распространения отходов: Отчет ФЭИ, Инв. №9791, 1998, 52 с. - Исполн. Зинин А.И., Зинина Г.А.
36. Дрожко Е.Г., Зинин А.И., Зинина Г.А., Самсонов Б.Г., Самсонов Л.М. Моделирование миграции радиоактивных загрязнений в подземных водах // XVI Менделеевский съезд ''Химия и проблемы экологии, анализ и контроль объектов окружающей среды'', Санкт-Петербург, 1998. / Рефераты докладов и сообщений. Т. 3, с. 88.
37. V.P. Ginkin. Problems of Numerical Simulation of the Single Crystal Growth Process. Proc. of the Fives International Conference on Simulation of Devices and Technologies. Cape-Town, South Africa, October 11-20, 1998.
38. Пупко С.В., Кагаленко А.Б. Задачи планирования оптимальных дозных полей в лучевой терапии: Препринт ФЭИ-2739, Обнинск, 1998, 20 с.
39. Гинкин В.П. Проблемы численного моделирования процесса роста монокристаллов. // Труды Второго Российского симпозиума "Процессы тепломассопереноса и рост монокристаллов и тонкопленочных структур НТ&CG'97". Обнинск, ГНЦ РФ-ФЭИ, 1998, с.148-157.
40. Галкин В.А., Гинкин В.П., Драков А.А., Озерных И.Л., Забудько М.А., Свириденко И.П. Моделирование и оптимизация теплофизических процессов роста монокристаллов в условиях микрогравитации. // Труды Второго Российского симпозиума "Процессы тепломассопереноса и рост монокристаллов и тонкопленочных структур НТ&CG'97". Обнинск, ГНЦ РФ-ФЭИ, 1998, с.140-147.
41. Кудрявцев А.И., Андросенко П.А. Методы Монте-Карло для решения задач тепломассопереноса в условиях неоднородной геометрии. // Труды Второго Российского симпозиума "Процессы тепломассопереноса и рост монокристаллов и тонкопленочных структур НТ&CG'97". Обнинск, ГНЦ РФ-ФЭИ, 1998, с.247-255.

HIGH-VOLTAGE ACCELERATORS DIVISION

1. V.S.Bashmakov, S.V.Bazhal, A.I.Glotov, V.K.Debin, A.S.Feigin, B.V.Kuprijnov, E.I.Lobanov, A.A.Malygin, V.A.Nikitin, V.A.Romanov, K.A.Rezvykh, V.I.Spirin, V.I.Volodin. The Obninsk EGP –15 tandem (status and development), IPPE, Obninsk, Russia. 6th European Particle Accelerator Conference. EPAC-98.
2. K.A.Rezvykh, V.A.Romanov. Systematic error estimation of an electric field strength for high- voltage devices. Journal «Electricity» , 1999, № 4.
3. K.A.Rezvykh, V.A Romanov. Breakdown Voltage Calculation for Gases with Non-uniform Field of an Accelerator by Base Method. //Nucl Instr and Meth. A423 (1999).203.
4. K.A.Rezvykh. Substantiation of breakdown voltage calculation for high – voltage accelerators, insulated by binary mixtures N_2 / CO_2. Proceedings of the XII International Conference on Electrostatic Accelerators 25-28 November 1997, Obninsk: IPPE Publishing, 1999.
5. S.V.Bazhal, V.A.Romanov. Calculation and preliminary analysis of optical characteristics of the ion beam injection system into accelerating tube of tandem accelerator.

6. K.A.Rezvykh, V.A.Romanov. High–voltage structure development for the EGP-15 tandem (Project). 6th European Particle Accelerator Conference. EPAC-98. Proc. of the 6th European Particle Accelerator Conference, Bristol and Philadelphia: Institute of Physics Publishing, 1998, p. 696-698.
7. V.A.Romanov, A.A.Malygin, A.S.Feygin, T.A.Krasavina et al. Track membrane production of EGP-15 accelerator complex. Performance and properties. Contribution submitted on MEMBRANY_98 All-Russian Scientific Conference, Moscow, 28 September-3 October 1998.
8. Глазков А.А., Диденко А.Н., Коляскин А.Д., Шмелев А.Н., Хорасанов Г.Л. Оценка параметров электроядерной установки для трансмутации радиоактивных отходов. // В сб.: Аннотации докладов XVI Совещания по ускорителям заряженных частиц, 20-22 октября 1998 г., Протвино: Изд. ГНЦ РФ ИФВЭ, с.106-107, 1998.
9. Хорасанов Г.Л., Иванов А.П., Шимкевич А.Л. Потенциальные возможности использования жидкого олова в качестве теплоносителя электроядерных установок. // В сб.: Тезисы докладов конференции "Тяжёлые жидкометаллические теплоносители в ядерных технологиях", 5-9 октября 1998 г., Обнинск: Изд. ГНЦ РФ ФЭИ, с.36, 1998.
10. Хорасанов Г.Л., Иванов А.П., Коробейников В.В., Блохин А.И., Шимкевич А.Л. Свинцовый теплоноситель для быстрого реактора - выжигателя с жестким спектром нейтронов. // В сб.: Тезисы докладов конференции "Тяжёлые жидкометаллические теплоносители в ядерных технологиях", 5-9 октября 1998 г., Обнинск: Изд. ГНЦ РФ ФЭИ, с.50, 1998.
11. G.L.Khorasanov, A.P.Ivanov, A.N.Didenko, A.D.Koljaskin, A.A.Glazkov. Accelerator - Driven Subcritical Fast Reactors for Closing the Nuclear Fuel Cycle. In: Proceedings of the 9-th Int. Conf. on Emerging Nucl Systems, ICENES'98, Iune 28- Iuly 2 1998, Tel Aviv, Isracl, v.I, p. 227-234,1998.
12. G.L.Khorasanov, A.P.Ivanov, A.Yu.Konobeyev, A.N.Didenko, A.D.Koljaskin, A.A.Glazkov. Accelerator- Driven Subcritical Fast Reactors for Closing the Nuclear Fuel Cycle. In: Proceedings of the 6-th Int. Conf. on Nuclear Engineering, ICONE-6, May 10-15 1998, San Diego, California, USA, 1998.
13. G.L.Khorasanov, A.P.Ivanov, A.I.Blokhin, V.A.Apse, A.N.Chmelev, A.A.Glazkov and A.D.Koljaskin. Low-Activation Materials with Isotopic Tailoring for Future NPPs, Accepted at the Int. Conf.on Future Nuclear Systems, GLOBAL'99, August 30 - September 2, 1999, Snow King Resort, Jackson Hole, Wyoming, USA, (in press).
14. G.L.Khorasanov, A.P.Ivanov, V.V.Korobeinikov, A.I.Blokhin and A.L.Shimkevich. Lead Coolant for Fast Reactor-Burner With Hard Neutron Spectrum. Ibid, (in press).
15. A.N.Didenko, A.A.Glazkov, A.D.Koljaskin, A.N.Chmelev and G.L.Khorasanov. Parameters of Electroneclear Facility for Radiowastes Transmutation. Ibid, (in press).

5. MEETINGS AND CONFERENCES

(These are Meetings and Conferences where NPD IPPE played a major role in the organization)

1. XIV Meeting on Physics of Nuclear Fission 12-15 October, IPPE, Obninsk.
   About 100 participants from Russia and Foreign Parts.
   Topic: static properties of fission, mass, charge and energy distribution of fission fragments, cold fission, prompt neutron emission, delayed neutrons, fission dynamics, fission of hot nuclei and heavy ion induced fission, nuclear data, related with the fission process.

2. Meeting of Russian Nuclear Data Commission. 16 Oktober IPPE, Obninsk.
   About 20 participants from Russia.
   Topic: Nuclear Data Activity of Russian Institutes.

6. PARTICIPATION IN INTERNATIONAL AND NATIONAL CONFERENCES AND MEETINGS

1. **EPAC-98 6th European Particle Conference.**
   Stockholm, 22-26 June 1998.
2. **MEMBRANY-98 All-Russian Scientific Conference.**
   Moscow, 28 September-3 October 1998.
3. **XVI WORKSHOP on charged particle accelerators.**
   Protvino, 22-24 October 1998.
4. **V International Conference on High Nitrogen Steels.**
   Espoo-Finland, Stockholm-Sweden, May 24-28 1998
5. **XXXI Совещание по физике низких температур.**
   Москва, 2-3 декабря 1998
6. **Topical Conference on Giant Resonances.**
   Italy, Varenna, May 11-16, 1998.
7. **The 6th International Spring Seminar on Nuclear Physics "Highlights of Modern Nuclear Structure".**
   Italy, S.Agata Sue Due Golfi, May 18-22, 1998.
8. **International Conference "The structure of Mesons, Barions and Nuclei".**
   Poland, Cracow, May 26-30, 1998.
9. **The 6th International Seminar on Interaction of Neutrons with Nuclei.**
   Russia, Dubna, May 13-16, 1998.

7. COOPERATION

№№	Topic	Organization	Country
1	Accelerator system "SPRUT" with overlapping low energy electron and proton beams for use in simulating facility KOBE	Deutsches Zentrum für Luft-und Raumfahrt. V Berlin.	Germany
2	Charging belt system for electrostatic accelerators	Institute of Ion Beam Physics and Materials Research, Rossendorf	Germany
3	Condensed matter study and the neutron spectrometry methods development.	Frank Laboratory of Neutron Physics, Joint Institute on Nuclear Research, Dubna.	Russia
4	The partial dynamical structure factors study of the crystalline and amorphous compounds Ni-B by the inelastic neutron scattering.	Russian National Centre-"Kurchatov Institute", Moscow	Russia
5	Study of the microscopic dynamics of the aqueous and nonaqeous solutions by the inelastic neutron scattering.	Kurnakov Institute of General and Inorganic Chemistry, Russian Academy of Sciences, Moscow	Russia
6	Investigation of the influence of high frequency nonlinear vibrations - biphonons, biexitons, solitons - with their energy near the lattice stability barrier on the phase transition kinetic in the crystalline and the disordered solid materials.	Institute of Spectroscopy, Academy of Sciences of Russian Federation, Troisk, Moscow Region	Russia
7	The investigation of the quantum liquids fundamental properties by neutron scattering.	National Scientific Centre of Ukraine -"Kharkov Institute of Physics and Technology".	Ukraine
8	The investigation of hydrogen effect on the crystal and lattice dynamics of the austenitic Fe-Cr-Mn steels by the neutron scattering.	Institute for Metal Physics, Ukraine Academy of Science, Kiev	Ukraine
9	The investigation of the excitation spectrum of the superfluid helium.	Institute of Laue-Langewin, Grenoble	France
10	A study of the lattice dynamics of fast ion conductors with the fluorite structure at the transitions temperatures.	Institute for Physics and Nuclear Engineering, Bucharest	Romania
11	Interstitial atom effect on the crystal structure and lattice of the triple Nb-O-H(D) solid solutions and high nitrogen steels.	Darmshtadt University of Technology	Germany